The spatial variation of minimum near-surface temperature in complex terrain: Marlborough vineyard region, New Zealand

---

A thesis submitted in partial fulfilment of the requirements of the degree of
Doctor of Philosophy in Geography
in the University of Canterbury

Stuart Powell

University of Canterbury 2014

Abstract

The economic impact of frost on agriculture remains a global problem. It is a particular concern for the New Zealand wine industry, where the consequences of an unexpected spring frost can be disastrous. Marlborough is located in the north-eastern corner of the South Island and is the largest grape-growing region in New Zealand. The region is surrounded by complex mountainous terrain that gives rise to extremes of climate, particularly large spatial variations of minimum temperature and the frequent occurrence of spring frost. The high spatial variation of near-surface minimum temperature can lead to under-preparedness among grape growers who rely on accurate frost forecasts as part of their frost mitigation systems.

Field campaigns of the 1980's and 90's extended the understanding of the physical meteorological processes that affect cooling in complex terrain. More recent modelling efforts continue to refine this knowledge, although much less attention is given to the effects of different cooling processes on near-surface temperature. Agricultural developments in areas of complex terrain would benefit from an increased understanding of the meteorological processes that govern near-surface cooling, as this will help with the local prediction of frost.

The spatial variation of near-surface minimum temperatures is first explored by identifying relationships with synoptic weather patterns using the Kidson (2000) synoptic classification scheme. Analysis revealed that Kidson types associated with the largest daily variations in near-surface minimum temperature (T, TNW and H) are not always associated with the occurrence of frost. Frost is more likely to occur during the cooler airflows of Kidson type HW, HNW and SW, or during the settled anticyclonic conditions that follow cooler airflows.

The relationship between the spatial variation of near-surface minimum temperature and regional airflow patterns is explored using numerical weather prediction (NWP)

modelling. Results indicated that a high σ T_{min} around the region is a product of interaction between the region's complex terrain and ambient meteorology, and it could occur in both settled weather and more dynamic synoptic conditions. A high regional σ T_{min} during light ridge top winds could occur as a function of a location's relative susceptibility to ventilation from thermally-induced drainage winds, and it may also occur as a result of the simultaneous ventilation and stagnation of near-surface air layers as synoptic wind interacts with local topography.

The influence of the vertical structure of the nocturnal boundary layer (NBL) on near-surface minimum temperature was investigated with the University of Canterbury Sonic Detection And Ranging (SODAR). Measurements confirmed the formation of low-level jets (LLJ's) in the Awatere and Wairau Valleys during settled weather conditions, and that shear-induced turbulence beneath the jets was sufficient to mix warmer air to the surface and increase local temperatures. The process is sufficient to reduce frost risk to some of the region's upper valleys during clear settled weather. In stronger ridge top winds development of the LLJ's can be suppressed or eliminated and this was found to reduce shear-induced turbulence near the surface, allowing increased near-surface cooling.

While results from this study are of greatest value to the prediction of near-surface minimum temperature and frost in Marlborough, the results could be applied to improved prediction of near-surface minimum temperature in complex terrain around the world. Further research could be directed toward the interaction of synoptic winds with thermally-induced airflows, as the transition zone between these wind systems is believed to govern the temporal and spatial evolution of near-surface stagnation, and this is related to episodes of strong near-surface cooling.

Acknowledgements

For much of the time this research was conducted remotely, away from the University of Canterbury campus, on a part-time basis. While this brought about a number of logistical challenges, the exceptional support from a number of people provided the incentive to continue the course of study. First and foremost, I wish to thank Andrew Sturman and Peyman Zawar-Reza for your supervision. Your skill in guiding this research from a collection of disorganised theories into a meaningful and scientifically rigorous study has been invaluable. I have been tremendously educated along the way, in a professional, constructive, and friendly environment. I also wish to thank a number of staff and colleagues within the Department of Geography for their input to this research, by way of conversation, emails and technical support, in particular Iman Soltanzadeh and Marwan Katurji. A big thank you to Justin Harrison and Nick Key for the field work set up, including a number of trips onto the exposed Blackbirch Range in sometimes less than favourable conditions.

I would like to extend my thanks to the support team at Harvest Electronics in Masterton, for your help in keeping all the automatic weather stations recording, and resolving issues with sensors and communications. In addition, the friendly annual data fees on several automatic weather stations for the duration of this research have been greatly appreciated.

Thanks again to Godfrey Checkley at Welds Hill Vineyard in the upper Awatere Valley, and Willie Crosse at Korohi Vineyard in Rapaura, who allowed the SODAR to be deployed and accessed on their vineyards for several months during 2010 and 2011. Data from the SODAR has been an integral component of this research.

Finally, this research would not have taken place without a grant from the Ministry of Science and Innovation, which required the co-sponsorship from a local winery. A huge

thank you to Pernod-Ricard New Zealand Ltd for providing the sponsorship, together with industry mentors Andy Frost and Andrew Naylor.

Contents

List of Figures

List of Tables

Chapter 1 Frost and the grapevine: A cool climate perspective

1.1 Introduction

The natural distribution of plants on Earth is largely determined by temperature. Not only is the average temperature important, but also the daily and seasonal variations must lie within limits specific to each plant species (Ireland 2005). Climate change, unseasonable weather and frost events cause significant damage to plants and crops on a global scale. While there is no universal definition for 'cool climate agriculture', a number of useful criteria including upper limits on Growing Degree Days (GGD's), the requirement for four distinct seasons, and large variations in diurnal temperature are useful (*http://winemakerschoicewinedoctor.blogspot.co.nz/2008/10/what-exactly-is-cool-climate-wine.html)*. Cool climate crops are most at risk from frost in spring and autumn when the average monthly extreme minimum air temperature is a few degrees below zero (Ireland 2005). Several studies have considered the grapevine as one of the most responsive plants to its surrounding environment (Becker 1984, Jackson and Lombard 1993, Holland and Smit 2010), with air temperature recently acknowledged as the main determinant of wine quality in New Zealand (Sturman and Quénol 2013).

The onset of bud burst each spring is a period of anticipation and anxiety on a cool climate vineyard. With the exception of a minority of locations, "every year poses the possibility of a frost causing an economic disaster" Trought et al. (1999). Inexperienced growers are often ignorant of the potential economic ramifications that spring frost can incur (Stafne 2007). While adequate warning of an impending event provides an integral first step towards managing a location's frost risk, the economic and practical aspects of protection often limit the methods that can be used. Recent advances in viticultural practices such as irrigation, fertigation, pest and disease control, and automated frost protection, have not only contributed to larger yields of superior quality crop, but also allowed the growth of a range of crops, including grapes in areas that would have not been possible several decades ago.

While the concept of terroir affects every form of agriculture, it is seldom more evident than with the production of high quality wines. The narrow climate zones required for optimal grape quality create a particular risk from extremes in near-surface temperature that may be associated with longer-term fluctuations in climate. The term terroir encompasses the complex interplay of physical factors crucial to grape development, such as climate, soil type, terrain and the people who cultivate the grapes (Jones and Hellman 2003). Although average climate conditions are important, weather parameters that fluctuate on daily or hourly time scales are critical, such as solar radiation, extremes of temperature (including frost), diurnal temperature range, rain, wind and hail. Many of these parameters have been combined to produce bioclimatic indices that describe a region's potential for viticulture (Jackson and Cherry 1988, Kenny and Shao 1992, Stafne 2007).

In the following introduction to this thesis, the economic impacts of frost, frost mitigation and frost prediction in New Zealand are considered. The chapter concludes by describing the impetus for this research, together with the research aims and objectives, and overall structure of the thesis.

1.2 Grapevine distribution and sensitivity to frost

Practical experience accumulated over many centuries has resulted in the present day spatial distribution of grape varieties around many parts of the world, except in the New World including in New Zealand, where the industry is considerably younger. The global distribution of grape growing is mostly restricted to temperate latitudes of between 30 – 50 degrees (Figure 1) and this corresponds to mean annual air temperatures in the range of 10 – 20°C (Jackson and Schuster 1997). Many grape growing locations occupy highly complex topographical niches embedded in broader landscapes and climatic regimes that may not be suited to viticulture at all. Many examples of this are illustrated by pockets of grape growing outside the 10 - 20°C isotherms, such as in North America, Canada, Brazil and Central Otago (New Zealand). A number of wine varieties popular today, such as Pinot Noir,

Riesling and Sauvignon Blanc, favour the cooler end of the grape growing temperature spectrum and the narrow climatic zones required for optimum quality predispose these varieties in some locations to high risk of spring and autumn frost.

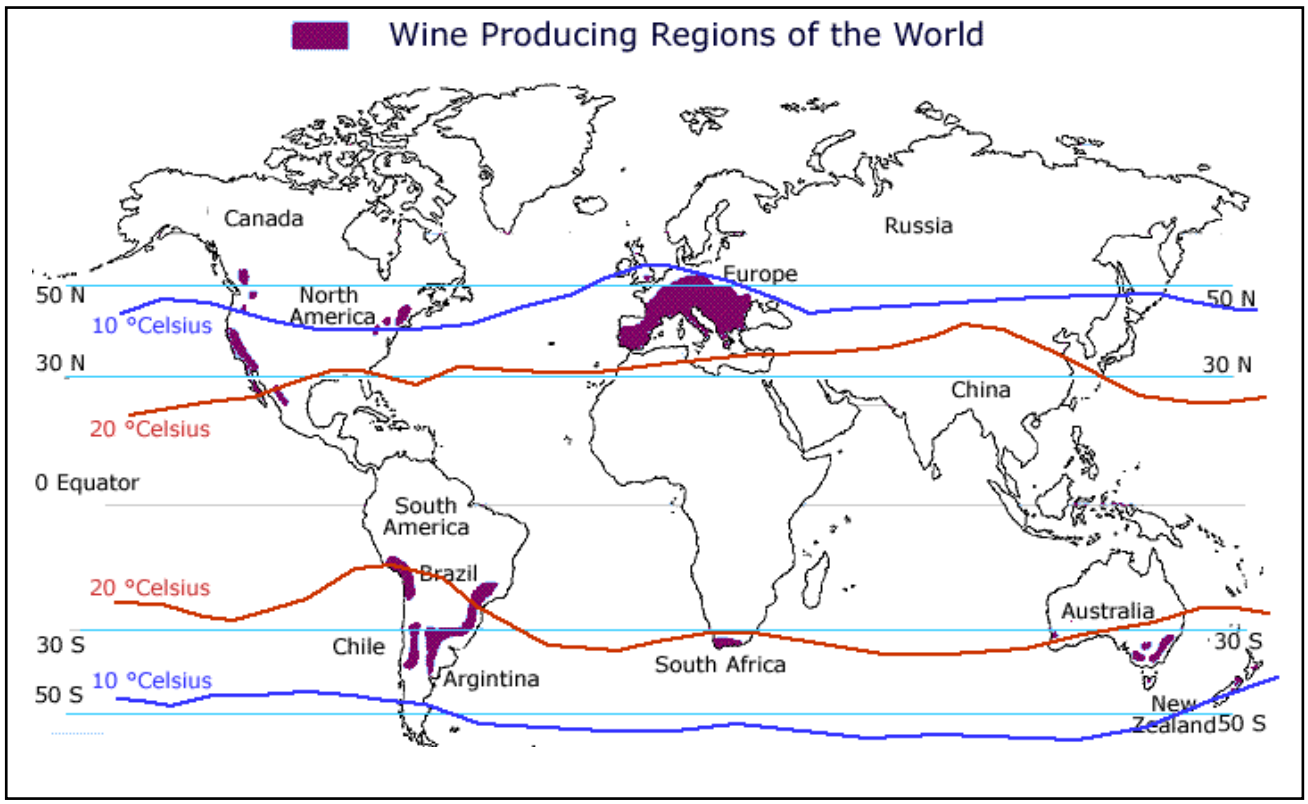

Figure 1.1 *Major wine producing regions of the world. (Source: http://www.thirtyfifty.co.uk/images/World-wine-map.gif)*

Although the mechanism of frost damage is still not completely clear, it may be either 'direct' when ice crystals form inside the protoplasm of cells (intracellular freezing) or 'indirect' when ice forms inside the plants but outside of the cells (extracellular freezing) (Synder and Paulo de Melo-Abreu 2005). The main cause of frost damage to plants in nature is extracellular freezing that causes secondary water stress to the surrounding cells. The subsequent disruption to membrane and enzyme functions causes widespread necrosis of affected tissue and results in the typical 'frost burn' symptom (Allard et al 1998). While -2°C is generally accepted as the critical temperature for damage, tissues vary in susceptibility and potential damage in any season depending on the time of the frost, its length and

severity, as well as the phenological stage of the crop (Trough et al 1999, Jones 2010). When damage from frost occurs, it not only reduces the quantity and quality of the crop for the current season, but also because of the perennial nature of grapevines, it can influence the productivity for several years into the future (Trought et al. 1999).

1.3 Economic consequences of frost

The economic consequences of frost affecting grapes and many other crops are well documented in the literature. Kalma et al. (1992) acknowledged substantial losses due to frost to the coffee industry in Brazil between 1963 – 1974, and the citrus crops of Florida in 1962, 1983, 1985 and 1989, with the latter frost in 1989 estimated to have cost over US $3.5 billion. More specifically, losses attributed directly to frost on vineyards are discussed by Jones et al. (2010), who noted that severe frost affected Tasmanian vineyards in October 2006. In a report to the New Zealand Wine Industry, McArtney et al. (2003) ascribe the low grapevine yields of 2000, 2001 and 2003 in Hawkes Bay directly to frost damage. The 2003 Chardonnay crop was reported to be down by 81% on the previous season (by 6000 tonnes) and so assuming an average price of NZ $1000 per tonne, this represents a $6 million loss in revenue for this one variety alone. In a personal communication with Pernod-Ricard New Zealand in November 2009, Andrew Frost (Research and Development Manager) estimated a loss of 7,000 tonnes of fruit from Hawkes Bay for the 2003 vintage, which equates to 5 million litres of premium wine. Pernod-Ricard provided a further example of the devastation wrought to a single Marlborough vineyard following an October frost in 2003, where the loss of 1000 tonnes of grapes is estimated to have cost the company $5 million in lost revenue. In 2007, New Zealand Winegrowers Chief Executive Officer Philip Gregan told a large audience at a Focus Vineyard Seminar in Marlborough, that a frost that affects just 10% of the country's production of grapes would cost New Zealand over $40 million in lost revenue. He went on to say that "the impact (of frost) can be absolutely massive for the grape grower and devastating for the wine company" (Local Industry Winepress Magazine, November 2007).

In spite of evidence pointing to a warming of mean global temperatures in many areas (*http://www.ipcc.ch/publications_and_data/ar4/wg1/en/tssts-3-1-1.html*), frosts continue to wreak havoc on vineyards. In 2012 alone, significant frost damage was reported in Southern Australia *(http://www.abc.net.au/rural/news/content/201210/s3611856.htm)*, Austria (*http://www.drinksint.com/news/fullstory.php/aid/2995*), the central mid-west of United States (*http://www.winesandvines.com/template.cfm?section=news&content=100413*), France (*http://jimsloire.blogspot.co.nz/2012/04/loire-frost-video-of-damage-in-touraine.html - France April 2012*) and Central Otago in New Zealand (*http://www.odt.co.nz/regions/central-otago/233634/harsh-frosts-could-cost-1000-tonnes-grapes*).There are several possible explanations for this, such as the continued expansion of vineyards into climatically marginal areas, new growers that do not understand the inherent risks associated with a frost or freeze conditions (Stafne 2007), and the manner in which some viticultural locations are responding to larger scale atmospheric circulation patterns (increasing local frost risk) brought about by climate change (Sturman and Quénol 2013).

1.4 Frost mitigation

Frost protection techniques used in agriculture are either active, where action is taken during a frost to modify the micro-climate of the air surrounding the plant, or passive where activities are carried out prior to a frost either on the plant or to the immediate surrounding environment. Three of the more commonly used active frost protection techniques include the use of wind machines, return stack heaters and sprinkler irrigation, and passive frost protection may include the application of sprays to the plant foliage or cutting grass between rows of vines.

During a radiation frost, ground-based inversions occur which are characterized by air temperatures above the canopy being higher than air temperatures within and below the canopy of an orchard or vineyard (Kalma et al. 1992). Wind machines are large 2 or 4 bladed

fans on 10 m towers, with a drive mechanism that rotates the fan assembly around the tower axis, usually once every 5 – 6 minutes. When a temperature inversion is present, the fans mix warmer air from above with colder air near the ground within the vineyard, and in addition provide a drying action to the surface of plants with each consecutive rotation. A large jet of air is produced from the wind machine, directed slightly downward. As the jet moves away from the machine, it slows (through turbulent mixing) and entrains surrounding air (Kalma et al. 1992). While wind machines have been in use since the early 1900's, recent modifications to engines and blades allows modern machines to protect a considerably greater area (up to 7 ha) than earlier models. The area protected by a wind machine is typically uneven and elliptical in shape, reflecting ambient wind drift speed and direction. Protection is greatest closer to the wind machine and decreases at distances further away. Typical capital costs (in 2013) associated with wind machine frost protection in New Zealand are in the order of $9,000 per ha.

Although a variety of heating systems have been used over the decades, the use of the return stack heater provided one of the most popular methods. Despite a decrease in popularity in recent years, they are still in use today on some New Zealand vineyards and orchards and can be seen lined up along property boundaries or spaced intermittently down vineyard rows. Recent hikes in fuel cost, together with tightening of local bylaws in an attempt to reduce air pollution have made alternative methods of frost protection more attractive. By and large, heaters protected the crop by transfer of radiant heat to the plant surface and offered protection to small areas immediately surrounding the heater. Most of the heat is lost very quickly from the heater via the chimney and the high buoyancy provides very little in the way of temperature modification to the surrounding environment.

Sprinkler irrigation is a widely used method of frost mitigation both internationally and in New Zealand. Irrigation on most New Zealand vineyards is carried out from large storage dams, which are recharged from local sources during wetter periods of the year. Sprinkler jets are usually mounted above canopy height and provide either full or intermittent

coverage of water to the crop. The amount of water application must be increased with lower temperatures and irrigation start-up is governed by wet bulb temperature. Protection by overhead sprinkler irrigation is through the continuous release of latent heat when the water (intercepted by the plant) is turned into ice, in such a way that the surface of the ice layer is not allowed to completely freeze (Kalma et al. 1992). In these circumstances, the release of latent heat as water turns to ice will maintain the plant tissue temperature at 0°C.

Passive (indirect) methods of frost protection include cultivation techniques that promote storage of heat in the soil between plant rows, application of sprays that attempt to alter the solute content of the plant prior to frost, methods of pruning, keeping grass and weeds short through and around the orchard or vineyard, and promoting airflow at night by trimming surrounding shelterbelts and trees.

A combination of at least one active and several passive frost protection techniques are employed by many New Zealand vineyards. Active frost mitigation systems installed within the last 10 years are automated and commence operation at a predetermined temperature. A variety of frost alarms and frost lights (that change colour in response to temperature) are also commonly used, together with subscription to one or more local frost forecasting services.

1.5 Minimum temperature prediction in complex terrain

Prediction of cold-air-trapping events in valleys and basins has proven to be one of the most difficult forecasting problems in mountain meteorology (Smith et al. 1997). Banta (2008) stated that suppressed mixing under stable conditions allows smaller scale features to persist, complicating nocturnal air flows. Suppressed vertical mixing facilitates layering so that near-surface observations are not representative of conditions aloft. Ghielmi and Eccel (2006) concluded that many of the best known empirical methods of predicting minimum air temperature have been developed for use in plains and open areas and that their

application in areas of more complex terrain would encounter considerable difficulty. The vast majority of empirical prediction methods appear to have been developed to predict temperatures on a “dusk to dawn” approach, involving rates of cooling in a static atmosphere, assuming highly stable atmospheric conditions, uniform topography and minimal local air mass change through the course of the night.

The use of numerical weather prediction (NWP) models for both general and extreme event forecasting has become common since the 1980’s as improvements in computer power have become available. Published literature on the use of high resolution NWP models for prediction of minimum temperature, in particular frost in complex terrain, is limited. However, several common problems appear to confront the models used for prediction. Cellier (1993) noted that early model simulations used for minimum temperature prediction in complex terrain encountered issues arising from the great variation in local conditions (soil and environment). It appears that early parameterizations of the small scale physical processes were crude, which proved hazardous for prediction of minimum temperatures under stable nocturnal conditions. Hauge (2006) acknowledged that the traditional approach of increasing model resolution to better represent areas of complex terrain has been flawed, as many parameterizations are tuned for coarser scale resolutions, in which case running such models at high resolution is futile. In a study by Chigullapalli and Molders (2008), the Weather Research and Forecasting model (WRF) was applied to the prediction of temperatures during a radiation frost over an area of complex terrain in Alaska. The subsequent poor simulation of temperatures was attributed to the way in which terrain data are represented in the model. It was concluded that accurate representation of terrain elevation and land use is essential to achieving reliable high resolution temperature simulations in complex terrain.

1.6 Wine regions and associated frost risk

The grape growing regions of New Zealand are spread over 10 degrees of latitude and extend from the north of the North Island (35°S) to Central Otago in the southern South Island (45°S) (Figure 1.2). A range of climatic conditions could be expected across these latitudes, including variable risk of frost, enhanced by mountainous and complex terrain. According to Trought et al. (1999) frost is a significant hazard to grape production in many parts of New Zealand. The susceptibility of a vineyard to damage from frost is a function of the grape variety, the susceptibility of the wine region to frost, and the location of the vineyard within the particular wine region.

In Table 1.1, the mean air temperature, the diurnal temperature range, the average number of air (screen) frosts per growing season (October – April inclusive) has been presented for six major wine producing regions in New Zealand. An air (screen) frost is defined as a temperature of 0°C or less, recorded inside an approved solar radiation screen at a height of 1.3 m above the ground. Although a trend is evident toward warmer mean temperatures and fewer frosts in the north and a greater incidence of frost further south, the trend is not linear. Complex terrain that surrounds most of New Zealand's grape growing areas produces regional peculiarities that predispose a region to a particular range of temperatures, including frost during certain synoptic weather conditions. The effect is further enhanced on a local scale by the interaction of daily weather and local terrain. For example, the grape growing region of Central Otago has the greatest diurnal temperature range but also the highest incidence of spring frost. Generally, grapes grown in New Zealand are susceptible to frost from mid-September until the end of April, although the risk of frost during the summer months of December, January and February is very low.

Marlborough is classified as a cool climate growing region for grapes, based on grapevine climate/maturity groupings, according to Jones (2003). Marlborough has a mean temperature through the growing season (October – April) of 15.2°C, a mean diurnal

temperature range of 11.2°C and can expect an average of 3.0 air frosts during the two spring months of October and November.

Based on the mean temperature through the growing season, Marlborough is very similar to the grape growing areas of Champagne, France (14.5°C), the middle Rhine Valley, Germany (14.9°C) and Pendalton, North Oregon (15.2°), although the differences in latitude and proximity to the coast produce dissimilar temperature distributions, as well as the frequency of spring frost. The mean diurnal temperature ranges of 10.5°C in Champagne, 9.0°C in the Rhine Valley, and 13.0°C in North Oregon, show an association with the average number of spring frost events at these locations. Champagne can expect an average of 3.0 frost events each spring, Rhine Valley 2.6 and North Oregon 4.5.

Table 1.1 *Mean air temperature, diurnal range and average number of air frosts, per growing season* (*Source: http://cliflo.niwa.co.nz*)

Wine growing region	Mean temp °C	Diurnal range °C	Ave No. frosts / growing season	Latitude °
Gisborne	16.5	10.9	0.8	38.4
Hawkes Bay	16.7	10.6	1.2	39.4
Wairarapa	15.0	12.2	5.8	41.1
Marlborough	15.2	11.2	6.1	41.3
Canterbury (Waipara)	15.0	11.6	4.2	43.0
Central Otago	14.7	13.0	15.0	45.0

The response of each of these regions to climate change scenarios cannot be accurately predicted, although the effects of recent climate trends on several grape growing regions around the world were discussed by Jones (2003). The effects of recent climate trends on frost for selected northern hemisphere vineyards, show fewer frosts with the median date of the last frost occurring earlier in the growing season. The effects of climate change on temperatures in Marlborough have been reviewed by Sturman and Quenol (2013). Marlborough does not follow the warming trends evident in many northern hemisphere grape growing regions and the average number of frost days (per annum) appears to be

increasing. Frost occurrence in Marlborough is more strongly associated with circulation patterns, in particular the frequency of northerly and southerly airflows. Sturman and Quenol (2013) have shown that an increase in southerly airflow over New Zealand since 1958, is associated with an increase in frost incidence in some regions such as Marlborough.

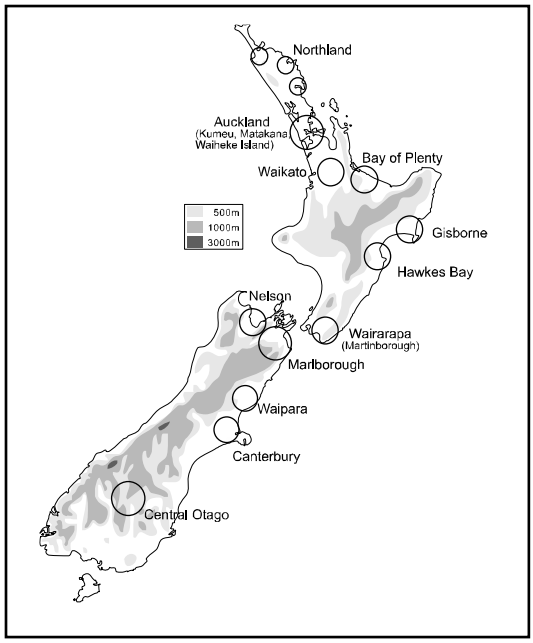

Figure 1.2 *The wine-producing regions of New Zealand (from Sturman and Quénol 2013).*

1.7 Predicting frost in New Zealand

Snyder (2005) stated that accurate frost forecasting can potentially reduce frost damage because it provides growers with the opportunity to prepare for an impending frost event. While daily minimum temperatures are predicted for major towns and cities in New Zealand by MetService, the complex terrain that surrounds many of New Zealand's viticulture regions can lead to large discrepancies between predicted minimum temperatures and those that are observed at the very local scale. Trought et al. (1999) suggested that it is possible to establish long-term temperature relationships between major towns and other points of interest, although earlier research by Laughlin and Kalma (1987) acknowledged

that the regression procedure becomes unreliable in areas of more complex terrain. This is likely to be a result of the ventilation and stagnation of near-surface airflow which can greatly influence near-surface temperature.

1.7.1 Private weather forecasting services

It is not clear when the earliest private weather forecasts commenced. However, their survival is governed by the demand from end-users that have specific forecast requirements not covered by public forecasting agencies. Brooks et al. (1996) suggested that as long as public sector forecasting agencies continue to produce forecasts of basic weather elements based almost entirely on numerical weather prediction output, the private sector will be able to package that output and provide detailed, tailored forecasts for specific users that either improve upon the NWP products or make it easier for users to interpret. They concluded by acknowledging that future sales of private forecasts will depend heavily upon the ability to demonstrate the economic benefit of the forecasts, so that verification of weather forecasts will be an important issue.

At present, three private forecasting enterprises operate in New Zealand and provide minimum temperature predictions to the wine industry. The private forecasters may operate NWP models such as the Weather and Research Forecasting (WRF) model to predict local near-surface climate variables such as wind and near-surface temperature, and modify these predictions based on knowledge of local climate and terrain interactions. The private forecasts are subscription based and uptake by the local wine industry is high. It is not uncommon for corporate wineries to subscribe to more than one forecasting service and then call for additional commentary when discrepancies between forecasts arise.

1.8 Impetus for research

The impetus for this research has its genesis in the early 2000's resulting from commercial experience working for the New Zealand wine industry on matters concerning frost protection. The succession of particularly frosty spring seasons of 2002, 2003 and 2004 caught many grape growers by surprise, costing the wine industry millions of dollars in lost revenue. A severe and unpredicted frost that caused considerable damage to Marlborough vineyards in April 2005 prompted the commercialization of one frost forecasting service. The central problem was that until this time, forecasts only provided one indication of minimum temperature for central Blenheim. The regional variation around this prediction would regularly exceed 5°C and the variation would change from one night to the next, as a function of the synoptic situation. The circumstances would leave vineyard managers guessing as to whether to take precautions against an impending prediction for cold temperatures, which would frequently result in frost damage to the some of the regions vines.

Until the commencement of local frost forecasting in 2005, little was known locally about the physical processes that were causing variations of near-surface minimum temperature and, the variation in occurrence of frost around the grape growing areas of Marlborough. It was realized, however, that an improved understanding of these physical processes, in particular the interaction of meteorology with local topography, would benefit the rapidly expanding grape industry by providing area-specific information of an impending frost. Improvements in frost forecasting create an opportunity for grape growers to better prepare for an impending event. Output from this research will directly benefit grape growers by providing improved capacity for frost prediction to the local industry. Furthermore, many of the findings will be applicable to similar areas of complex terrain around the world.

The following chapters of this PhD thesis will explore relationships between synoptic climatology represented by the Kidson classification scheme, local surface-based meteorological observations and spatial variations of minimum near-surface temperature. It is important to emphasis here an association between the incidence of frost in complex terrain, and a large spatial variation of near-surface minimum temperature. A study of vineyard frost in Marlborough cannot be achieved without investigating the role of meteorological processes in creating the large spatial variation of near-surface minimum temperature, which at times results in frost.

This is followed by the application of state-of-the-art NWP models that are used as heuristic tools to examine area-specific meteorological relationships that account for regional variation in minimum temperature. Finally, data from deployment of the University of Canterbury SODAR is used to study the vertical structure of the lower nocturnal boundary layer (NBL) in a range of stable boundary-layer (SBL) conditions.

1.9 Research aims and objectives

While the broader aim of this research is to account for the evolution of near-surface minimum temperature in complex terrain, three research objectives have been identified and these will be explored in subsequent chapters. The research objectives are:

1. ***To identify relationships between synoptic scale weather systems and variations in near-surface minimum temperature.*** *Are there broad relationships between synoptic scale weather systems, the spatial variation of near-surface temperature and the occurrence of frost? Are these relationships supported by local observations from automatic weather stations (AWS)?*

2. ***To explore the relationship between mesoscale airflow, as represented by ridge-top winds, and spatial variation of near-surface temperatures using numerical***

weather prediction models. *What do the models reveal to us about the occurrence of local meteorological processes that create the variations of near-surface temperature? How well do the models predict the local variations of near-surface wind velocity and minimum temperature in complex terrain?*

3. ***To investigate the relationship between the vertical structure of the atmosphere within the Awatere and Wairau Valleys of Marlborough's vineyard regions and near-surface temperature variations.*** *Can the University of Canterbury SODAR (SOund Detection and Ranging) identify meteorological processes such as the development of LLJ's and determine a mechanism by which they influence near-surface temperatures?*

1.10 Thesis structure

This chapter has provided a general background on the incidence and world-wide importance of improving the prediction of frost. The research theme is crucial to high value cropping in areas of complex terrain. The thesis adopts a structure that sequentially addresses each of the research objectives, but with a particular focus on an exploration of the spatial variation of near-surface minimum temperature. Chapter 2 will provide background to the research by way of a literature review. It addresses what we know about cooling of near-surface air in a valley system by describing how the atmospheric boundary layer works in complex terrain, with a particular focus on how and why cold air becomes trapped. It concludes by outlining the international significance of this research, and specifically how it is expected to extend knowledge of minimum temperature prediction. Chapter 3 introduces the methodology for the research. It describes the research area and the rational for its study, data collection techniques, and the existing status of minimum temperature prediction in the Marlborough region. This is followed by an overview of the region's climate in Chapter 4 using nine AWS to represent climate of Marlborough's grape growing region, particularly the local incidence of frost. The first set of results is presented

in Chapter 5, following an analysis of the synoptic climatology using Kidson weather types, in conjunction with local surface-based climate observations and near-surface minimum temperature. In the second results chapter (Chapter 6), two NWP models are used to explore relationships between ridge-top wind velocity and near-surface minimum temperature. The models' ability to capture sub-regional variations in meteorology and portray the spatial extent of surface-based climate variations is of primary interest. The third results chapter (Chapter 7) examines the vertical structure of the lower NBL using data obtained from the University of Canterbury SODAR. Data from the SODAR are used to investigate meteorological processes and identify the key mechanisms that influence near-surface minimum temperature. Further analysis then illustrates the role of LLJ's for mixing warmer air downward to the surface in light ambient wind conditions. The final chapter of the thesis (Chapter 8) presents a short summary of results, including their implications, as well as suggestions for further study.

1.11 Summary

This introductory chapter outlines the international and national importance of frost prediction and protection. The association between frost and a large spatial variation of near-surface minimum temperature in complex terrain has directed the research towards an examination of local scale meteorological processes. Frost damage to food crops, including vineyards, continues to cause widespread losses every year. The problem is exacerbated by greater demands for food and beverages, as production is expanded into increasingly climatically marginal areas. While findings from this research will be directly applicable to the grape growing areas of New Zealand, they are also expected to be applicable to many agricultural areas in close proximity to complex terrain around the world.

Chapter 2 Formation of cold air in complex terrain

2.1 Introduction

Nocturnal cooling of near-surface air during radiative cooling events is generally well understood and predictable for flat terrain (Cellier 1982). However, the physical processes affecting near-surface temperatures in complex terrain, such as the effects from thermally driven wind regimes, varies from valley to valley and from time to time in the same valley, and even from segment to segment along a valley's length (Whiteman 1990, Zardi and Whiteman 2012). While the major causes of significant horizontal temperature differences in undulating or dissected terrain can be identified, defining the relative importance of each remains a challenge. Smith et al. (1977) stated that the prediction of cold-air trapping events in valleys and basins has proven to be one of the most difficult forecasting problems in mountain meteorology.

In this chapter, the general principles of cold air formation in valleys are reviewed, commencing with present day understandings of cooling of the ground surface, the lower atmosphere, and the role of radiational cooling with respect to basic surface energy budget principles. Following this, a discussion of mesoscale processes that can affect, or occur as a result of, cooling of the near-surface environment will be introduced. This discussion will describe many effects of topography, including sheltering, ventilation, katabatic winds, cold air drainage flows, and development of LLJ's. The focus of the chapter will then move on to the importance of empirical and NWP modelling; in particular, what modelling attempts have revealed to us about the mechanisms of cooling and how they have refined data collection campaigns over a number of years. Finally, the chapter will conclude with a discussion of the way in which results from this research are intended to build upon what we know about spatial variation of minimum temperature in complex terrain.

While much of the material covered by this review provides a sound foundation for this research, it is realised that the terrain surrounding Marlborough's high-value agricultural lands presents a number of differences from landscapes described by international research, and so the significance of some cooling mechanisms may differ from those described elsewhere. For example, Sturman and Quenol (2013) have shown that frost risk to the Marlborough region during spring is associated with several atmospheric circulation factors including the Southern Oscillation Index (SOI), but that it is more closely linked to an M1 index which describes the predominance of either northerly or southerly airflow. While there is significant inter-annual variation, there has been a general increase in spring frost risk to the Marlborough region since 1958, reflecting an increase in the M1 index and southerly airflows.

2.2 The surface energy budget

Air temperature is a gauge of the thermal energy content of the atmosphere and is related to the fundamental energy of the Earth-atmosphere system (Oke 1988). Temperature change near the surface is a response to an energy flow process, with the amount of temperature change determined by what goes on inside the Earth-atmosphere system. The temperature, for example, is a function of the system's physical properties, such as its ability to absorb, transmit, reflect, or emit radiation, as well as conduct, convect and store energy (heat). Horizontal temperature variations in the Earth-atmosphere system give rise to horizontal pressure differences which result in wind. In this manner, thermal energy from the solar energy cycle is converted into kinetic energy of wind systems. The energy is then in a kinetic energy cascade involving the transfer of energy to increasingly small scales of motion by turbulence and eventually heat (Oke 1988).

For most situations, the net all-wave radiation (Q*) is the primary component of heat exchange as it represents the total available energy source or sink. It is also the basic input to the surface energy balance. Q* is usually positive during the day when the net short-

wave (solar) input generally exceeds the net long-wave (terrestrial radiative) loss, and negative at night in the absence of solar radiation. At any given time, and in accordance with the principle of conservation of energy, the surface radiative surplus or deficit is balanced by a combination of convective exchanges to or from the atmosphere as sensible (Q_H) or latent (Q_E) heat, and by conduction to or from the underlying substrate as soil heat flux (Q_G). In this respect, the complete energy balance for a system is $Q^* = Q_H + Q_E + Q_G$ and is encapsulated by Figure 2.1 (Oke 1987). As the focus of this study is on the formation of cold air at night, the mechanisms associated with heat loss are of primary interest.

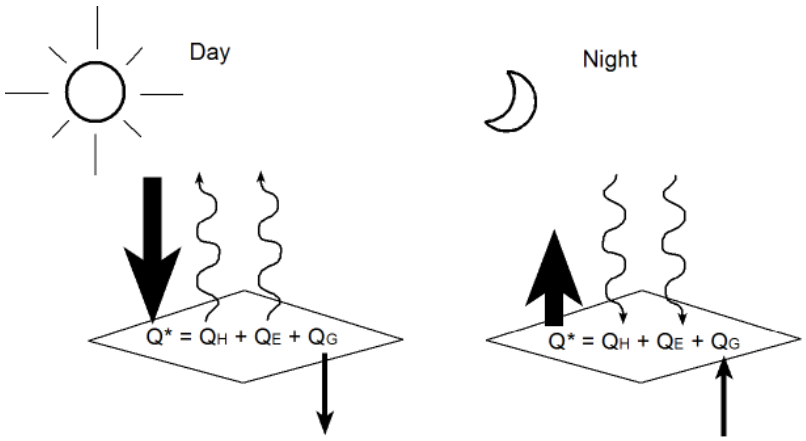

Figure 2.1 *Surface energy fluxes by day and by night (Oke 1987)*

At night, excess heat is radiated back to space as longwave radiation. The amount of radiation emitted by the Earth is governed by the temperature of the surface and its relative radiating power (emissivity). The Earth, however, also receives radiation back from the atmosphere (counter-radiation) which is a function of the atmosphere's temperature and emissivity (Kalma et al. 1992). The emissivity of the atmosphere is highly variable in time and space and is related to the amounts of water vapour, carbon dioxide and other gases that it contains.

The accepted view is that air cools primarily because of its proximity to the radiating (and therefore cooling) Earth's surface. It then cools from the bottom up, by transferring heat to the surface by convection and to a much lesser extent conduction. On a clear calm night, the sensible heat flux (Q_H) depends on the temperature difference between the surface and the air and on the degree of atmospheric turbulence, which then depends on atmospheric stability, wind speed and surface roughness (Kalma et al. 1992). On a still clear night, radiative loss from the Earth's surface is replaced inefficiently, so that both surface and adjacent air layers cool to a greater extent as convective (and turbulent) heat transfer from above is reduced.

2.2.1 Cooling of the ground surface

Many early attempts at predicting atmospheric cooling were based upon the surface energy balance equation, as described previously in this section by $Q^* = Q_H + Q_E + Q_G$. The relative success of this approach depended on the relationship between the temperature of the surface and that of the atmosphere at some given height. The equation assumes no horizontal advection into or from the system and that heat exchange by thermal radiation is independent of Q_H (Kalma et al. 1992). The soil (or ground) heat flux Q_G is a function of the thermal conductivity of the soil, which is influenced by soil moisture and other characteristics of the soil, such as porosity and thermal conductivity. When thermal conductivity is considered in conjunction with a soil's volumetric heat capacity, its rate of heating and cooling can be determined. This value, however, changes markedly both spatially and temporally with changes in soil moisture content. The latent heat term Q_E is often considered to be small at night but, although difficult to measure accurately, can have a profound influence on minimum temperature by way of dew condensation, frost formation and modern water irrigation frost protection systems (Kalma et al. 1992).

Surface soil temperatures are closely linked with the surface energy balance and are a function of rates of energy exchange between the atmosphere and the underlying soil. An

experiment by Cremer and Leuning (1985) found that temperatures in dry soils continued to decline through the night, reaching values at dawn several degrees lower than for moist soils at the same depth. This occurred because of the greater volumetric heat capacity and thermal conductivity of the wet soil. The effect of wet soils after rain on delaying the rate of decrease of near-surface temperature in the Marlborough region has been observed on numerous occasions. These observations are supported by studies such as Connell and Snyder (1989), who concluded that up to a 1.7°C increase in air temperature was measured (at an unspecified height above the ground) within the irrigated area during a radiation frost when a 16.5 m^2 was continually saturated with water at 4.4 mm per hour.

2.2.2 Cooling of the lower atmosphere

Early researchers, such as Funk (1960), examined the cooling of a column of air between two vertical coordinates. He found that the actual cooling rate was due to the divergence of both the net longwave radiation and turbulent heat transfer to the Earth's surface. Funk's findings implied that air may cool at night by radiating more at the top (of the air column) than the bottom (divergence of the radiation flux). He found that the calculated values of the radiative cooling rate between the vertical coordinates exceeded what was observed, which implied that the turbulent heat flux offsets otherwise larger amounts of cooling that would take place from unhindered radiative heat flux divergence.

Later work by Kondo et al. (1978) found that under stable conditions, turbulent heat flux directed toward the surface (implying surface heating and air cooling) dominated the cooling of the near-surface layer up to a height of about 10 m. Above 10 m radiative flux divergence dominated the cooling of the air column. It was observed that the cooling rate approximated the sum of the radiative and turbulent cooling rates.

Andre and Mahrt (1982) confirmed the earlier findings of Kondo et al. (1978) that cooling due to divergence of sensible heat flux is confined to the lower part of the surface inversion

layer. Cooling due to radiative cooling extended to several times the height of the turbulent cooling and acts to deepen the inversion layer through the night. While the shallow turbulent layer remained constant during the night, it may vary widely from one night to the next. Their work reinforced the notion that surface (energy budget) observations alone accounted for less than 25% of the variation in nocturnal boundary layer (NBL) height, and furthermore that near-surface air temperatures could not be predicted satisfactorily from only surface energy balance considerations. Kalma et al. (1992) suggested that observed atmospheric cooling rates are the result of interactions between turbulent heat flux divergence and radiative heat divergence.

2.3 The effects of topography

According to Whiteman (1990), Wagner (1932) first conceived the idea of a Topographical Amplification Factor (TAF), which describes the tendency of a reduced volume of a valley atmosphere to heat up and cool down more quickly than the atmosphere over an adjacent plain. The ideas have been reworked by Neininger (1982) and Steinacker (1984) to account for more realistic topographical shapes. McKee and O'Neal (1989) made further contributions by calculating TAF ratios along several valleys in Colorado and discovered that it was possible to determine whether cold air would stagnate and pool in one or more segments of a valley. Whiteman (1990) then suggested, however, that the influence of the TAF on thermal structure of a valley may be strengthened or weakened by other physical processes.

The ideas supporting cooling processes in valleys were also refined by studies examining the direct sheltering effects of topography. One such study by Thompson (1986) investigated the formation of cold air pools within complex topography of the Niagara peninsula, near lake Ontario, Canada. He was most interested in attributing the initial formation of a cold layer within a topographical hollow to a process he called skin flow, consisting of a very shallow layer of cold air moving down slope into a topographical depression. He found that

on over half the cases studied, skin flow did not occur and that the initial development of cold air formation was due to the early diminution of turbulent heat transfer within sheltered locations. He concluded that katabatic flow only ensued after a surficial cold air mass had become established in the bottom of a valley. Results from this study were extended by Hunt et al. (2007) in which researchers investigated the rapid near-surface cooling and associated strong inversion development shortly after sunset at the El Reno Oklahoma Mesonet. Authors of the study suggested that the rapid formation of very strong inversions within an inversion sub-layer was the result of radiational cooling, as turbulent exchange of energy with the surface is suppressed. The air within the overall inversion layer cooled as a result of conduction (with the ground surface) and weak convective or shear-induced mixing until sunrise. The strongest temperature gradients occurred when the wind profile was very weak. The cooling process was further accentuated during clear sky, dry atmospheric conditions, promoting large longwave losses of radiation.

The amount of incoming longwave and diffuse radiation received on a surface depends on the fraction of the sky visible in the viewing hemisphere of the surface, and is called the sky view factor (Whiteman 1990). According to Whiteman, this causes complicated spatial variation in the downward longwave and diffuse solar radiation components. Locations with higher sky view factors (such as upper valley side walls and ridge tops) are exposed to the cold radiating sky and receive smaller downward longwave radiative fluxes. For this reason they are thought to be more effective generators of cold air at night than areas on lower slopes and in the centre of a deep valley. The sky view factor is also affected more locally by buildings and trees. Proximity to these structures can offset surface longwave radiation from larger areas and cause significant variations in near-surface temperature over short distances.

Finally, in a recent study by Smith et al. (2010) a series of surveys carried out using an instrumented vehicle in the south-west of England during clear calm nights, revealed that the cooling of air within moderate valleys (where valley depth is generally < 100 m) was the

result of topographic sheltering, which reduces the turbulent flux of heat down from aloft. Valleys that recorded the largest amounts of cooling were those that became fully decoupled, allowing the near-surface air to cool rapidly in response to surface longwave radiative cooling.

In a range of studies detailing nocturnal cooling processes, the primary mechanisms appear to include cold air drainage (Thompson 1986; Gudiksen et al. 1992; Kondo 1995), katabatic flow (Thompson 1986; Sturman et al. 1985; Whiteman and Zhong 2008), and in situ cooling (Thompson 1086; Gustavsson et al. 1998; Clements et al. 2003), although the larger scale development of mountain winds should also be considered (Manins and Sawford 1979; Whiteman 1990). These processes are of mesoscale origin and will be reviewed in the following section with respect to their effects on cooling of valleys. Depending on the synoptic situation they may each play a dominant role in cooling the lower atmosphere and affect near-surface temperatures of the Marlborough region.

2.4 Mesoscale effects

In this section a number of processes are described that account for different cooling rates within the same valley and between adjacent valleys in the same region on the same night. A clear understanding of these processes is vital for subsequent data interpretation from the Marlborough region.

2.4.1 Katabatic flow, cold air drainage and mountain winds

For the purposes of this review, katabatic flow, cold air drainage and mountain winds have been categorised together, for all of these processes provide mechanisms for transporting air within a valley during cooling regimes. For the purposes of this research, a katabatic flow is assumed to transport the least amount of air within a valley, while mountain winds entrain a significantly greater volume of air.

Katabatic flow has been extensively addressed in the literature over many decades (Oke 1988; Doesken et al. 1989; Stone and Hoard 1989; Kalma et al. 1992, Barry 1992, Gudiksen et al. 1992; Poulos 1996; Shapiro and Fedorovich 2007; Poulos and Zhong 2008). Barry (2008) defined a katabatic wind as a local scale down-slope gravity flow caused by radiative nocturnal cooling of the surface under light wind, clear sky conditions. The term "down-slope flows" is used by Whiteman and Zhong (2008) to collectively describe winds of katabatic origin, other thermally driven flows such as down-valley flows and combinations of down-slope and down-valley winds.

While katabatic flow is still regarded as an important mechanism for the transport of cool air from valley side walls to the centre of the valley, earlier work by Gustavsson et al. (1998) and more recent studies by Bodine et al. (2009) have shown that katabatic flow may also contribute warmer air to a cold pool and, in fact, significantly limit further cooling from a valley system. The process by which this occurs was described in a study by Shapiro and Fedorovich (2008), who concluded that when a sloping surface is cooled, the temperature difference between the air closest to the ground and the free-air at the same elevation induces a down-slope (katabatic) flow. However, this process does not require that the along-slope temperature gradient be positive or negative and so both along-slope warm- and cold-air advection are consistent with katabatic flows. In the case of valley cooling, the contribution of katabatic flow to the formation of a near-surface cold pool may vary as the night progresses. Initial contributions to cooling early in the evening may be significant if the valley floor is warmer than the valley side-walls. As the valley floor cools and a cold pool develops, in situ cooling becomes the dominant cooling process, and contributions of air from a katabatic origin become less significant, as the now, relatively warmer katabatic air is less likely to penetrate into the cold pool. In cases, however, where katabatic flows or other drainage winds become strong enough, they may penetrate the valley cold pool and mix relatively warmer air from surrounding slopes to the valley floor. This process is of great

interest to this research, where at times, local observations have shown a reduced rate of cooling, or even warming of the near-surface air, following the onset of katabatic flow.

The process is summarised in a schematic illustration (Figure 2.2), modified after Fernando (2010), who proposed a mechanism for cold air filling a valley by entrainment. As a cold pool develops, further contributions of air from the katabatic flow begin to peel away from the valley side-walls and disperse into the stable valley atmosphere.

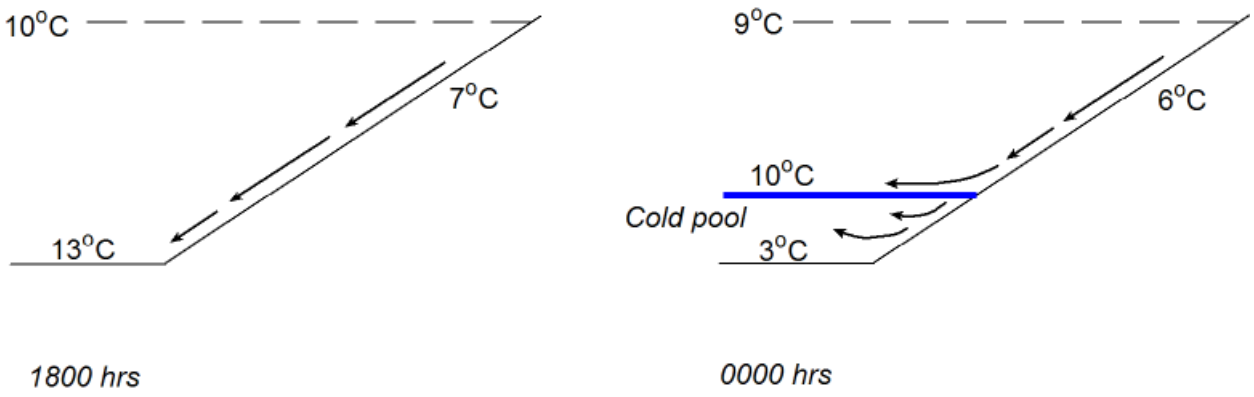

Figure 2.2 *The process of cooling within a valley, modified from Fernando (2010). At 1800 hrs katabatic flow from valley side-walls is the dominant cooling process within the valley. By midnight, katabatic flows become less significant to the development of the cold cool and flows peel away from the valley side-walls and inject into the stable valley atmosphere.*

Drainage winds are defined by Sturman (1987) as "downslope flow more extensive than a simple katabatic wind and 'which may derive some of its volume from adjacent slopes and higher terrain' (Garrett, 1983, 1979)". It therefore describes a downslope flow of intermediate scale between a katabatic flow and a mountain wind, although no specific range of wind velocities are mentioned. While drainage winds have been described by numerous researchers (Gudiksen et al. 1992; Kondo 1995; Mahrt et al. 2001; Soler et al. 2002), they are expected to play a major role in shaping the spatial variation of nocturnal near-surface temperatures around Marlborough.

Mountain winds are both local and regional scale phenomena that form in response to nocturnal along-valley pressure gradients as a result of different rates of cooling brought about by the topographic amplification factor. Mountain winds have been observed extensively in alpine areas, with specific New Zealand examples detailed in McGowan and Sturman (1996) and Sturman et al. (2003). In the Lake Tekapo Experiment (LTEX) mountain winds were observed using pilot balloon and free-flight radiosonde ascents. Mountain wind depths ranged from 200 - 1000 m, about 200 m short of the ridge tops surrounding the Godley Valley, near Lake Tekapo, South Island, New Zealand. Barr and Orgill (1989) suggested that mountain wind depths of this nature are common as under 'ideal conditions' a mountain wind may grow in depth to fill the volume of an entire valley.

2.4.2 Ventilation and stagnation

The degree of ventilation or stagnation has significant effects on near-surface air temperatures. In the case of ventilation, losses of thermal energy from the Earth's surface and near-surface air layers are readily replaced from above. During stagnation, strong positive vertical temperature gradients develop in the air layers near the ground forming an inversion. The inversion layer represents the vertical extent of cooling due to turbulent and radiative heat fluxes. Coolest temperatures are observed nearest the surface and increase with height, to the top of the inversion layer, known as an inversion cap. In these situations, much of the energy lost by the radiating ground surface is replaced by the transfer of sensible heat from the near-surface air, which therefore decreases in temperature (Kalma et al. 1992). Stagnation occurs when buoyancy forces associated with stably stratified air exceed inertial forces of an overlying crosswind.

The Froude number represents the ratio of the natural wavelength of the air to the wavelength of a mountain barrier (Sturman and Tapper 1996). It has important implications for determining the theoretical atmospheric conditions required to cause ventilation or

stagnation of a valley, with respect to wind speed at ridge height, valley depth and/or width of the mountain barrier. The Froude number is expressed as:

$Fr = \pi \frac{U}{Nx}$

where U = horizontal wind speed

x = width of the mountain barrier

$N = \left[\frac{g}{\Theta}\frac{d\Theta}{dz}\right]^{0.5}$ (the Brunt – Vaisala frequency).

The Brunt – Vaisala frequency represents a stability factor which helps to determine the natural wavelength of oscillation of the air if it is disturbed (Sturman and Tapper 1996).

While Snyder et al. (1985) found that *Fr* is linearly related to the height of the stagnant air layer, Manins and Sawford (1982) suggested that the critical Froude number (required to produce ventilation) is more variable and reflects the subjectivity in determining the "controlling "ridge height in complex terrain, particularly when there may be a number of parallel ridges. In addition, if wind direction on adjacent ridge tops changes through the night, then this alters the apparent height of the barrier, as it may in fact change the controlling ridge to an adjacent ridge further away from the valley floor. The effect of katabatic wind and cold air accumulation may also contribute to enhance stagnation in a valley. The potential energy required to ventilate an accumulation of cold air near the bottom of a valley, will be considerably greater than would be required if no accumulation of cold air were present. In such cases, the "critical" Froude number would be larger than a theoretical value.

There are a number of occasions when a theoretical calculation of the critical Froude number required to ventilate parts of the Marlborough region under stable atmospheric conditions would be under-predicted. Firstly, the accumulation of cold air in the slightly concave-shaped lower Wairau Valley floor (near Fairhall) has been observed to persist, in spite of remarkably strong winds (15 m s^{-1}) on surrounding ridge tops. Secondly, predicted

ventilation (based on *Fr*) of other areas that are subject to strong cold-air drainage, such the upper Awatere Valley and parts of the Waihopai Valley may also be under-predicted. In these cases higher values of *Fr* (in association with stronger ridge top wind speeds) are required to ventilate these regions during frost conditions.

Much lower Froude numbers (0.2) in association with very stable conditions and light or moderate ridge top winds are believed to affect the incidence of frost in parts of the Southern Valleys region of Marlborough. During light to moderate north-westerly synoptic winds, some airflow is blocked near the base of the upwind side of the Wither Hills, while remaining airflow is believed to flow around and over the hills. The phenomenon is supported by local observations of wind speed and temperature, where the Automatic Weather Station (AWS) in the lower Awatere Valley at Seddon can record higher wind speeds than the ridge top AWS, on top of the Wither Hills. The light to moderate north-westerly wind is channelled around the north-eastern base of the Wither Hills and through several low passes between the Wairau and Awatere Valley of 2 – 300 m in elevation. The simultaneous occurrence of upwind blocking has been observed to cause local stagnation of air, and has resulted in frost. The phenomenon is illustrated by the schematic diagram in Figure 2.3.

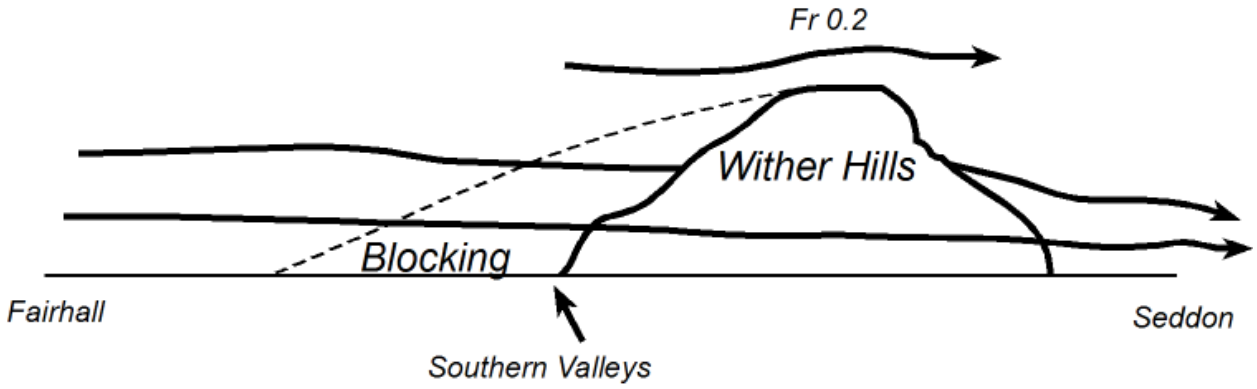

Figure 2.3 *Up wind blocking and acceleration of airflow associated with light to moderate north-westerly winds during very stable conditions and low Froude numbers (~0.2) over the Wither Hills, near Blenheim, Marlborough.*

An important mechanism of cooling during stagnation is in situ cooling. It occurs when air near the surface does not mix with the surrounding air and can be associated with wind obstructions, such as hills and trees. The obstructions block the wind and can aid in the creation of large horizontal temperature gradients if skies are clear (Hunt et al. 2007). Cooler air forms more readily either behind, or within the shelter provided by the obstruction, relative to adjacent areas that are exposed to mixing from prevailing airflows. Thompson (1986) verified that in situ cooling begins and is most intense immediately after sunset and is associated with the rapid formation of cold pools in the absence of measurable cold air drainage. In valleys, Gustavsson et al. (1998) found that the greatest cooling often occurred during the first two hours after sunset and that the cooling rate slowed for the remainder of the night. Edwards (2009) used an idealised model to study the interaction between radiation and turbulence in the stable boundary layer, with a focus on the surface layer after the evening transition period. It was concluded that radiational cooling is less significant within the developed stable boundary layer than during the evening transition.

A good example of in situ cooling is provided by Clements et al. (2003), in which the evolution and structure of a cold air pool is investigated in the Peter Sinks limestone sinkhole in Utah. The study demonstrated that under ideal clear settled conditions, light katabatic flows were initially recorded, but that they became detached from the valley side-walls, and ran out over the basin centre on top of a shallow stable layer above the basin floor (Figure 2.2). The flows ceased 2 hours after sunset, yet air temperatures between 0.1 and 10 m continued to cool until sunrise. The authors concluded that the cold-pool build up within the basin did not fit the conceptual model of cold pool formation in valleys and basins, in which a cold pool deepens as cold air running down the side-walls converges within the pool. Down-slope flows played a minor role in the formation of the atmospheric structure and the observed continuation of cooling after the cessation of katabataic flows were attributed to turbulent sensible heat flux divergence and then radiative flux divergence.

2.4.3 Interactions between ambient meteorology and thermally-induced wind flow

Many observational studies in the recent past have described the interactions of ambient meteorology with local thermally-induced wind flow. One of the key acknowledgements common to most studies is that local, thermodynamically driven wind systems are seldom completely decoupled from the ambient atmosphere above the ridge tops. The following brief overview presents a summary of findings from related research of the past few decades.

Some early investigations by Nappo and Snodgrass (1981) identified effects of ambient winds on nocturnal drainage winds in the Anderson Creek Valley, as part of the Atmospheric Studies in Complex Terrain (ASCOT) research programme. They observed the increased thickness of drainage winds within the valley as ambient wind speeds decreased. Local research by Sturman et al. (1985) on airflow regimes in the Chilton Valley determined the presence of an intermediate layer between underlying katabatic flow and gradient winds above. The structure of the intermediate layer was found to respond to variations in gradient wind velocity. Following the ASCOT experiments, Barr and Orgill (1989) demonstrated the presence of a "dynamically active" transition layer that varied in time and space. While they stopped short of describing the influence that a transition layer might have on near-surface temperatures, they acknowledged that it has important implications for local and regional transport and diffusion of pollution. They concluded by suggesting a number of mechanisms for the coupling of underlying drainage winds to synoptically governed winds, such as evidence of stationary and travelling internal buoyancy waves, small scale dynamical turbulent mixing and mechanically-induced cross-valley eddies, all of which are supported in later work by Banta et al. (2004). Further related literature as a result of the ASCOT programme includes that of Gudiksen et al. (1992) and Orgill et al. (1992), while later investigations by Poulos et al. (2000) reworked ASCOT data using a

Froude number climatology to determine the influence of mountain waves on katabatic wind formation.

Sturman et al. (2003) examined the interactions of synoptic meteorology and thermal regimes in the Lake Tekapo Basin, South Island, New Zealand. Data were collected over two field campaigns in 1997 and 1999 using a variety of techniques including SODAR, pilot balloon soundings and light aircraft to investigate the contribution of surface heat fluxes, the effects of localised heating and cooling, and advective processes on atmospheric boundary layer development. The presence of katabatic flows and mountain winds with a down-valley jet structure were observed during clear, settled weather over several special observation periods, followed by their interaction and eventual termination by dynamic channelling of gradient winds into the valley.

Down-valley flows with a LLJ structure have also been observed by other researchers, such as Kraus et al. (1985) during PUKK (Projekt zur Untersuchung des Kusten-Klimas or project for the investigation of the coastal climate) and Banta et al. (2004) in the Great Salt Lake Basin, Utah, as part of the Vertical Transport and Mixing (VTMX) field campaign. The down-valley jet observed during VTMX was a feature connecting a complex string of basins that drained toward the Great Salt Lake. The timing of the down-valley jet development was found to be influenced by synoptic pressure gradients over the region. Pinto et al. (2006) also described the mixing processes of warmer air from beneath the down-valley jet by analysis of data from a SODAR, collected during VTMX.

In a thorough review of observations of katabatic winds by Poulos and Zhong (2008), they acknowledged much earlier work by Cornfield (1938) that recognised the influence of ambient winds on the development of katabatic flows. It was suggested that an opposing wind to the katabatic flow in the lee of a hill would create a calm zone on the hillside, where, without ambient winds, a katabatic flow would otherwise develop. It is unclear

whether such observations present a grounding of the transition zone or a combination of topographic sheltering and decoupling of the synoptic flow.

Finally, Schmidli et al. (2009) investigated the evolution of nocturnal flows in the Owens Valley, California, as part of the Terrain-Induced Rotor Experiment (T-REX). While further evidence was presented that supports earlier findings on the relationship between drainage flows and meteorology above surrounding ridge tops, the Advanced Regional Prediction System (ARPS) model was used to replicate observations and demonstrate the interactions of opposing flow at different heights within the valley to produce a resultant surface flow on any one given night.

2.5 A summary of relevant field campaigns

Several large scale cooperative atmospheric research campaigns relevant to this research have been undertaken over the past few decades. Each of these campaigns has produced numerous publications on cooling processes in valleys, the formation and structure of thermal wind regimes, as well as interactions of thermal wind regimes with ambient meteorology. In addition, the larger scale campaigns were generally combined with numerical modelling efforts. Zardi and Whiteman (2012) suggested that much confidence is gained when comprehensive field observations are available for comparison with model results, so that simulations are usually done in conjunction with large observational programmes.

The Atmospheric Studies in Complex Terrain (ASCOT) programme was initiated in 1981 to investigate the role of local winds in the dispersion of pollutants, particularly at night, and was centred on the complex terrain of Brush Creek in Western Colorado (Gudiksen 1989). One objective of the research was to relate different terrain-induced airflows to specific landforms and time and space scales, while a second objective investigated the influence of broader scale winds on local nocturnal drainage winds. Of particular interest to this

research are the studies conducted by Clements et al. (1989) and Barr and Orgill (1989) who investigated the structure of drainage flow in relation to ambient atmospheric conditions. They found that increasing the strength of ambient winds appeared to diminish thermally induced wind regimes, a phenomenon that appears to significantly affect the horizontal (spatial) variation of near-surface temperatures in Marlborough.

The Cooperative Atmosphere-Surface Exchange Study 1999 (CASES-99) was the product of scientific interest in stable boundary layer conditions. At the time it was acknowledged that the stable boundary layer was the source of a number of outstanding problems in atmospheric science and agricultural meteorology. CASES-99 observation periods were focused on clear, settled weather which were conducive to stable and very stable boundary layer conditions, with the field campaign conducted through October 1999 near Luon, Kansas. Several key objectives were identified prior to commencing the field campaign, as reviewed in Poulos et al. (2002), but the overall aim of the project attempted to identify the sources, and quantify the physical characteristics, of atmospheric phenomena occurring during the formation, progression and breakup of the NBL. The study provided impetus for this research by demonstrating that turbulence from elevated shear layers within a stable NBL are directly responsible for contributions of intermittent heat and momentum fluxes to the surface. With regard to these findings, elements of the CASES-99 experimental design were incorporated into instrument deployment within the Marlborough region, to determine whether similar profiles of shear-induced instability contributed to the spatial variation of near-surface minimum temperatures. The CAESE-99 experiments provided a number of opportunities for modelling the evolution of the NBL, as demonstrated by Steeneveld et al (2006).

The Vertical Transport and Mixing (VTMX) field experiment took place in October 2000 at the southern terminus of the Great Salt Lake Valley, which separates the Great Salt Lake and Utah Lake Basins. The field experiment was sponsored by the United States Department of Energy's Environmental Division, and designed to study the way in which thermally

driven circulations affect vertical transport of heat, momentum, air pollutants and the development of cold pools in complex terrain. One of the main thrusts of the research was to quantify the impact of a down-valley jet on the evolution of underlying cold pools and, in particular, the impact of the jet on turbulence and mixing near the surface. Several papers published from this research are of great importance to research in the Marlborough region, such as that of Pinto et al. (2006), Banta et al. (2004), and Darby et al. (2006). Pinto et al. (2006), Banta et al. (2004) and Darby et al. (2006) all discussed the structure of a down-valley jet (DVJ) as it emerged from the Utah Lake Basin; in particular, the effect that the DVJ had on turbulence and mixing near the surface, including on the thermodynamic structure of the nocturnal boundary layer. Banta et al. (2004) proposed five mechanisms for the vertical mixing of cold air within a valley or basin, as illustrated in Figure 2.4. It was suggested that breaking waves, and shear-driven turbulence were important factors in the erosion of surface-based inversions and cold pools, resulting in increased near-surface temperatures.

The Terrain-induced Rotor Experiment (T-REX) commenced in Owens Valley, California in 2006. Among a variety of campaign objectives (reviewed by Grubisic et al. 2008), it aimed to examine the structure and evolution of a complex terrain boundary layer under clear quiescent conditions. Instrumentation included the use of wind profilers, radio acoustic sounding systems (RASS), aerosol and Doppler lidars, as well as sonic anemometer and profile measurements from a number of meteorological towers. The campaign culminated with a number of NWP model simulations of nocturnal valley wind structure, including predicted influences of upper-level synoptic flow. It was found that the evolution of thermally generated wind regimes was highly susceptible to mid-level pressure gradients above the valley, well below the heights of surrounding ridge tops. The larger scale synoptic gradients over the region were shown to influence the development and structure of a low-level thermal jet (Schmidli et al. 2009).

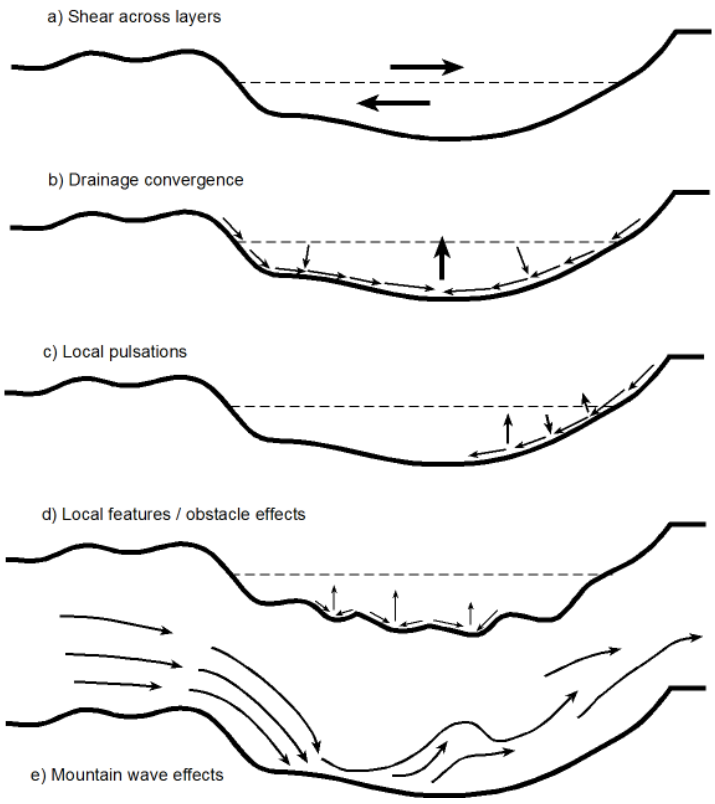

Figure 2.4 *Processes that can produce vertical transport and mixing in a mountain valley under stable NBL conditions (from Banta et al. 2004):a) Shear between flow in the cold pool and ambient winds aloft can produce waves and mixing; b) Acceleration of drainage flows down slopes can produce divergence and draw air downward toward the surface; c) Nonstationarity of drainage flow along slopes is observed to produce pulsations, which in turn produces localized up and down valley motions; d) Topographic features within the valley such as hills, ridges or cliffs, act as obstacles to the flow and induce mixing by convergent channelling effects, or by diverting or focussing drainage flows; e) Wave effects downwind of basin sidewalls can produce significant vertical mixing.*

Other international collaborative research efforts, such as the Mesoscale Alpine programme (MAP) in southern Switzerland, were reviewed by Rotach and Zardi (2007). One of the scientific projects was devoted to the study of 'Boundary Layers in Complex Terrain'. The most important result of the MAP boundary layer studies is that despite the highly complex structure of typical valley atmospheres, it was shown that characteristic, reproducible and transferable patterns in the turbulence structure could be identified and successfully

simulated with numerical models. However, appropriate numerical simulations of boundary layer processes over complex terrain require spatial resolution in the order of a few hundred metres in connection with detailed knowledge of surface conditions.

The Alpine Experiment (ALPEX) conducted a series of experiments in the European Alps in spring 1982 and produced a number of publications on airflows over mountains (Hafner and Smith 1985) and cyclogenesis in the lee of mountain ranges (McGinley and Goerss 1986, Alpert et al. 1996). While the these publications and many others are acknowledged for their contributions to understanding boundary layer evolution over complex terrain, results from the field programmes were of limited value to this research, as their experiments did not focus on the processes or mechanisms that are associated with development of spatial variations in near-surface temperature.

Projekt zur Untersuchung des Kusten-Klimas (Project for the investigation of the coastal climate; PUKK) investigated the formation of a nocturnal LLJ in north-western coastal Germany in 1981. Kraus et al. (1984) observed the jet flowing from mountainous terrain to the coast with a horizontal wind speed maximum at 400 m above ground level. In addition, a steep gradient of potential temperature was observed beneath the jet. Subsequent simulations of the LLJ using a Planetary Boundary Layer model resolved the basic features of the LLJ quite well in settled conditions, but problems were found to arise during events with stronger geostrophic winds.

Finally, The Lake Tekapo Experiment (LTEX) provided an example of successful collaborative research within New Zealand and findings are summarised by Sturman et al. (2003) in the preceding section. Some of the results from this study are of interest to this research, in particular, the descriptions of interactions between local thermally generated wind regimes and synoptic airflow. Powell (2000) also describes the evolution and vertical structure of a mountain wind, including development of a LLJ in an area of complex terrain, just north of Lake Tekapo.

2.6 Modelling the cooling processes within a valley

The complexity of real mountain valleys provides a challenge for numerical model simulations. As the spatial resolution of present models is not yet fine enough to present all the small scale features of valley winds, they could not be expected to accurately represent the diurnal fluctuations of near-surface temperature. However, regardless of a model's spatial or temporal resolution, the ultimate objective of all modelling studies is to provide insight into the workings of a given system (Steyn and Galmarini 2008), and a useful approach to investigating the mechanisms and processes responsible for cooling within valleys has been to focus on simulations using idealised topographies (Zardi and Whiteman 2012). Although the primary focus of this section will review the findings from several high resolution NWP model simulations applicable to the Marlborough region, the intrinsic value of establishing local climatological relationships should not be forgotten and as such will be the focus of a subsequent chapter in this thesis.

Many empirical models developed for the prediction of minimum temperature exist in the literature, and semi-empirical approaches that include calculations of energy balance and heat transfer processes near the surface are also plentiful. While many documented empirical models have been "tweaked" or modified to enhance prediction of local climate conditions, the modifications are rarely published (Synder 2005). Ghielmi and Eccel (2006) concluded that many of the empirical methods best known from the literature have been developed for use in plains and open areas, and that their application in areas of more complex terrain would encounter considerable difficulty. Although Snyder (2005) suggested that a temperature prediction model should incorporate energy balance calculations, earlier reviews by Kalma et al. (1992) concluded that for a number of reasons, air temperatures cannot be predicted satisfactorily from surface energy balance considerations alone. More recent studies by Verdes et al (2000) noted that many of the more sophisticated non-linear techniques of temperature prediction, provide only slight improvements in model performance over the standard (linear) regression approach, with the vast majority of

models developed to predict temperatures on a “dusk to dawn” approach, assuming highly stable atmospheric conditions, with minimal local air mass change through the course of the night.

High resolution NWP models are increasingly used to simulate observed cooling processes and predict horizontal differences of near-surface temperatures in complex terrain. Up to the present time, NWP models have been routinely operated using horizontal resolutions of several kilometers, whereas many hills and valleys in areas of complex terrain have widths of only several hundreds of metres and are therefore not resolved. Smith et al. (2010) suggested that an improved understanding of the physical mechanisms involved in producing cold air in valleys will increase the success of model downscaling techniques that are used for prediction of near-surface air temperatures in complex terrain.

Among the earlier computer-based models used to predict cold air drainage and air temperatures in hilly terrain was one presented by Mattson and Nordbeck (1981). The model predicted the horizontal extent and thickness of cold air at different times of the night. The model considered the physical properties of cold air, topography, land use and vegetation cover, but did not incorporate regional weather conditions, and was not compared with observations (Laughlin and Kalma 1990). Although several detailed three-dimensional meso-scale boundary layer models were developed through the 1980’s, most were inadequately validated against observations.

In the latter half of the 1980’s and early 1990’s many numerical modeling papers were produced from the ASCOT experiments in Brush Creek, such as Yamada and Bunker (1989) and Leone and Lee (1989), who utilized a nonhydrostatic, finite-element model to examine drainage flow in Brush Creek with zero ambient wind conditions. Doran (1991) used Clark’s non-hydrostatic model to investigate the interaction of katabatic winds with ambient winds for an idealized valley. This numerical study was important as simulations not only showed a decreasing strength and depth of drainage wind as adjacent ridge top wind velocities

increased, but also little effect was found by changing the angle that the ambient wind made with the valley axis. It was concluded that enhanced mixing of air within the valley at larger approach angles of the ambient wind, was partially compensated by a smaller up-valley component of the ambient wind, resulting in negligible effect on the cold air drainage in the centre of the valley, and the effect is illustrated in Figure 2.5. The conclusions from this study may help explain the high incidence of thermally generated drainage flows in parts of the Marlborough region, especially the upper Awatere Valley.

Numerous modeling studies from ASCOT found that large horizontal flow divergence in a valley could not be adequately explained using realistic values of vertical subsidence over the valley. O'Steen (2000) attempted to resolve this by using the Colorado State University Regional Atmospheric Modeling System (RAMS) to simulate drainage flow in an idealized valley-tributary system, to evaluate the tributary and main valley interactions. Simulations supported many field observations which suggested the idealized valley-tributary geometry was sufficient to describe salient features of drainage flows, including the notion that tributary valleys can lead to additional valley drainage, compared to that produced from a simple valley sidewall section. This finding is also important to Marlborough and is supported by numerical modeling, as discussed later in Chapter 6. During critical ambient wind flows, wider valleys can become ventilated, whereas for the same wind conditions smaller steeper tributary valleys may not. In these conditions, cold air drainage may continue to affect small localized areas of the wider valley that are adjacent to smaller tributary valleys, and this has been associated with observations of steep horizontal temperature gradients in parts of Marlborough's Wairau Valley.

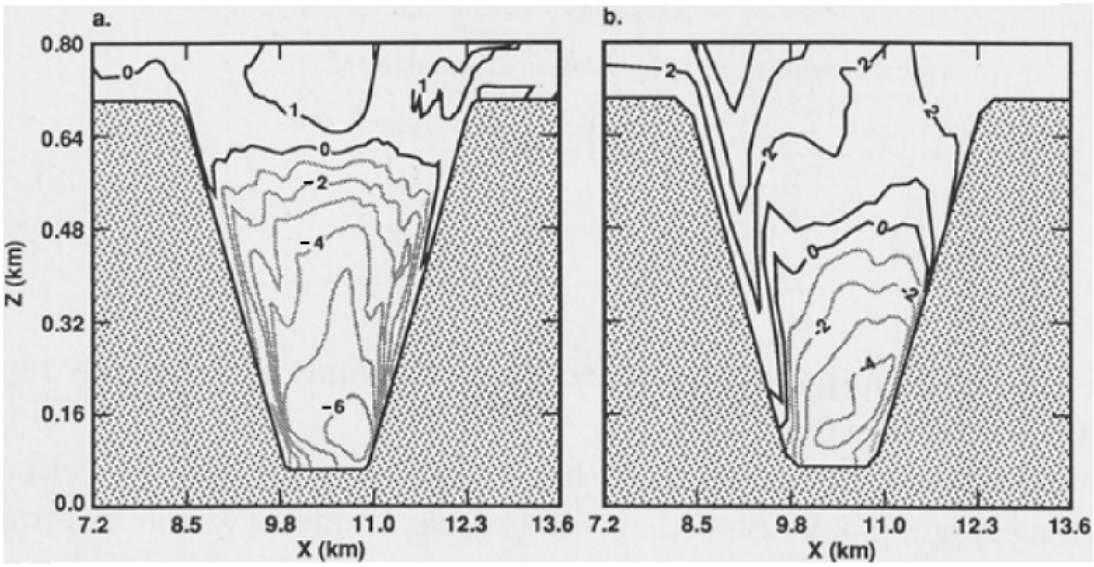

Figure 2.5 *Contours of along-valley wind speeds in an idealised valley. Heavy lines: up-valley winds; light lines: down-valley winds. Ambient winds at 60° to valley axis, with ridge top speeds of (a) 0.5 ms^{-1}, and (b) 4 ms^{-1}(from Doran 1991).*

As mentioned in the preceding section, numerical modeling of NBL development in complex terrain using the Advanced Regional Prediction System (ARPS) by Rotach and Zardi (2007) established that a sub-kilometre model resolution (of a few hundred metres) in connection with detailed knowledge of surface conditions (soil moisture) was required to resolve fine-scale flow structures. It was found that simply increasing model resolution without incorporating improved surface data produced poor results. They suggested that improved parameterisations of subgrid-scale turbulence processes that account for relationships between true and modeled topography will enhance future simulation accuracy.

Fernando (2010) acknowledged that transition periods between periods of up-valley and down-valley flow remain problematic in numerical modelling, given their rapid flow evolution and non-equilibrium turbulence. While the paper focussed on the implications for air pollution dispersion, near-surface temperature observations from Marlborough suggest that the spatial and temporal distribution of transition periods can have a significant effect on the spatial distribution of minimum temperatures.

The modelling component of this thesis uses The Air Pollution Model (TAPM) and the Weather and Research Forecasting (WRF) numerical weather prediction models. As is the case with most modelling studies, the models are used as heuristic tools, with an expectation that they will reveal something of value, in this case about the meteorology and mesoscale flow interactions that determine the near-surface temperature variations throughout the region. As they are, the models cannot be applied directly to create frost risk frequency plots for the Marlborough region. The models would require extensive configuration and calibration specifically for the region, to ensure the reliability of predicted temperature values. If however this was carried out and model simulations were produced for a number of years, the data could be analysed to create binomial distributions of the probability of an event occurring for any given year. The compilation of temperature frequency distributions in this manner is beyond the scope of this research. A further introduction and history of these models are provided in Chapter 6.

2.7 Contribution to science

By accounting for the spatial variation of minimum temperatures in the complex terrain of the Marlborough region, this research attempts to improve our understanding of the physical mechanisms involved in producing not only cold stagnant air, but areas of persistent warmer temperatures that have been observed to occur simultaneously around the region. Output from the research is expected to aid the development of downscaling techniques for the forecasting of local air temperatures, in an area of significantly high-value agriculture and this is achieved through a variety of data collection and analysis techniques.

The research in Marlborough will demonstrate the effects of topographic sheltering on minimum temperature evolution in complex terrain and, through the use of NWP models, identify the meteorological processes that determine the spatial variation of temperatures.

Prior to commencement of this research, little was known about the evolution and structure of the NBL above the Marlborough region, and in particular, its effect on near-surface temperature. This research is expected to extend the early work of Barr and Orgill (1989) by not only investigating the existence of transition layers between thermal wind regimes and overlying synoptic flow, but quantifying the effect on near-surface temperatures when the transition layer “couples” with the surface.

Chapter 3 Methodology and research area

3.1 Introduction

This chapter of the thesis introduces the research field area of Marlborough. The topography of the area is described, and the rationale for choosing the area for study. A detailed account is provided of data collection techniques using automatic weather stations (AWS) and the University of Canterbury's SODAR (SOnic Detection and Ranging).

The incidence of frost to the grape growing areas of Marlborough is associated with a large spatial variation of near-surface minimum temperature. A methodology for acquiring a better understanding of frost events during the spring season must arise from an investigation into the processes and mechanisms that drive the spatial variation of near-surface minimum temperature. In this respect, the method of investigation commences with an analysis of the broader synoptic influences that affect the spatial variation of near-surface temperature for the three spring seasons of 2009 - 2011. Analysis is then extended by drawing upon local meteorological data to establish relationships between ridge top wind velocity and the variation of near-surface minimum temperature for the same period. The data set for the three spring periods includes a number of frost events, as recorded by vineyard AWS.

High resolution numerical weather prediction models provide an explorative tool for investigating the relationships that were found to exist between the region's terrain and the spatial evolution of near-surface minimum temperature. Model simulations are evaluated using data from local AWS. Furthermore, numerical models reveal a great deal about other meteorological processes that are creating the region's large spatial variations of near-surface temperature, such as the sub-regional prominence of strong drainage winds, and the topographically induced ventilation and stagnation of near-surface air.

As one of the leading meteorological processes that influence near-surface temperature is wind speed, it was important to ascertain the mechanisms through which near-surface temperatures were affected. This was investigated using the University of Canterbury's SODAR to take vertical soundings of wind velocity at specified locations. Subsequent plots of vertical wind shear reveal the extent of shear-induced turbulent mixing under different synoptic conditions, which may lead to the simultaneous ventilation and stagnation of the near-surface air in different parts of the region.

3.2 The Marlborough region

The Marlborough region is located in the north-eastern corner of the South Island (41.5° south and 174° east). It is bounded in the south by the Clarence and Conway River catchments, to the west by the Spensor and St Arnaud Ranges, and by further mountainous terrain to the north between Tasman Bay and Pelorus Sound (Figure 3.1). There are three main catchments, the Wairau, Awatere and Clarence, all of which flow north-eastwards to the Pacific Ocean (Pascoe 1983). The region's predominantly mountainous terrain extends in a north-east to south-west direction and from south to north includes the Seaward Kaikoura Range, the Inland Kaikoura Range, the Blairich Range and furthest west, the Richmond Range. The mountainous region to the south-west is comprised of the St Arnaud, Traverse and Spensor Mountains. Many of the ridge tops within these ranges exceed 2000 m in elevation, including Mt Tapuaenuku at 2885 m. Much of the region's flat arable land is located either side of the Wairau and Awatere Rivers.

Both the Wairau and Awatere Valleys owe their existence to the historic movement of major fault lines that lie beneath the region, but within these larger river valleys numerous smaller hills and tributary valleys create a region of highly complex terrain. The Wairau Valley is almost 108 km in length and ranges from 3 km wide near Wairau Valley township to almost 12 km in width near Blenheim. The Awatere Valley is a little shorter, but narrower with many parts of the valley extensively planted in grapes where the valley width is only

1.5 – 2 km wide. The side walls of both valleys are steep with many surrounding ridge tops rising in excess of 1200 m. The two most prominent grape growing areas of the region, the Wairau and Awatere Valleys, are separated by a prominent range of hills south of Blenheim which are an extension of the Blackbirch Range.

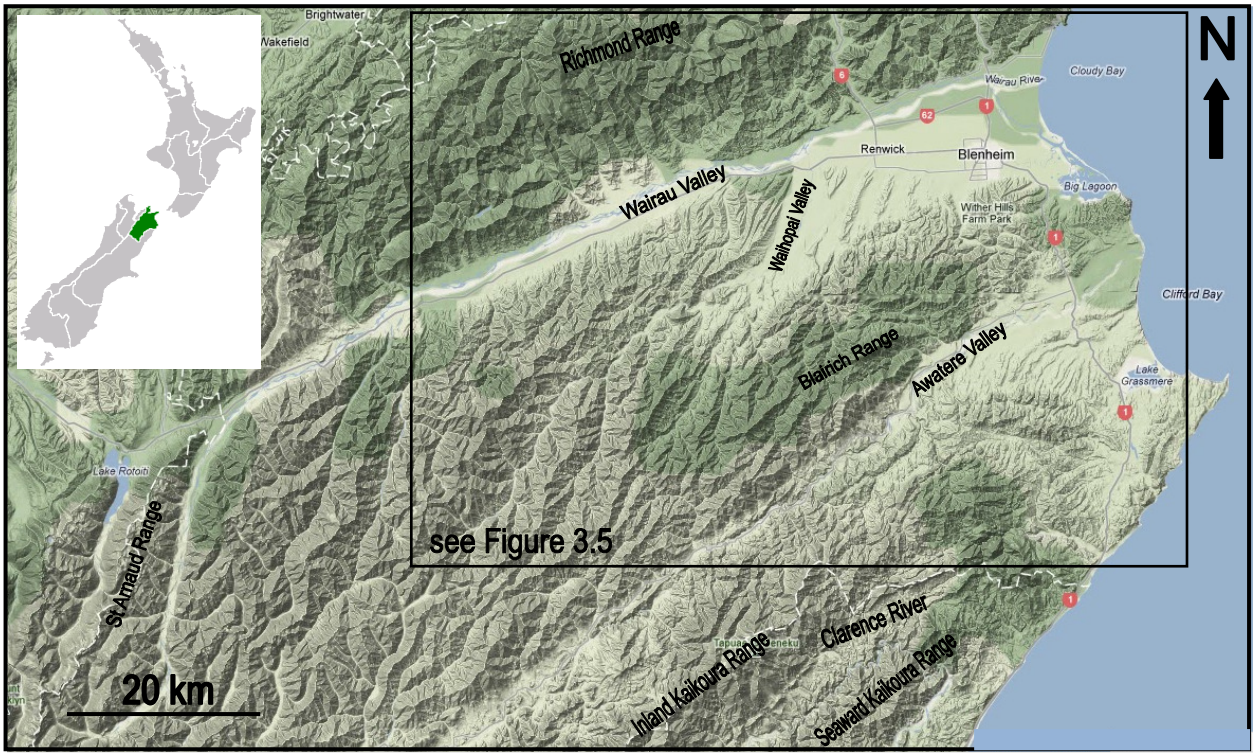

Figure 3.1 *Topographic map of Marlborough (coloured) green in the insert map. A detailed map of the field area is provided in Figure 3.5.*

Understanding the topography encompassing the Marlborough region is crucial to this research, for it has a massive impact on the spatial variability of day-to-day weather and the evolution of minimum temperatures. The topography surrounding the region effectively blocks, channels and interacts with a range of synoptically driven wind systems and exposes the region to a high diurnal range of temperatures and weather extremes. It also predisposes the region to frost, which is a major hazard to its buoyant wine economy.

3.2.1 The Marlborough wine industry

Traditionally, Marlborough's economy was focused on agriculture. The extensive areas of sheep and beef farming were interspersed with pockets of orchards, market gardens and forestry (Pascoe 1983). In the last 25 years (since about 1990), the region has experienced a rapid expansion of grape growing. As of January 2011, 24,000 ha of grapes had been planted (Figure 3.2) with the region acquiring a worldwide recognition for its outstanding Sauvignon blanc.

The vast areas of grape planting that are spread over extensive flatter areas of the river plains are surrounded by the region's complex topography (Figure 3.3). The regular occurrence of spring frost over much of the region necessitates frost protection systems, such as wind machines (Figure 3.4), helicopters, dams and water irrigation systems, and examples of these pepper the landscape.

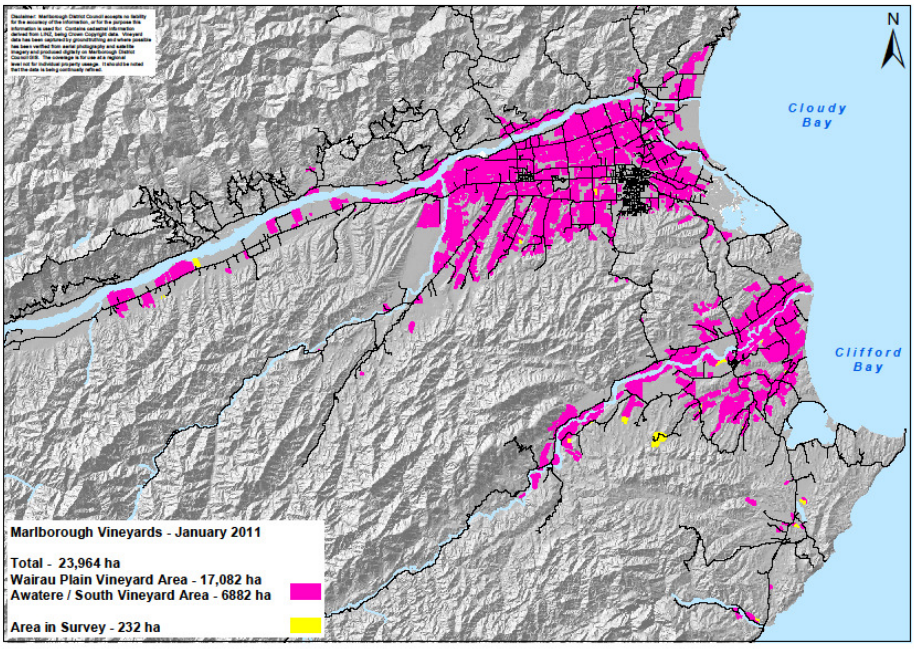

Figure 3.2 *Extent of grape planting in Marlborough as of January 2011.*
*(*http://www.marlborough.govt.nz/Environment/Land/Land-Cover-Land-Use/~/media/Files/MDC/Home/Environment/Land/Viticulture%20January%202011.ashx*)*

Figure 3.3 *A river terrace planted with grapes in the upper Awatere Valley. The complex topography that surrounds the vineyard is typical of many grape growing areas in the region.*

Figure 3.4 *A wind machine located in Fairhall, Marlborough, in operation during an early morning frost October 2007.*

Seventy seven percent of New Zealand's grape production is now grown in the Marlborough region *(http://www.wine-marlborough.co.nz/)*. Although the rate of expansion all but ceased from 2009 – 2011 due to a global recession and saturation of existing markets for New Zealand wine, the latter months of 2012 and 2013 have seen resurgence in the grape

economy. As of April 2009, the value of New Zealand wine exports reached $900 million and accounted for 20% of the Marlborough region's economy (*http://www.nzwine.com/assets/sm/upload/v9/q6/e9/ls/NZIER_Rep_April_09.pdf*).

3.2.2 An opportunity for research in Marlborough

The expansion of vineyards throughout the complex terrain of the Marlborough region predisposes a high value, cool climate crop, to frost. With the exception of occasional warmer seasons, the ongoing success of Marlborough's wine economy relies heavily on both fixed and ad hoc measures of frost protection, and in the early 2000s a demand for accurate local frost forecasting was recognised. The recent installation of dozens of privately owned, modestly priced AWS revealed the extent of Marlborough's variation in near-surface minimum temperature, and these data sets provide a unique opportunity to explore the relationships between the local climate and surrounding topography.

3.3 Data collection

The data collection process commenced in February 2009. The data have been sourced from MetService, NIWA and privately owned AWS, most of which had been in place prior to commencement of study. Three new privately owned AWS were installed as part of the extended field campaign to coincide with use of the University of Canterbury's SODAR.

Data collection from such an extensive AWS network, including that of a high elevation ridge top station, is not commonly reported in the literature, although studies using similar data collection strategies have been described by Doran and Horst (1990), Gudiksen et al. (1992) and Gustavsson (1995). Traditionally, the acquisition of upper-level (ridge top) climate data is achieved using SODAR, LIDAR and tethered or free-flying balloon ascents. There are, however, several advantages in using a fixed ridge top AWS overlooking a

research area, such as collection of data during increasingly dynamic synoptic conditions and the real time correlation of ridge top and valley floor data.

3.3.1 Automatic Weather Stations (AWS)

Data were collected from a total of thirteen AWS from around the Marlborough region. The locations of privately owned AWS and official stations (e.g Dashwood) used in this study are illustrated in Figure 3.5. The SODAR was deployed at the Awatere and Rapaura AWS sites. Automatic weather station locations at Scrub Rough Spur and Blairich were installed temporarily, while the SODAR was deployed at the Awatere Valley location.

Ten of the thirteen AWS were in place prior to commencement of this research and continue to support a privately owned frost forecasting service for the region. Each of these stations record temperature, humidity, wind speed and direction and rainfall. Several sites also record inversion strength by recording temperature at 12 m as well as 1.2 m. The AWS named “ridge top 902” is shown in Figure 3.6a on privately owned farmland on an exposed ridge behind the Wither Hills. The stations were installed through the period of 2005 – 2008 in areas surrounded by extensive grape plantings. A third privately owned AWS was installed in 2010 at the Wairau Valley Coast. It has since become part of the network of AWS to aid frost forecasting in the region. Observations regularly demonstrate that the network of privately AWS is able to resolve much of the spatial variation of minimum temperature around the region. In this respect, each of the AWS is well positioned to meet the research objectives defined in the preceding chapter.

The temporary AWS at Scrub Rough Spur in the upper Awatere Valley was only in place for the period of SODAR deployment. Its function was to validate observations from the SODAR, at some 220 m above the valley floor. The Blairich site at 1502 m (Figure 3.6b) was intended to be long-term, but only survived 8 months in the severe alpine conditions. Its operation was to help assess the impact of upper level wind velocity on the spatial variation

of minimum temperatures. Unfortunately, for much of the time, one or more of the sensors at the station gave erroneous data and as the station was remote, it was particularly expensive to access and service. The station collapsed as a result of icing during a storm in July 2010 which produced severe gales and below freezing conditions.

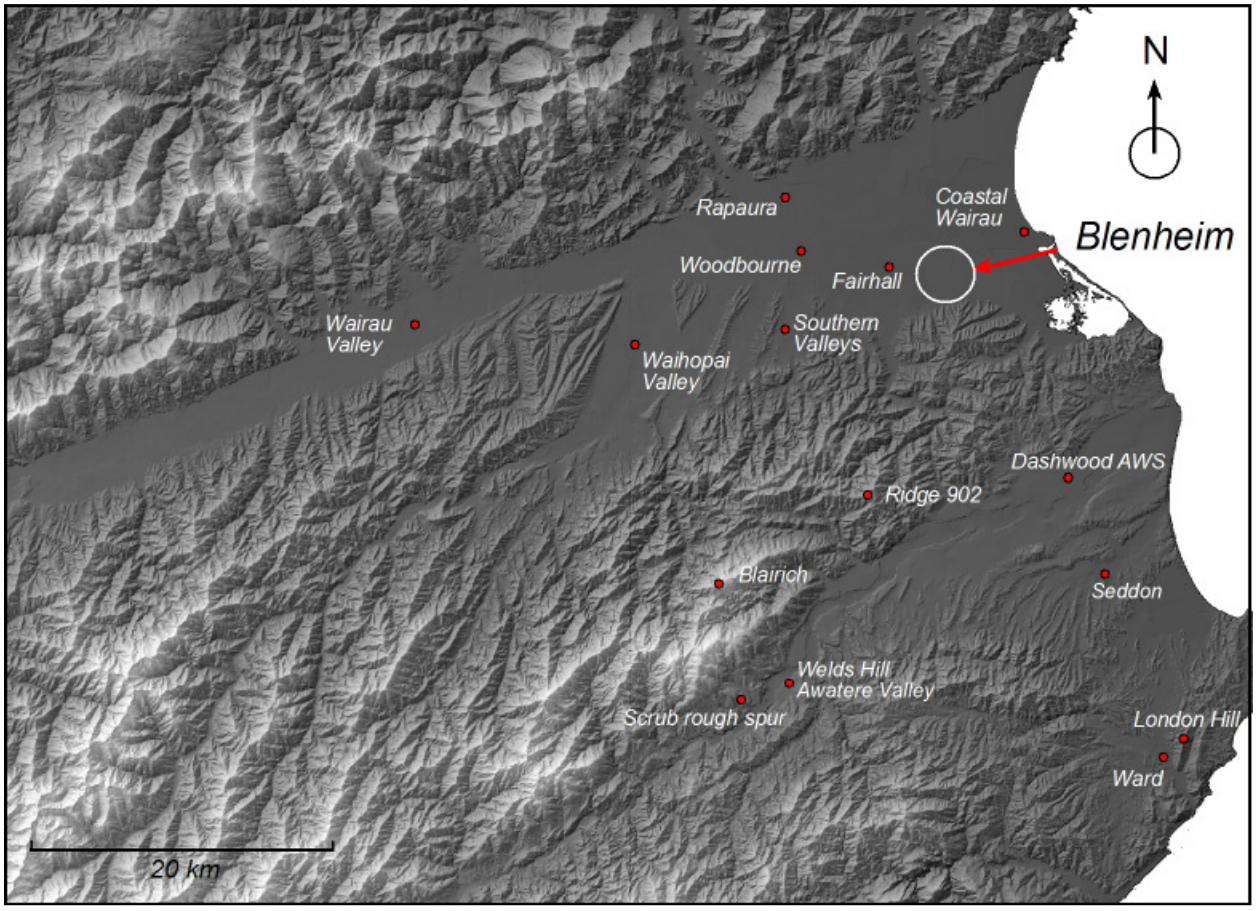

Figure 3.5 *Data collection points from AWS located throughout the Marlborough region.*

The network of privately owned AWS is expected to provide representative near-surface climate data for the grape growing region, and be suitable for the subsequent application of numerical modeling. Both the spatial and temporal evolution of modeled temperatures will be compared with observations in Chapter 6. Although long term temperature records have been used from the two official MetService AWS sites in the region at Woodbourne and Dashwood, no daily or specific event data from these stations has been analysed.

Figure 3.6 *(a) Ridge 902 AWS, and (b) the temporary Blairich AWS at 1502 m.*

Temperature at the Dashwood AWS is modified by the close proximity of local frost protection systems, and hourly meteorological data from the Woodbourne AWS did not provide a satisfactory observation frequency for integration with surrounding privately owned AWS. In this case, data from the privately owned Seddon AWS was used in place of the Dashwood AWS, and the Woodbourne AWS was replaced with data from the privately owned Southern Valleys AWS. Proximity of these privately owned AWS to the Dashwood and Woodbourne AWS are illustrated in Figure 3.5.

3.3.2 The SODAR (SOnic Detection and Ranging)

Wind measurements in the vertical plane were made using a Scintec Flat Array SODAR (SFAS) (Figure 3.7). The SFAS model provided an option for continuous remote measurement of wind speed and direction without the need for tethered balloons. The SODAR antenna emits a short acoustic pulse into the atmosphere which is scattered by temperature in-homogeneities in the atmosphere. The antenna then receives the

backscattered signals and converts the signal to a shift in Doppler frequency, which reveals wind speed and direction

(http://www.scintec.com/english/Web/Scintec/Details/A031002.aspx). It was set up to collect data up to the maximum height range of 500 m, with a resolution of 5 m. The antenna height above ground level was set to 0.8 m and a mean data collection temperature of +10°C. The instrument was validated using data from the Welds Hill, Awatere AWS. Antenna azimuth was aligned as accurately as possible with respect to true north, and recording time adjusted to NZST. The SODAR calibration was adjusted after redeployment at Rapaura.

Figure 3.7 *The Scintec Flat array SODAR deployed at Welds Hill near the upper Awatere AWS.*

The integration of SODAR as part of the data collection process was essential in helping to understand the region's spatial evolution of minimum temperature. The measurement range of the SODAR would provide vital information on wind conditions above the valley floor, but below the level of surrounding ridge tops. Early observations from the region during frost conditions, suggested that the interaction of synoptic and local thermally driven

wind systems would occur within the range of the SODAR and that a greater understanding of these interactions would improve the robustness of local frost forecasting.

The first SODAR deployment on Welds Hill Vineyard near the Awatere AWS consisted of 3 months from 27 July – 24 October 2010. During this time, the instrument was connected to a permanent power supply and ran continuously, apart from one short power outage for 3 days. The SODAR was checked and data were collected from the unit every 7 days. The 7 day data collection cycle was a compromise between costly return trips to the SODAR site and minimizing data loss in the event of a power outage. Although data collection was good, the vertical range of the unit was at times compromised, particularly by high surface winds or the proximity of vineyard machinery. As previously mentioned, SODAR data were also validated through the short-term deployment of an AWS on an adjacent (Scrub Rough) spur, 2 km west-south-west (up-valley) from the SODAR. The AWS was located 220 m above the height of the SODAR, so this provided a useful check of wind speed and direction in the vertical profiling data.

The second SODAR deployment at the site of the Rapaura AWS was also located on an actively managed vineyard (Figure 3.8). It was operated remotely at this location from 5 November 2010 to 1 May 2011, although a number of problems took months to unravel as a permanent power supply was not available at this site. The power requirements were considerably higher for one component of the unit than the initial set up allowed and this was only resolved by tripling the original battery configuration. Even then, the unit would only run for a maximum continuous period of about 2 days before running low on power. The vertical range of data collection was severely compromised at times at this site, as it was closer to an urban environment and a busier time of year for machinery on the vineyard, both day and night. There may have been some further obstruction to the SODAR signal due to the close proximity of trees, particularly during stronger surface winds. Noise complaints from a neighbouring residence were also received. As a result of all the above,

the SODAR was only operated for specific special observation periods, not usually longer than 18 hours, to capture an overnight period of interest.

Figure 3.8 *Remote SODAR deployment at Rapaura AWS.*

3.4 Analytical techniques

In the three results chapters to follow, a variety of statistical and climate-related software packages are used to explore the region's variation in near-surface minimum temperature. A brief summary of the main techniques and software are provided in the following section.

3.4.1 Statistical analysis

The analysis of climate data employed a number of rudimentary statistical approaches. A number of techniques were available as part of the Excel spreadsheet package, and involved the use of column graphs, box plots, scatter plots and data sorting analysis, to compare two or more sets of time series data. For example, much of the data from privately owned AWS logged anywhere from 7 to 13 times an hour, and consequently, required formatting to a common 10 minute logging interval so that data could be compared from different AWS between different parts of the region.

Chi-square(x^2) tests were performed in Chapter 5 in conjunction with a contingency table analysis to determine the significance of differences between the observed and expected frequency of Kidson synoptic type, in association with the standard deviation of minimum near-surface temperature around the Marlborough region. The null hypothesis to be tested was that no statistically significant difference existed between the observed and expected frequency of Kidson type, in association with the near-surface spatial variability of minimum temperature.

The t-test is also used to determine the significance of the difference of the means between two sets of data. Using a similar null hypothesis to that of the Chi-square tests, the t-test were used to assess the relationship between predicted and observed values of near-surface wind speed and temperature.

3.4.2 Climate and weather-specific analytical software

Several climate-specific software applications were used to analyse data from AWS and SODAR. These included WRplot to create wind rose plots displaying frequency of wind speed and direction (*http://www.weblakes.com/products/wrplot/index.html*). Integrated Data Viewer Version 4.1 (IDV) is a Java based software framework for analyzing and visualizing geo-science data. It is used to analyse and plot output from the WRF modeling procedures in Chapter 5. It enabled the creation of a high resolution topographic map, upon which three-dimensional displays of wind velocity or temperature can be superimposed. The data plotting functions that form part of the TAPM Graphical User Interface (GUI) were used to display output from TAPM in Chapter 4. The TAPM GUI offers significantly reduced control to the user for analysis and display of meteorological data when compare with IDV. Finally, data plotting functions that accompanied the SODAR provided analysis and visualization of the vertical wind velocity profiles.

3.4.3 Miscellaneous software applications

Matlab provides a high-level technical and interactive environment for data analysis, visualization, and numerical processing. A student version of the software provided a user-friendly, Windows-based platform for analysis of wind speed data, in particular, to generate three-dimensional plots of wind shear that are presented in Chapter 6. Surfer version 8 is a contouring and 3-dimensional surface mapping programme. The software was applied in Chapter 3 to produce co-ordinate based near-surface temperature contour maps.

3.5 Summary

The Marlborough region presents a unique and challenging stage on which to perform three-dimensional atmospheric research. The highly valued grape growing economy has evolved amongst complex terrain where regular spring frosts (average of 6.1 per growing season) can wreak havoc on unprepared vineyards in a matter of hours. One of the more important tools used by vineyard owners is a frost forecast. Improved forecasting will provide a better prediction of the near-surface minimum temperature variation. It can be achieved by enhancing our understanding of the relationship between synoptic conditions and the smaller-scale atmospheric features located within the region's complex terrain. The methodology by which this research attempts to address several key questions is summarised by the flow chart in Figure 3.13.

It is important to acknowledge at this point of the thesis that data collection from multiple sources within complex terrain is inherently difficult. There are significant periods when weather conditions are not conducive for data collection and many times when equipment failure from preceding extreme weather causes periods of missing data.

Data collection formed a significant component of this PhD research. It is thorough and provides many examples of the interactions between weather, topography and the

influence on minimum temperature, as well as frost. The following three results chapters explore a number of these interactions and extend our knowledge of the spatial variation and prediction of minimum temperatures in complex terrain.

	Objective 1	Objective 2	Objective 3
Key research phases	Identification of relationships between synoptic weather patterns and spatial variability of near-surface minimum temperature and frost	Exploration of the relationship between regional airfow patterns and spatial variation of near-surface minimum temperature and frost	Investigation of the influence of the vertical structure of the nocturnal boundary layer on near-surface temperature variations
Sources of information required	**1.** Synoptic weather maps for New Zealand **2.** The local/regional temperature field in the complex terrain of Marlborough from AWS network	**1.** Airflow data for the Marlborough region **2.** The local/regional temperature field in the complex terrain of Marlborough from AWS network	**1.** Vertical atmospheric structure within the Wairau and Awatere Valleys **2.** Temperature measurements at specific sites within the Marlborough region
Analytical tools used	**1.** Kidson daily classification of synoptic weather patterns for New Zealand **2.** Statistical analysis using Chi-square **3.** Visualization software (WRPlot, Surfer)	**1.** Ridge top wind measurements **2.** Mesoscale atmospheric numerical models (WRF & TAPM) **3.** Visualization software (IDV & TAPM GIS) **4.** Statistical analysis using t-test	**1.** SODAR wind profile measurements **2.** Visualization software (Matlab & Scintec APRun)

Figure 3.9 *The methodology of analysis is summarized by the flow diagram. Three research objectives are identified and key research phases, sources of information and analytical tools required for analysis are outlined.*

Chapter 4 Background climatology of Marlborough

4.1 Introduction

The complex topography that surrounds the Marlborough region creates significant spatial variation of climate. Although the weather and climate of the region was described in some detail by Pascoe (1983), the climate data were obtained from a relatively sparse network of weather observation sites. Only one of the weather observation sites at Blenheim was located within the present grape growing areas of the region. This chapter aims to extend the description of climate by Pascoe (1983) with data from nine privately owned AWS located within the grape growing areas of the region. In particular, a greater emphasis will be placed on the analysis of local meteorology that is associated with the incidence of large spatial variations of near-surface minimum temperature, which may result in frost.

Broadly speaking, the weather and climate of Marlborough is governed by the eastward progression of anticyclones with intervening troughs of low pressure. When the centres of anticyclones pass close to the region and ridge top winds are light, thermally induced wind regimes often become established. In warmer months, clouds form by day as cooler moister air moves onshore, although skies will clear again at night if synoptic gradients from the south or westerly quarter strengthen. Only active troughs that pass over the region bring significant rain, usually in the form of spill-over from the western ranges. Marlborough's location on the east coast of New Zealand predisposes the region to a significant rain-shadow effect and it is one of the three driest regions in the country. Inland Marlborough (including Blenheim) remains particularly sheltered from cooler southerly airstreams behind the Seaward and Inland Kaikoura Ranges and any associated cloud or shower activity clears the region quickly. Sunshine hours in the north-east of the

region are among the highest in New Zealand, with an annual average of 2446 hours (*http://cliflo.niwa.co.nz*).

4.2 Temperature

Pascoe (1983) stated that mean temperatures in New Zealand at sea level range from 15°C in Northland to 12°C near Cook Strait and 9°C in Southland. The mean temperatures for Marlborough were said to conform to this general scheme. In Table 4.1 the mean near-surface temperatures (T_{mean}) have been calculated for a network of eight privately owned AWS located within the grape growing areas of the region, as illustrated in Figure 3.5. Mean temperatures range from a low of 11.6°C at Waihopai Valley and Wairau Valley township AWS, to 12.6° at Rapaura. The monthly mean near-surface temperatures have been plotted for each AWS in Figure 4.1. There is a slightly increased range of mean temperatures in the winter month of July (σ = 0.65°C), compared to January (σ = 0.40°C), and this reflects the incidence and severity of frosts in cooler locations during the winter months.

Table 4.1 *The mean annual near-surface temperature at eight of the nine privately owned AWS in Marlborough, 2008 – 2013. The coastal Wairau Valley site has not been included as observations from this site are intermittent.*

AWS	T_{mean} °C
Fairhall	12.0
Rapaura	12.6
Southern Valleys	12.0
Waihopai Valley	11.6
Wairau Valley town	11.6
Seddon	12.4
Upper Awatere Valley	11.7
Ward	12.1

Mean monthly maximum and minimum near-surface temperatures for the network of privately owned AWS have been calculated, and are shown in Figures 4.2 and 4.3. The spatial variation of the mean annual monthly maximum temperature in January is slightly smaller (σ = 1.22°C) when compared to the mean annual minimum temperature in July (σ = 1.28°C). Warmest temperatures in Marlborough occur during summer months when winds arrive from the west or north-west. Winds from these directions have traversed the Southern Alps and as they descend down into Marlborough's river valleys, they often bring dry, foehn wind conditions. On these occasions near surface temperatures usually exceed 30°C across many parts of the region. Warmest extreme maximum temperatures occur in February at all AWS locations, except Ward which often records highest maximum temperatures in January. The warmest maximum temperature recorded in Marlborough of 42.2°C was observed at The Jordan, only a short distance up-valley from the upper Awatere AWS. This temperature is 0.1°C cooler than the official New Zealand record, but was recorded on the same day (7th February, 1973) as the extreme high temperature in Rangiora, near Christchurch.

Conversely, coldest weather arrives from the south or south-west. Showery conditions often accompany the colder weather nearer the coasts, although conditions often remain dry further inland. The colder change in weather is often followed by air frosts during cooler months of the year, and this can result in large spatial variations of near-surface temperature.

4.2.1 Soil temperatures

Long-term soil temperature data are available from Dashwood AWS and the Marlborough Research Centre AWS and recorded at depths of 10 cm and 30 cm. The average annual monthly soil temperatures for Dashwood and Marlborough Research Centre for the years 2002 – 2012 are presented in Figure 4.4. Minimum soil temperatures at both depths occur in July and maximum soil temperatures occur during January and

February. The 30 cm soil temperatures are slightly warmer most of the year, except at Dashwood where 10 cm soil temperatures are briefly warmer during spring. This may reflect soil type and moisture levels.

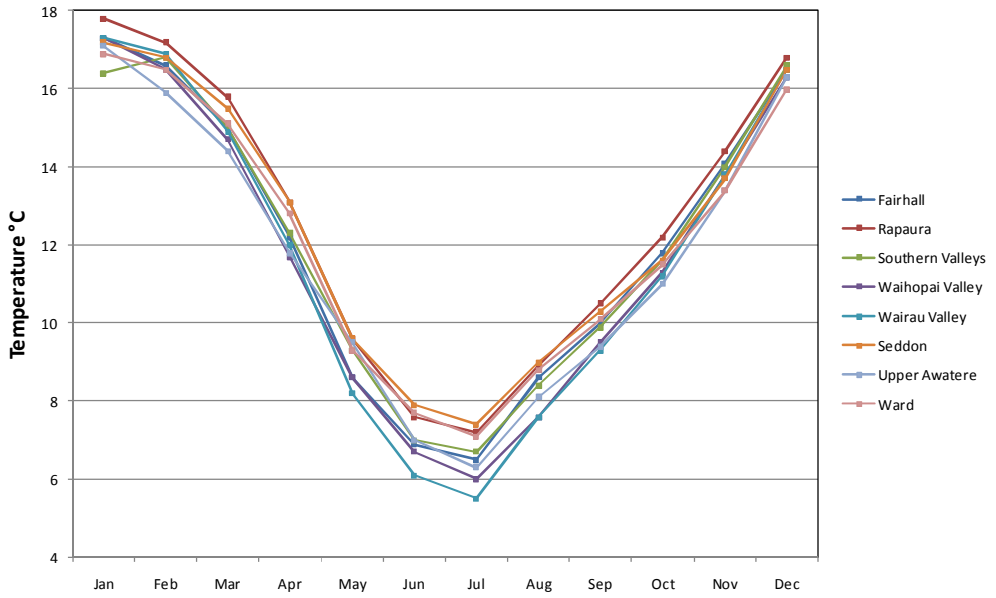

Figure 4.1 *Mean monthly near-surface temperatures for eight privately owned AWS in Marlborough, 2008 – 3013.*

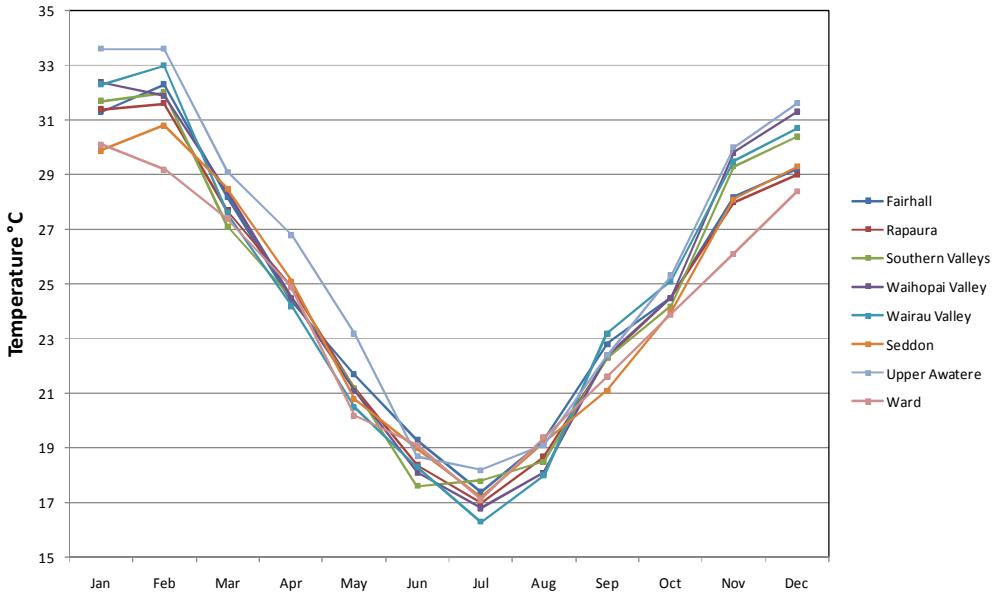

Figure 4.2 *Mean monthly maximum near-surface temperatures for eight privately owned AWS in Marlborough, 2008 – 3013.*

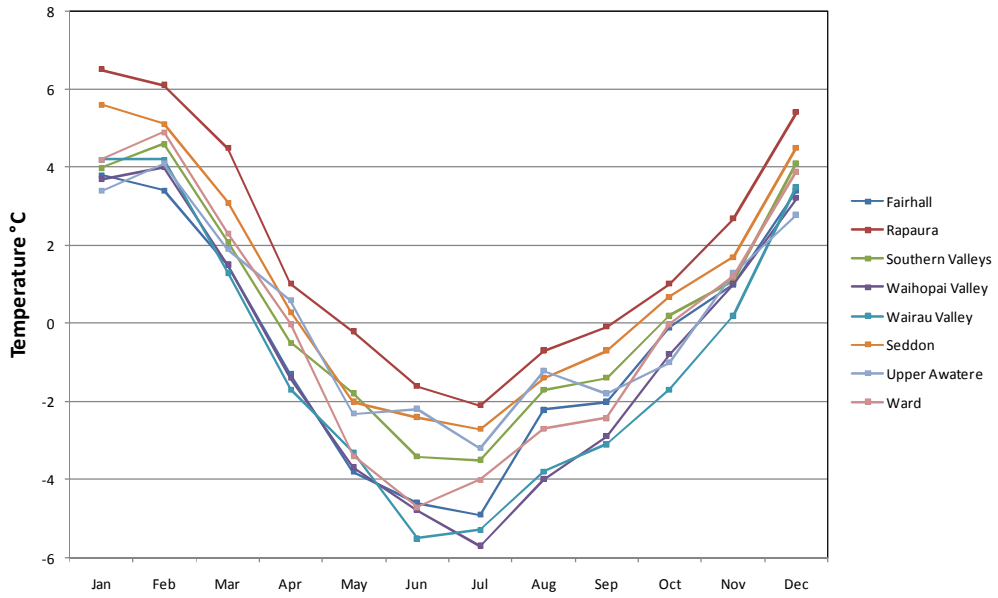

Figure 4.3 *Mean monthly minimum near-surface temperatures for eight privately owned AWS in Marlborough, 2008 – 3013.*

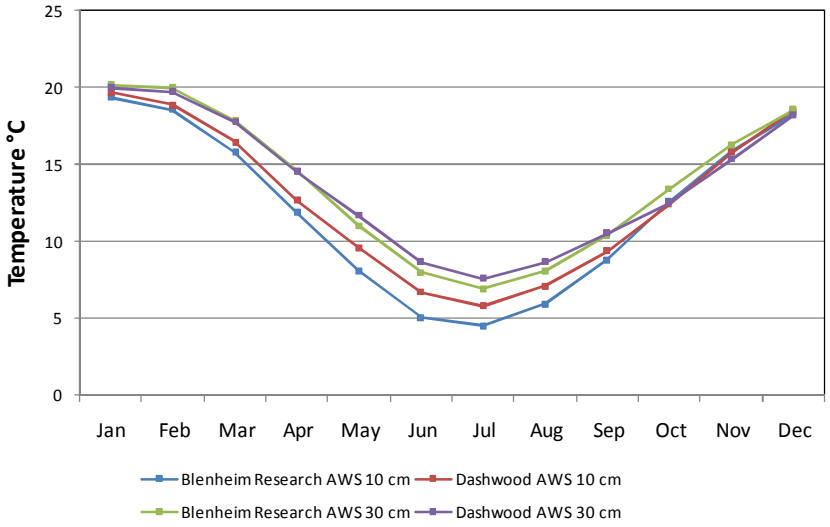

Figure 4.4 *Average annual soil temperatures at Dashwood and Marlborough Research AWS for the period 2002 – 2012.*

4.2.2 Incidence of frost

Air frosts are a common occurrence in Marlborough during winter and spring. These can be a significant hazard to agricultural crops, in particular the extensive grape plantings around the region. One of the region's longest recording climate stations at Woodbourne Aerodrome receives an average of 30 air frosts over the three winter months of June, July and August, although long-term records suggest an average of only 3 frosts can be expected during spring (September, October and November). The latitude and elevation of the region renders all frosts radiational in nature and they occur predominantly during clear settled conditions. Frost maps (produced by the National Institute of Water and Atmospheric Research, NIWA) are available for the region from the Marlborough district council website (*http://www.marlborough.govt.nz/Environment/Climate/Reports-and-Special-Investigations/Frost-Indicators-and-Maps.aspx*). These maps display a range of related information, such as projected dates of first and last frost, frost free periods and mean dates of first frosts. Trought et al. (1999) demonstrated that the dates of the last spring frost vary markedly from one season to the next.

The occurrence of frost around the region varies both spatially and from one year to the next. Figure 4.5 shows the incidence of frost conditions during spring for a 3 year period (2009 – 2011), from the network of privately owned AWS. Frost conditions are triggered when the air temperature at 1.3 m above ground falls below +1.4°C, and this is usually associated with the commencement of automated frost protection systems. The greatest occurrence of frost conditions occurs at Waihopai Valley with over 100 events for the 3 year period, while only 31 were recorded at Rapaura. Analysis has shown a weak correlation between distance from the coast and frost frequency, which suggests other mechanisms are responsible for the regional variation. Figure 4.6 illustrates the annual frequency of frost conditions (temperatures at 1.3 m in height above the ground are +1.4°C or less) and air frost (temperatures at 1.3 m in height above the ground are 0°C or

less) from the Dashwood AWS in the Awatere Valley. The graph shows a considerable fluctuation of frost occurrence over the past 18 years.

4.2.3 The spatial variation of near-surface minimum temperatures

The extensive shelter provided by terrain surrounding the region's grape growing areas contributes to a high diurnal range of temperature, in particular cold nights, independent of synoptic situation and under a range of atmospheric stabilities. High spatial variations of near-surface minimum temperature (which may result in frost at some locations), have been recorded when moderate or even strong west or north-westerly winds blow across surrounding ridge tops. On these occasions the winds have been observed to exploit gaps in the surrounding terrain and cause ventilation to some sub-regions, while leaving other areas undisturbed allowing cooling to continue. Spatial temperature variations of up to 13°C have been recorded by the network of privately owned AWS.

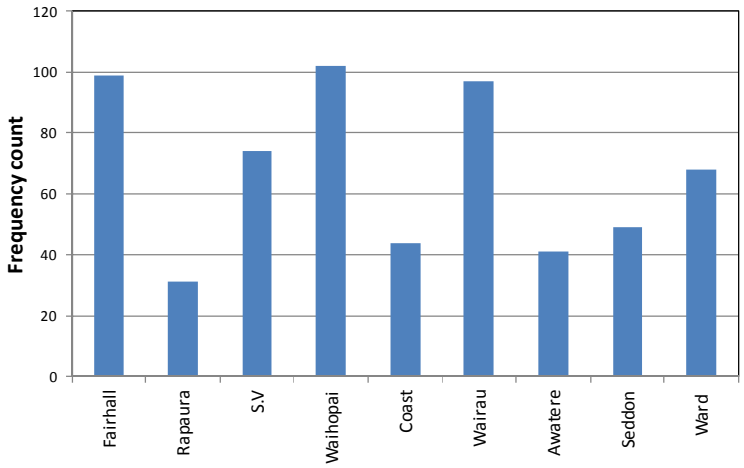

Figure 4.5 *Episodes of frost conditions (air temperature <1.4°C) from 9 AWS sites around the Marlborough region over the period 2009 – 2011 (refer Figure 3.5 for site locations).*

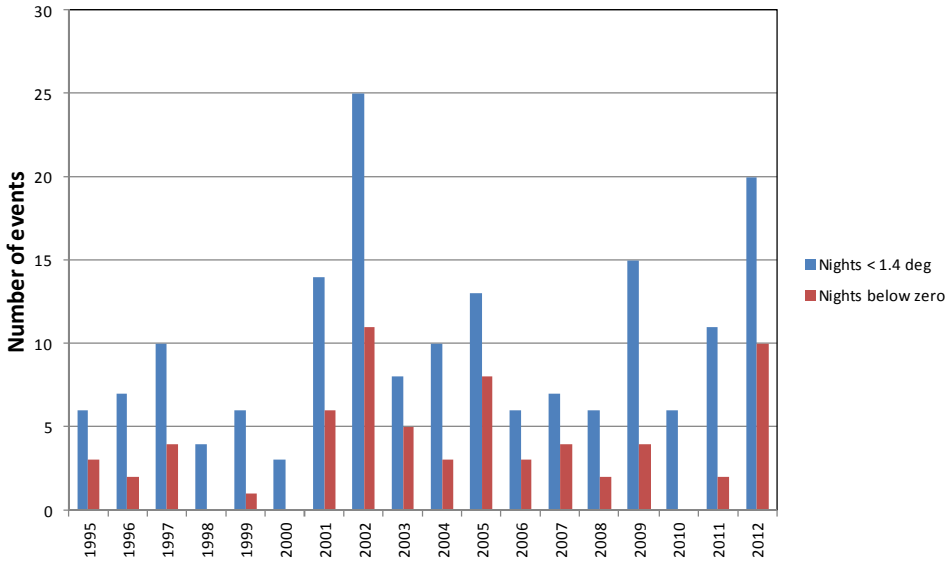

Figure 4.6 *Variation in the annual occurrence of frost conditions (blue) and air frost (red) from Dashwood AWS 1995 – 2012 (see Figure 3.5 for site location).*

Figure 4.7a – d compare near-surface minimum temperature for spring 2009 – 2011 (September and October only) for four selected AWS, with a two-way synoptic pressure gradient measured in hectopascals (hPa) across the region. The scatter plots provide a method of comparing near-surface minimum temperatures, with a synoptic pressure gradient between Cape Campbell and Nelson, and Cape Campbell and Kaikoura. The magnitude of the synoptic pressure gradients on any one night has been used as a relative indication of ambient wind speed and direction above Marlborough's grape growing region. Observations of synoptic pressure gradient that are positioned closer to the intersection of zero-pressure gradient between Cape Campbell – Nelson and Cape Campbell – Kaikoura, are indicative of light ambient winds, whereas points positioned further away from the centre of the graph, are assumed to reflect stronger ambient winds. Each observation of synoptic pressure gradient has been classified into one of three categories of near-surface minimum temperature, warm nights (minimum temperature > 8°C), cool to mild nights (minimum temperature 1.5 to 7.9°C) and frost conditions (minimum temperature < 1.4°C), and the four plots reveal the frequency of

each class of minimum temperature as a function of the regional synoptic pressure gradient.

Figure 4.7a shows that Rapaura records the lowest incidence of frost conditions, and they are recorded over a narrow range of weak regional synoptic pressure gradients. By contrast Waihopai Valley (Figure 4.7b) is likely to record frost conditions more often, and they were recorded over a greater range of synoptic pressure gradients. Seddon (Figure 4.7c) and the upper Awatere Valley (Figure 4.7d) record a similar frequency of frost conditions, however, frost conditions at the upper Awatere AWS is spread over a greater range of regional synoptic pressure gradients, and this suggests that frost conditions occur during stronger ambient winds and for a wider range of ambient wind directions.

There are several examples where a specific synoptic pressure gradient will result in frost conditions at one AWS location and a warm night at another location, and this can result in a large spatial variation of near-surface minimum temperature. On one occasion a synoptic pressure gradient of -4.8 hPa between Cape Campbell and Kaikoura and +2.0 hPa between Cape Campbell and Nelson, (indicative of a strong north-west airstream over the region) resulted in frost conditions at Waihopai Valley (<1.4°C), and a warm night in Seddon (>8°C).

Two further examples where subtle changes in synoptic pressure gradient have produced large regional variations of near-surface temperature are illustrated in cases A and B in Figure 4.7. Case A is indicated by the larger red square and case B as a larger green square in Figure 4.7. Case A (10th April 2010) represents an overnight period of weak regional pressure gradients associated with light to moderate north-west winds, while case B (11th April 2010) is characterized by a greater regional pressure gradient and stronger north-west winds. The 0000 NZST sea level synoptic charts are displayed for April 10th and 11th 2010 in Figures 4.8a and 4.8b, while the effect of these synoptic situations on the near-surface temperature at 60 privately owned AWS is presented in

Figures 4.9a and 4.9b. The data used to create these plots is independent of the nine AWS that are used through the remainder of the thesis and accuracy of the data from these stations cannot be guaranteed. However, the most striking change between the temperature contour plots in Figures 4.9a and 4.9b is the spatial shift in the areas with coolest temperatures. During weaker synoptic pressure gradients (case A) the coolest 0600 NZST near-surface temperatures are distributed amongst several pockets in both the Wairau and Awatere Valleys. These areas represent known low spots within the surrounding topography, and coolest air has a tendency to stagnate in these areas during light wind conditions. As the synoptic pressure gradient over the region increases (case B), the areas of coolest near-surface temperatures are redistributed to the regions upper valleys (including the Waihopai and upper Awatere Valley), while remaining parts of the region are flushed of cold air by synoptic winds.

a)

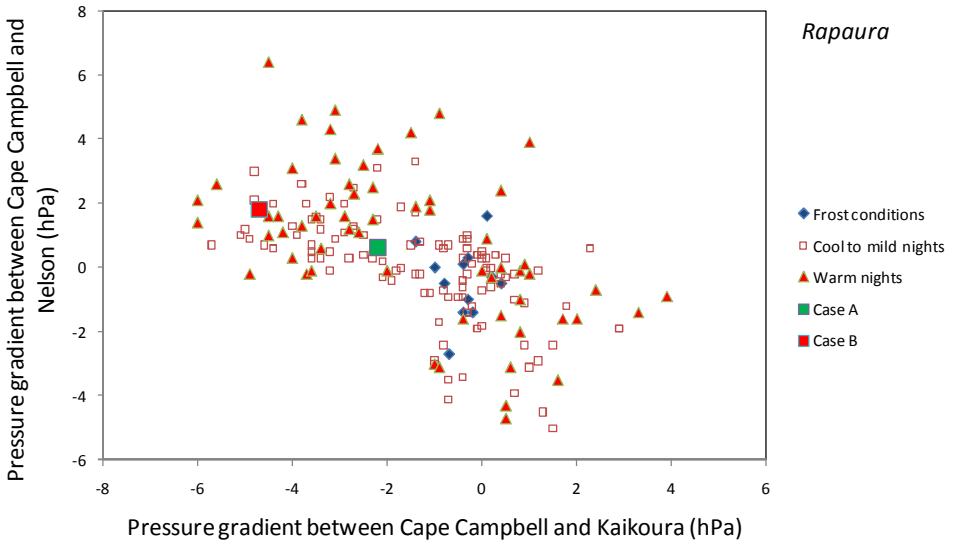

b)

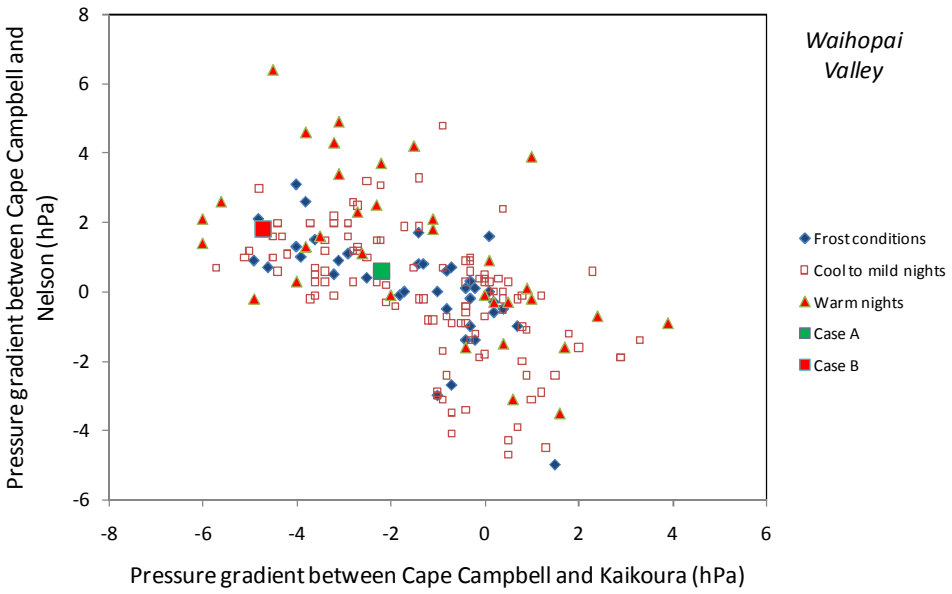
Waihopai Valley
Pressure gradient between Cape Campbell and Nelson (hPa)
Pressure gradient between Cape Campbell and Kaikoura (hPa)
8
6
4
2
0
-2
-4
-6
-8
-6
-4
-2
0
2
4
6
Frost conditions
Cool to mild nights
Warm nights
Case A
Case B

c)

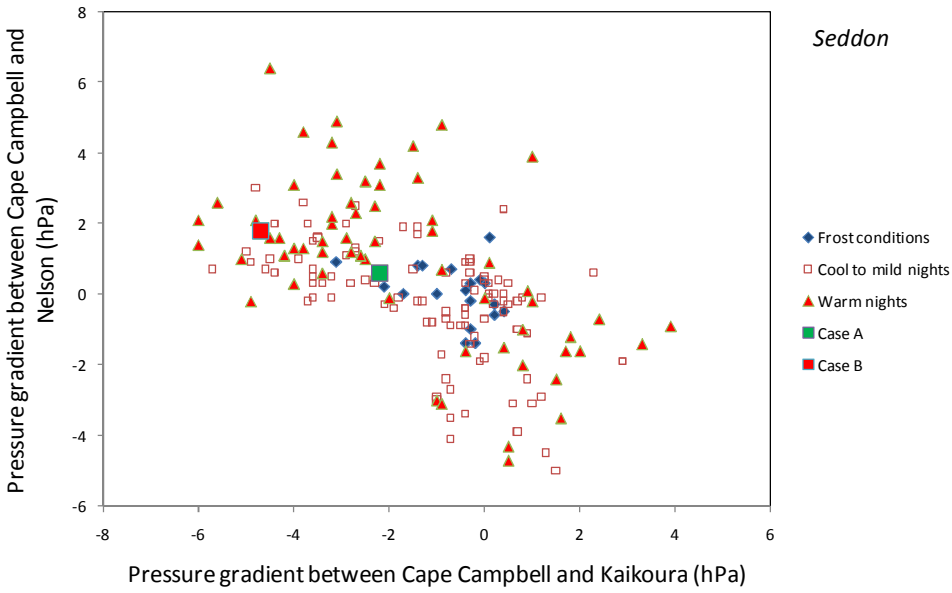
Seddon
Pressure gradient between Cape Campbell and Nelson (hPa)
Pressure gradient between Cape Campbell and Kaikoura (hPa)
8
6
4
2
0
-2
-4
-6
-8
-6
-4
-2
0
2
4
6
Frost conditions
Cool to mild nights
Warm nights
Case A
Case B

d)

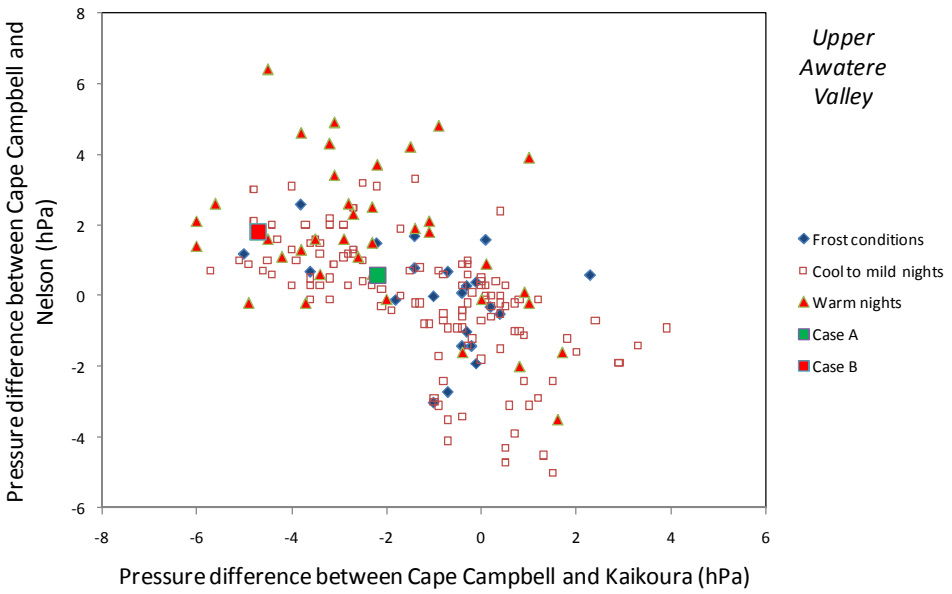

Figure 4.7 *Regional synoptic pressure gradients in hectopascals (hPa) at 0000 NZST between Cape Campbell, Nelson, and Kaikoura, and near-surface minimum temperatures for September and October 2009 – 2011 at a) Rapaura, b) Waihopai Valley, c) Seddon and d) Upper Awatere Valley. The 0600 NZST near-surface temperatures are categorized as a warm night (> 8°C, red triangle), cool to mild night (1 – 7.9°C red open square) or frost conditions (< 1.4°C, blue diamond). The atmospheric gradient over the region for case studies A and B are indicated by the larger green and red squares.*

a)

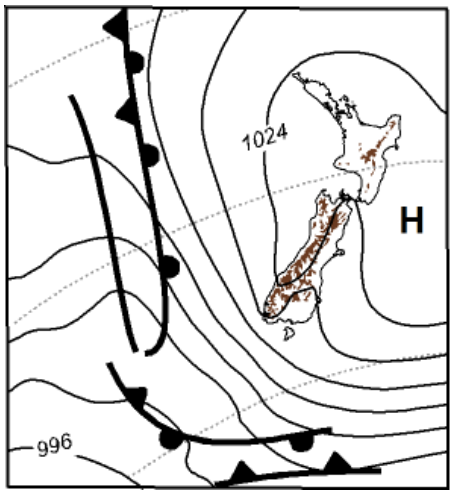

b)

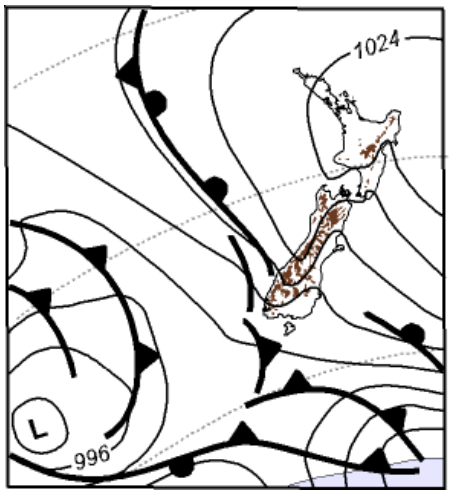

Figure 4.8 *Mean sea level synoptic charts for 0000 NZST a) April 10th 2010 and b) April 11th 2010.*

a)

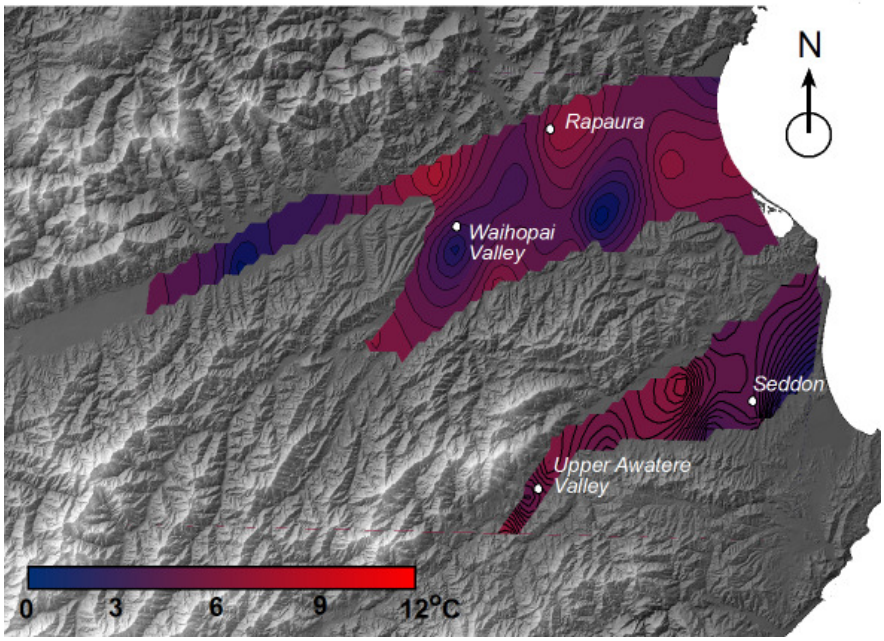

b)

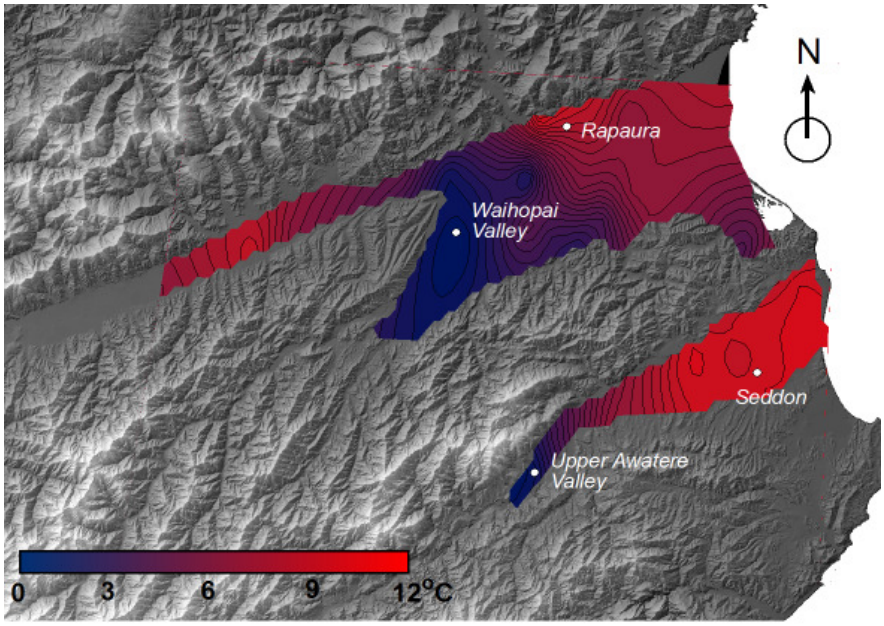

Figure 4.9 *Near-surface air temperatures as observed from 60 private weather stations on two consecutive mornings in April 2010: a) weak – moderate atmospheric pressure gradient across the region, whereas in b) moderate – strong atmospheric pressure gradient across the region. The subtle change in the pressure gradient across the region amounts to a marked re-distribution of coolest air (deeper blue shading).*

4.3 Wind

Pascoe (1983) identified the prevailing wind direction at ridge top height above the region as almost due westerly throughout the year. However, he also acknowledged that wind directions at the surface are greatly influenced by local topography. Figure 4.10 displays the mean hourly daytime wind velocity between 0800 – 2000 NZST from the network of privately owned AWS for the period 2008 – 2013. The wind rose plots confirm a modifying effect from the local topography, as prevailing wind directions vary considerably around the region from a relatively even spread of directions at Wairau Valley coast, compared to the strong topographically aligned winds at Wairau Valley Township and the upper Awatere Valley. West to south winds dominate the daily wind regimes of areas further inland at Wairau Valley Township and Waihopai Valley, while north or north-east winds prevail in areas closer to the coast. A large component of the wind regime of the upper Awatere Valley is believed to be thermally-induced, where north-easterly winds blow up-valley by day and south to south-westerly winds blow down-valley at night. When synoptic gradients from the west become very strong, the area may be subject to quite sudden ventilation, with very strong damaging winds.

Wind data for the Marlborough region has been displayed using WRPLOT software and the results have been superimposed on a topographic map of the Marlborough region. WRPLOT creates multi-functional wind rose plots of wind speed and direction where the orientation of each segment indicates wind direction and the length of each segment determines the frequency of occurrence. Wind speed is illustrated by the colour and scale to the bottom left of the map. Each wind segment is representative of a 15° increment of wind direction.

The wind rose plots for areas south of Blenheim (Seddon) and coastal areas of the Wairau Valley reveal a secondary maximum of southerly winds, while other locations around the region remain completely sheltered from winds of this direction. Pascoe

(1983) acknowledged that southerly winds may be of storm-force in Cook Strait while at Blenheim, only 30 km away, conditions will often be perfectly calm. This phenomenon is attributed to shelter provided to inland Marlborough from the Kaikoura Ranges. The incidence of strong south to south-westerly winds at the Waihopai AWS, are actually observed during west or west-south-westerly airflow, which is topographically aligned to blow down the valley.

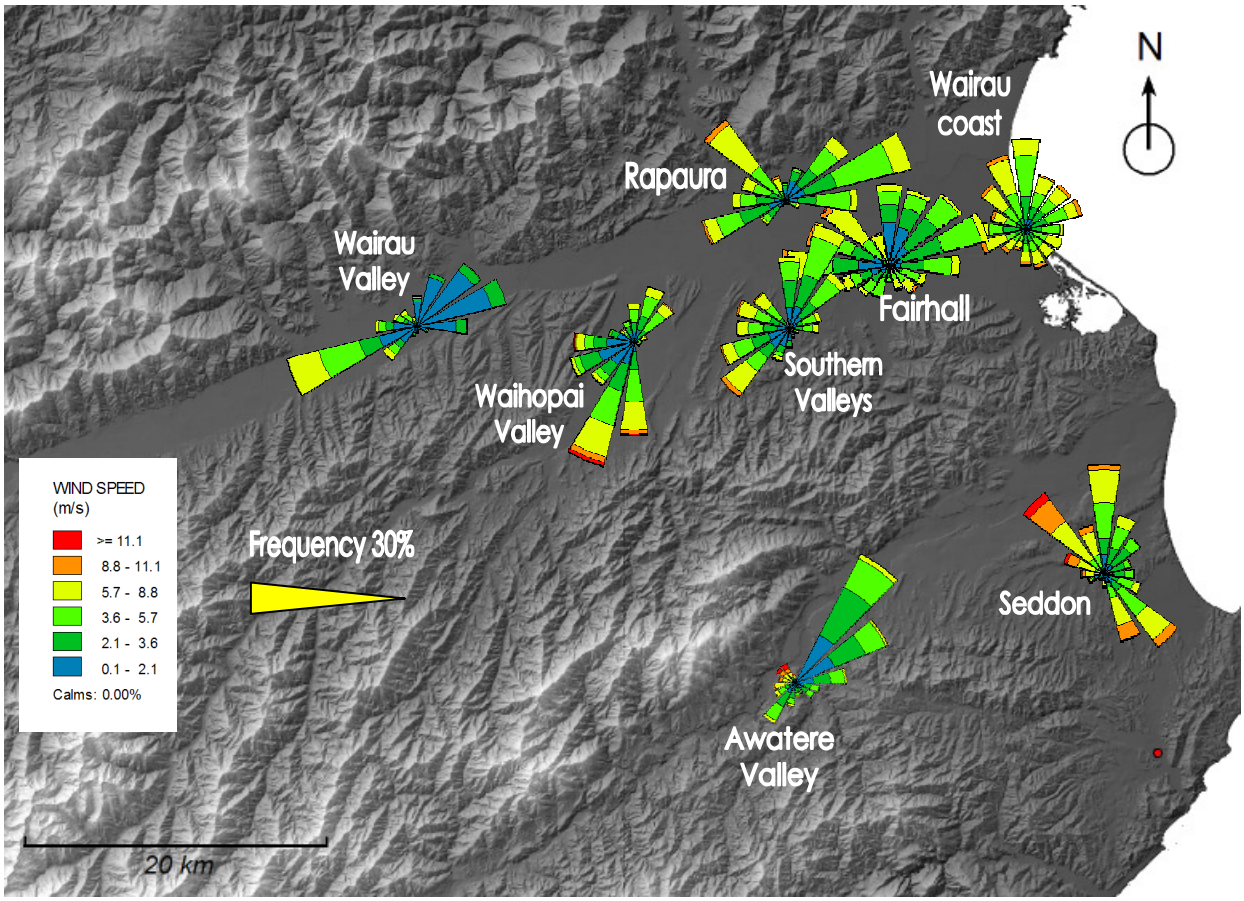

Figure 4.10 *Wind rise plots showing mean hourly wind speed and direction for the network of privately owned AWS between the daytime hours of 0800 NZST and 2000 NZST, 2009 – 2011. Averaged hourly wind directions reveal strong topographic alignment in Wairau and Waihopai Valley. Long-term wind data from Ward is not available.*

The contribution of thermally-induced winds to a location's wind regime can be significant in areas that remain sheltered from synoptic airflows, such as Waihopai Valley

and the upper Awatere Valley. The wind rose plots superimposed on the region in Figure 4.11 illustrate the mean hourly night time wind data, between the hours of 2100 NZST and 0700 NZST. Wind conditions during these times are frequently associated with minimum near-surface temperatures, and the presentation of wind data in this manner provides an opportunity to examine the spatial frequency of very light wind conditions that are related to cold-air stagnation events. Soler et al. (2002) defined the optimal near-surface wind speed required for cold-air stagnation as being less than 2 m s^{-1} and this is conveniently shown by the lightest wind category (blue colour) in the wind rose plots.

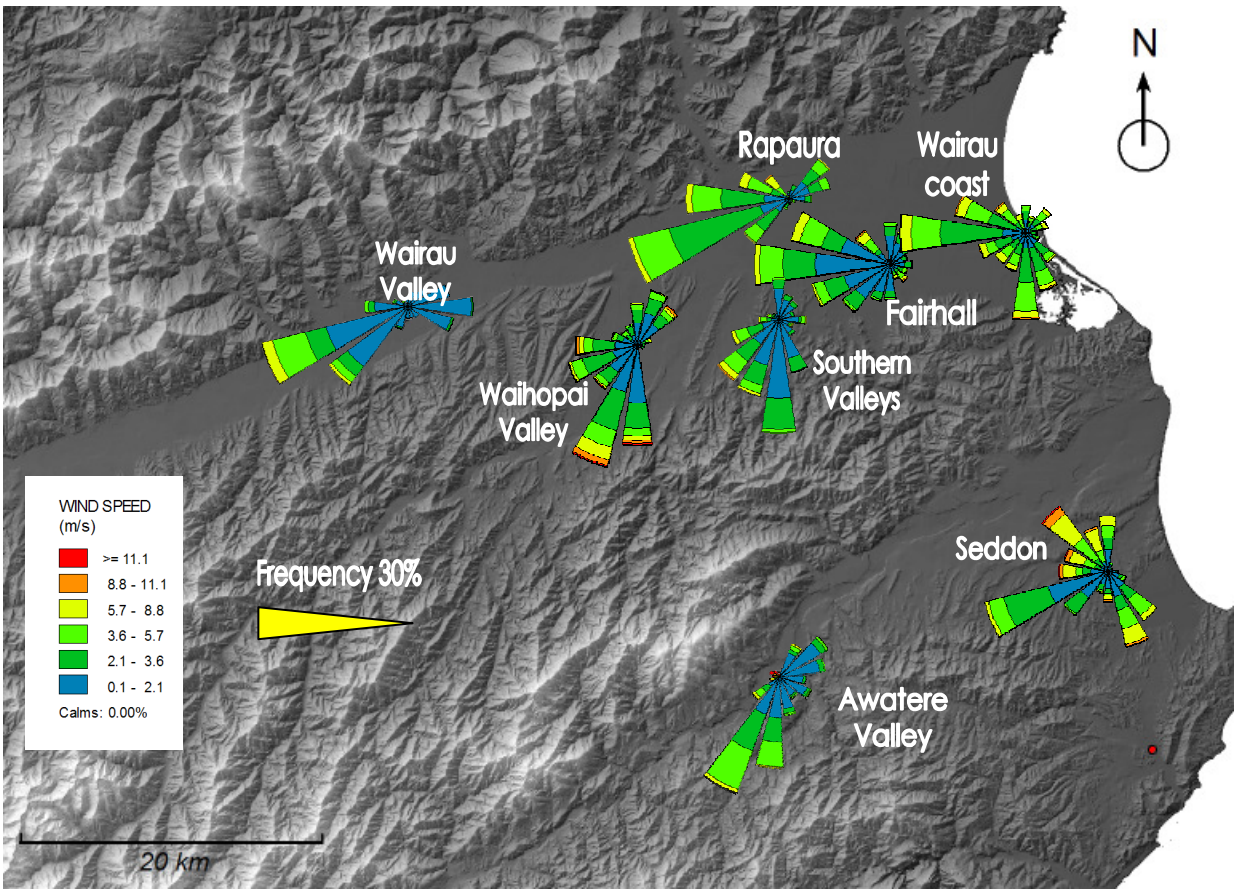

Figure 4.11 *Wind rose plots showing mean hourly wind speed and direction for the network of privately owned AWS between the night time hours of 2100 NZST and 0700 NZST, 2009 – 2011. Averaged hourly wind directions are increasingly dominated by thermal-induced drainage winds.*

The wind rose plots in Figure 4.11 reveal an increased frequency of light westerly and south-westerly winds and a reduced frequency of north-west and north-easterly winds, when compared with Figure 4.10. As the overnight data sets include periods of cloud and occasions when synoptic winds are strong enough to cause overnight ventilation, the wind rose plots do not show the true spatial magnitudes of cold-air drainage. However, the wind rose plots reveal a number of local terrain-induced peculiarities, such as a higher frequency of light southerly winds at Southern Valleys AWS, and south-south-westerly winds at the upper Awatere Valley AWS, which are known to conform to cold-air drainage in these locations.

In Table 4.2, the frequency of very light winds at (< 2 m s^{-1}) between 2100 NZST and 0700 NZST has been compared with the incidence of frost conditions (< 1°C) for the years 2009 – 2011. The r^2 for this relationship is 0.6, suggesting a strong relationship between the increased frequency of very light winds and increased incidence of frost. The association however is not perfect, and this is believed to reflect the presence of other meteorological variables that cannot be excluded from the data set, such as cloud cover.

Table 4.2 *Comparison of the frequency of wind speeds below 2.0 m s^{-1} with incidence of frost conditions around the network of privately owned AWS, 2009 – 2011.*

AWS location	Frequency < 2.0 m s^{-1}	Number of frosts
Fairhall	56%	99
Rapaura	30%	31
Wairau Coast	25%	44
Southern Valleys	63%	74
Waihopai Valley	49%	102
Wairau Valley	81%	97
Seddon	38%	49
Upper Awatere Valley	40%	41

4.4 Rainfall

The spatial variation of rainfall in Marlborough averaged for the years 1940 - 1971 suggests that annual rainfall totals range from less than 600 mm near Seddon, to over 5000 mm in the mountainous ranges in the south-west of region (Pascoe 1983). Blenheim was reported to receive an annual total of 664 mm. Pascoe (1983) also concluded that rainfall appeared to be evenly distributed throughout the year in the mountainous areas, but that areas nearer the coast revealed a slight wintertime maximum. Rainfall variability from one season and one year to the next is high in Marlborough, and droughts are a common feature of the climate.

The annual rainfall statistics were updated for the region by NIWA in 2012 for the period 1981 – 2010 and illustrated in Figure 4.12. In this most recent 30 year averaging period the annual rainfall for Blenheim Research AWS is 647 mm.

Long term rainfall statistics from the privately owned network of AWS are not available, for the relatively short-term data collection periods are not sufficient to provide an annual average. Until recently, the earlier versions of the rain gauges used in the privately owned AWS network were prone to blocking, and this had lead to erroneous monthly totals at times.

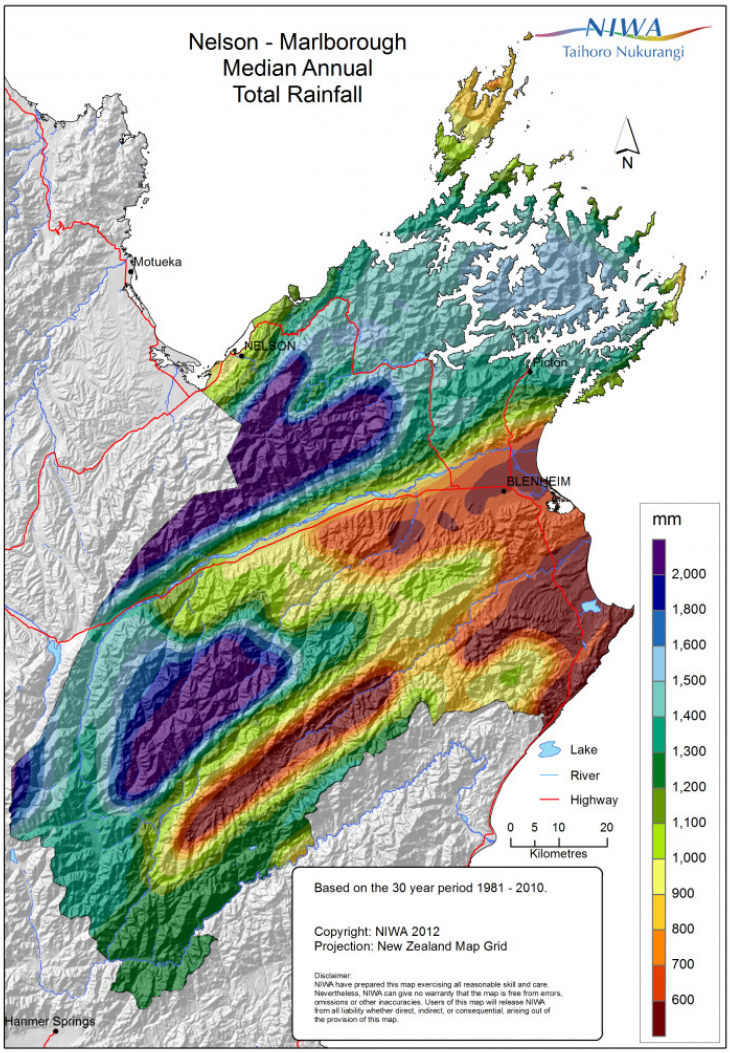

Figure 4.12 *Average annual rainfall for the Marlborough region, based on the 30 year period 1981 – 2010. (source http://www.niwa.co.nz/gallery/rainfall-14).*

4.5 Summary

The New Zealand MetService Publication by Pascoe (1983) has been extended by the inclusion of near-surface temperature and wind observations from nine AWS located within the grape growing areas of the region. Although analysis has revealed relatively small variations of mean temperature within the grape growing areas, there are large

variations in both the incidence and severity of frost. Some of this variation appears to be related to local frequencies of very light winds (< 2.0 m s^{-1}). The frequency of thermally-induced winds throughout the region is high, and is characterised by onshore (north-easterly) winds by day and west to south-west winds at night.

The climate of the Marlborough region could be summarised as having wide variations of both near-surface temperature and rainfall, with very high sunshine hours in the north-east. While the region is ideally suited for agriculture, the complex topography surrounding the region predisposes the region to a high spatial variation of minimum temperature, including the risk of spring frost. An investigation into the meteorological processes and mechanisms that create this phenomenon will form the basis of the following three results chapters.

Chapter 5

Effects of synoptic circulation and ridge top wind on minimum temperature

5.1 Introduction

In this first results chapter relationships are explored between Kidson synoptic types, local meteorological observations, the regional variation of minimum temperature and regional frequency of cold nights. The chapter examines the relationship between synoptic type over the New Zealand region as defined by Kidson (2000) and the regional variation of minimum temperature and occurrence of frost conditions.

A synoptic map classification system developed for New Zealand by Kidson (2000) distinguishes three broad weather regimes: trough, zonal and blocking. These regimes are based on twelve synoptic types that broadly encompass New Zealand's daily weather. Although many studies in synoptic climatology have been based on map classifications (as reviewed by Kidson 1997), analysis of the near-surface temperatures using Kidson types is uncommon in the literature. The following section describes the synoptic climatological approach and this is followed by a summary of local and international synoptic climatological studies.

5.2 Synoptic climatology

There is a long history of interest in classifying the pressure patterns on synoptic weather maps into a small number of categories for the purpose of studying local climatic conditions stratified on a meaningful basis. One of the many reasons for attempting these studies is the improvement of daily weather forecasting. However, according to

Barry and Carleton (2001) identification of discrete categories of pressure patterns or circulation types can present several problems:

1. Atmospheric modes are continuous which renders the delineation of boundaries between classes difficult.
2. Pressure systems arrive in varying intensities and decisions have to be made when to include or neglect small or weak features.
3. Addressing seasonal variation in type characteristics. For example, weather systems may be of greatest intensity in winter, when equator-pole heat differences are greatest.

Yarnal (1993) provided a definition of synoptic climatology as "relating the atmospheric circulation to the surface environment". He then refined the definition by saying "synoptic climatology integrates the simultaneous atmospheric dynamics and coupled response of the surface environment". Developments in synoptic climatology conform to either "traditional" or, from 1990, "empirical downscaling" techniques. Traditional climatology emphasised the use of 'classification schemes' that were derived from a variety of methods, such as manual typing, correlation based analyses, eigenvector-based analyses, compositing, indexing and self-organising maps. Yarnel et al. (2001) described each of these methods and provided recent examples of their use from the literature. He concluded by saying that traditional approaches to synoptic climatology remain popular and useful, but because the relationships between atmospheric circulation and the near-surface climate are empirical, the physical mechanisms that link the atmosphere to the environment must be inferred and cannot be certain. As the use of traditional synoptic climatological approaches for forecasting rely on small sets of discrete weather types, they are generally out-performed by other empirical and numerical predictive techniques.

Yarnel et al. (2001) distinguish empirical down-scaling from conventional synoptic climatology, by stating that the traditional goal of synoptic climatology is to understand

the relationships between the atmospheric circulation and the surface environment, while empirical downscaling focuses on trying to describe the relationships mathematically by development of NWP modelling. One important aspect of empirical down-scaling is the assumption that relationships between the atmosphere and the environment do not change over time. Yarnel et al. (2001) acknowledged the contributions that NWP modelling has provided to regional and local weather forecasting, however as a result, there has been a tendency to move away from describing physical interpretations of atmospheric - surface relationships, while attention has focussed on improving model accuracy.

5.2.1 International applications of synoptic climatology

A good international example of the use of traditional synoptic climatological approaches, relevant to this research, is the exploration of climate-viticulture relationships by Jones and Davis (2000). In this study, a regional circulation and local air mass synoptic climatology was developed for Bordeaux, France, to explain the relationship between climate variables of wind, temperature, moisture and cloud cover, and the mean phenology of the grapevine. This methodology was achieved by dividing the vintage into four phenological stages of bud break, floraison, véraison, and harvest, and this provided for a more comprehensive analysis of climatic influences on the timing and duration of each phenological stage. In this manner, the process allowed for the identification of specific air masses that are most influential in determining both yield and quality of grapes. It was found that a small number of synoptic clusters greatly affected viticultural potential throughout the growing season, and that these (short-lived) synoptic events would be masked by the use of many earlier traditional synoptic climatological approaches that use a greater proportion of averaged climatological parameters.

Nolan (2013) developed a synoptic climatology for Lake El'gygytgyn in Russia and explored modern climate trends affecting near-surface air temperatures to aid in paleoclimate reconstructions of a 3.6 million-year-old sediment core. Their procedure involved the traditional approach of 'self-organised mapping', and identified 35 synoptic weather patterns that influenced the study area from 1961 – 2009. The 50-year period of data indicated a 3°C increase in surface temperatures during the spring and autumn periods that they attributed, by an order of magnitude, to the effects of a general global warming, rather than changes in storm tracks.

Schubert and Sellers (1997) used a statistical model to downscale the local daily temperature extremes from synoptic-scale atmospheric circulation patterns in the Australian region. The aim of their research was to downscale climate predictions from GCM's to the mesoscale, so that the data could be used to form improved predictions of regional climate change scenarios, in particular, local daily extremes in temperature. While their study was successful in establishing a relationship between the GCM daily pressure fields, and occurrence of local extreme temperatures for four locations, their success could have been partly attributed to the continental land mass of Australia, that helps to create more predictable air-mass distributions for significant periods of the year.

5.2.2 Local applications of synoptic climatology

One of the earlier studies applying synoptic climatology to New Zealand by Sturman et al. (1984) used a subjective synoptic classification scheme to examine atmospheric circulation over the South Island. The classification scheme identified four circulation indices that displayed distinct monthly trends over a 20 year period. It was found that the monthly strength of each index could be related to short-term climate variations, which caused significant local weather events and affected the New Zealand economy.

Hay and Fitzharris (1988) found a strong relationship between the frequency of synoptic weather types and the long-term behaviour of the Ivory Glacier. Their research concluded that any trends in frequency of summer weather types will produce changes in ablation. In a similar study by Neale and Fitzharris (1997), a synoptic climatology of snow melt near the Main Divide of the Southern Alps, concluded that the synoptic situation exerts a strong influence on the magnitude of the melt. Snow melt was found to be greatest during north-westerly storms and anticyclonic conditions. Different synoptic situations were found to generate different energy budgets, and these were found to be associated with distinct pulses of melt lasting about one week.

Basher and Thompson (1996) examined the relationships between sea surface temperatures and regional circulation anomalies for 1992, the coldest year since 1942 in New Zealand. They found that the cold temperatures were primarily a result of frequent southerly wind outbreaks associated with a strong El Niño event, superimposed on the effect of the Mt Pinatubo volcanic eruption which occurred in 1991.

Salinger and Mullen (1999) then studied trends in atmospheric circulation patterns over New Zealand from 1930 – 1994 and identified three periods of distinctly different circulation. They broadly summarised the effects of these changes on rainfall and mean temperature patterns for some regions of the country.

Jiang et al. (2004) was first to apply an obliquely rotated T-mode Principal Component Analysis (PCA) (Eigenvector-based analysis) in New Zealand. The technique was applied to mean sea-level reanalysis data from 1958 to 1996, and identified ten representative synoptic types. The synoptic weather type-local meteorology relationship was found to be consistent over different phases of the Southern Oscillation Index (SOI). In Jiang (2011), PCA was used on an extended data set (1958 – 2008) to update the number of different daily weather types to twelve. The updated synoptic weather types were then used by Jiang et al. (2011) to provide a probabilistic description of daily rainfall in

Auckland. The study concluded that high rainfall conditions corresponded to varied cyclonic synoptic states, while low rainfall conditions were associated with anticyclones. Recently, Jiang et al. (2013) also used the climatological index defined by Jiang (2011) in environmental studies to describe the synoptic climatology of air pollution episodes over Auckland.

Kidson (1994a) was first to apply an objective weather typing approach to the New Zealand region that was subsequently developed further by Kidson (1994b, 1997, 2000) and Kidson and Waterson (1995). These applications proved helpful in interpreting climate variability, improving the ability to forecast daily temperatures, to validate performance of climate models, and indicate perceived changes in atmospheric circulation. In spite of these functions, Kidson (2000) concluded that "for the New Zealand region synoptic climatological techniques are largely of qualitative value, as the variability of a climate element within a synoptic class is typically too large relative to the differences between classes". The twelve synoptic types defined by Kidson (2000) have been reproduced in Figure 5.1, and these synoptic types will provide the basis of further analysis in this chapter.

Renwick (2011) provided an update of the Kidson (2000) original time series of synoptic type classifications. It was concluded that the relative frequencies of occurrence of the types and regimes have not changed significantly over the past decade. Renwick also stated that the original Kidson (2000) regimes are still associated in plausible ways to the phase of the SOI cycle and to the polarity of the Southern Annular Mode (SAM).

Finally, in a recent application of Kidson synoptic types in New Zealand, Sturman and Quénol (2013) analysed changes to atmospheric circulation patterns in relation to temperature trends in several winegrowing regions of New Zealand. Their study concluded that an increased range between mean maximum and minimum temperatures in Marlborough could be attributed to an increased frequency of clear skies along the

east coast of the country, resulting from more frequent anticyclones, fewer low pressure systems, and increased zonal and southerly flow.

While many investigators have applied synoptic climatological principles to describe regional weather conditions during each type of airflow, Barry and Carleton (2001) noted that few studies have addressed the problem of linking aspects of daily surface weather to synoptic classification schemes, although notable exceptions to this include the studies by Jones and Davis 2000a and 2000b). This chapter explores the relationship between Kidson synoptic types and the regional variation of near-surface minimum temperature. The unique approach demonstrates the value of synoptic climatology in accounting for an aspect of daily surface weather in an area of complex terrain.

5.3 Data and methodology of analysis

In the following analysis, minimum temperature data are analysed for three spring periods (September 1st – November 30th) for the years 2009 – 2011 from nine surface-based AWS scattered throughout the Marlborough region (Figure 3.5). The spatial range in temperature for any given night is measured by the standard deviation of minimum temperatures from the nine AWS. A lower standard deviation is indicative of less variability of minimum temperatures between the AWS.

Initially, the frequency of Kidson weather types was calculated for a range of minimum temperature standard deviation (σ T_{min}) categories, and the statistical significance is explored using a contingency table and the Chi-square (χ^2) test. The relationship is then examined in more detail using box and whisker plots. A case study is then conducted of the Awatere Valley by correlating the Kidson classification with the differences in overnight minimum temperature between Seddon (lower Awatere Valley) and Welds Hill (upper Awatere Valley). Following this section, Kidson types are related to the spatial variation of the region's minimum temperatures and then more specifically to the

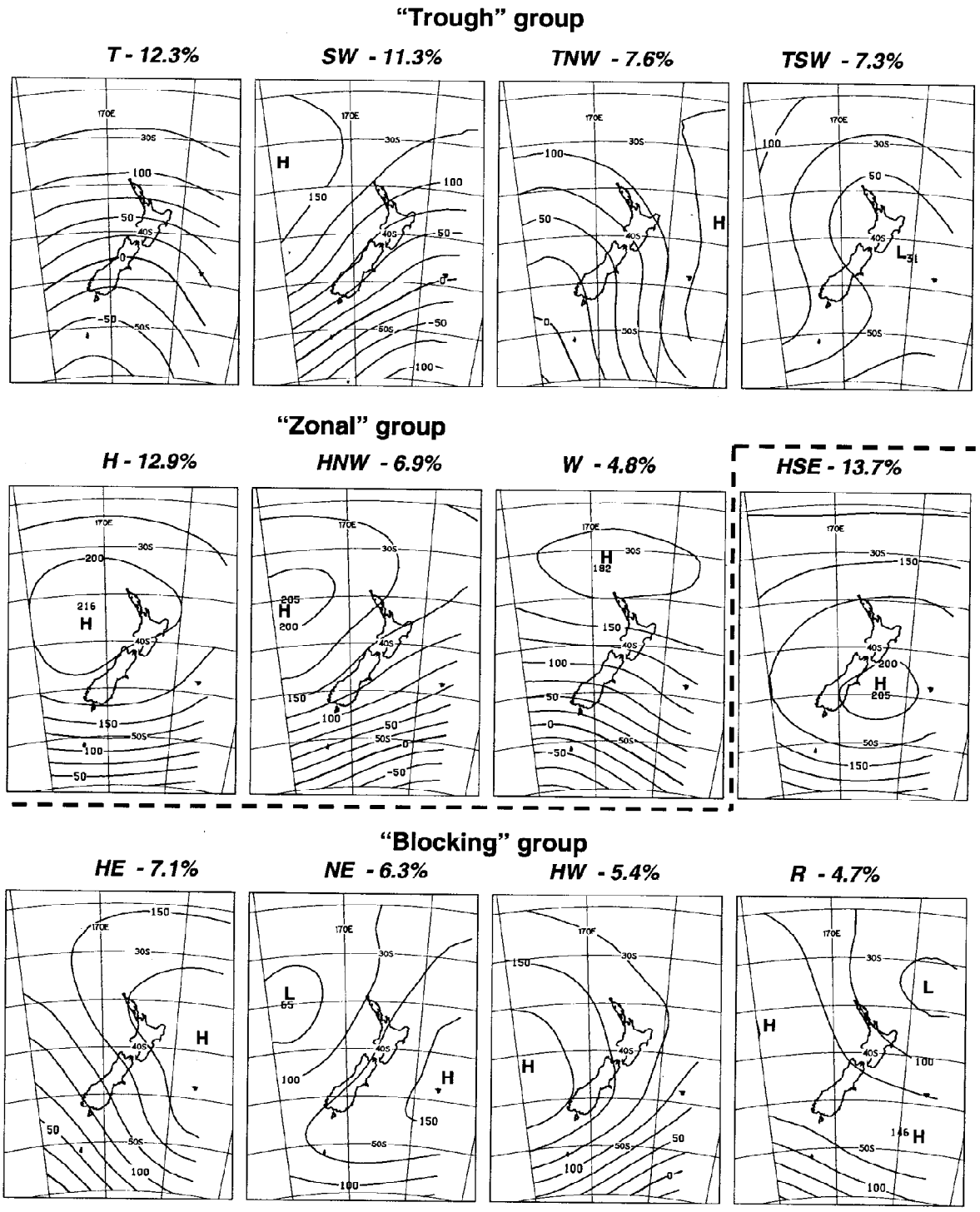

Figure 5.1 *Synoptic types as identified by Kidson (2000). Percentages denote climatological frequency of types. For an explanation of the groupings, refer to original text.*

incidence of frost conditions. In this chapter, frost conditions are defined as having a near-surface air temperature of < 1.4°C.

Finally, analysis draws upon meteorological data from an exposed ridge top AWS that is correlated with the region's spatial variation of minimum temperature and frost conditions. The aim is to reinforce the importance of interaction between synoptic weather, as defined by Kidson type, and the region's complex terrain. It is hypothesised that the analysis will provide evidence of the effects of local topographic sheltering on near-surface temperature.

5.3.1 The association between humidity, soil moisture and the spatial variability of minimum temperature

Humidity observations from the network of AWS were not considered as part of this research. The role of humidity in the development of frost and in frost prediction is multifaceted, and it is further complicated in Marlborough by the region's complex terrain. Results from early analysis of the role of humidity on frost in the region did not reveal significant associations between humidity prior to a frost and the occurrence of frost. Humidity was found to be unsuccessful as a predictor of frost as the region frequently undergoes air mass changes during the lead-up period to the time of the actual minimum temperature. Furthermore, under strongly stable atmospheric conditions, local AWS may remain completely decoupled from fluctuations in atmospheric moisture associated with interactions between the synoptic circulation and local terrain.

Reliable soil moisture observations are only available from two locations in the Marlborough region. These data are not expected to accurately represent the variability of soil moisture over the region. The role of soil moisture in frost occurrence is also highly complex, and is a reflection of the region's soil types and in particular water holding

capacities. Pascoe (1983) noted that the alluvial gravels of some parts of the region could mimic a continually dry surface, whereas areas of heavier soils could remain saturated for sometime following rain. Although a water-logged soil is more likely to hold heat during a radiation frost, the process is complicated by many other factors such as near-surface wind speed and vegetation cover.

5.4 Kidson synoptic type and spatial variability of minimum temperature

While each Kidson type can be associated with a predictable spectrum of local near-surface meteorological conditions by day, the interactions between synoptic winds and complex terrain are less predictable at night. Synoptic winds that are topographically channelled or forced through gaps in the terrain by day often decouple from parts of the region at night. The simultaneous ventilation and stagnation of different parts of the region can result in a large spatial variation of near-surface minimum temperature.

The overnight strengthening of a synoptic gradient under a particular Kidson type may not be reflected by a change in near-surface meteorological conditions in complex terrain. In these situations a change in near-surface wind and temperature can be abrupt, resulting in sudden ventilation of a particular area or sub-region. In complex terrain the relationships between synoptic gradient and near-surface weather are not linear as they also reflect parameters such as atmospheric stability and moisture.

In this section, the daily standard deviation of minimum temperature (σT_{min}) for three spring periods (2009 – 2011) are categorised into four classes: low (< 1), moderate (1 - 2), high (2 - 3) and very high (> 3). The midnight Kidson synoptic type is then ascribed to each day. The results are summarised in the contingency Table 4.1 below.

Analysis from the contingency table shows that Kidson types SW (trough), H (zonal) and HE (blocking) were among the three most frequent synoptic types governing the region's

climate over the analysis periods. However, they only account for 13% of σ T_{min} > 2°C. The Kidson synoptic type H was most frequently associated with a high spatial variation of minimum temperature, as 46% of cases recorded σ T_{min} > 2°C. When all the data are considered, only 20% of nights have σ T_{min} < 1°C, 51% of nights fall into the σ T_{min} 1 - 2°C range, 22% of nights have σ T_{min} of 2 - 3°C and only 7% have σ T_{min} > 3°C. The mean σ T_{min} for all nights (2009 – 2011) was calculated to be 1.7°C. The largest discrepancies between the observed and predicted frequencies occur when the count for the class of σ T_{min} or category of Kidson type is small, for example Kidson type TSW with σ T_{min} < 1°C had an expected frequency of occurrence of 2.7, yet it was observed 6 times.

Table 5.1 *Four classes of standard deviation representing the spatial variability of minimum temperature in the Marlborough region and associated Kidson type (2009 – 2011). Predicted frequencies for each class are indicated in brackets.*

Kidson type	**σ T_{min} < 1°C**	**σ T_{min} 1 - 2°C**	**σ T_{min} 2 - 3°C**	**σ T_{min}> 3°C**	**count**
T (trough)	2 *(5.5)*	13 *(13.8)*	8 *(5.8)*	4 *(1.9)*	27
SW (trough)	8 *(8.6)*	24 *(21.5)*	6 *(9.0)*	4 *(2.9)*	42
TNW (trough)	2 *(4.3)*	10 *(10.7)*	6 *(4.5)*	3 *(1.5)*	21
TSW (trough)	6 *(2.7)*	3 *(6.6)*	3 *(2.8)*	1 *(0.9)*	13
H (zonal)	4 *(8.3)*	18 *(20.9)*	13 *(8.8)*	6 *(2.8)*	41
HNW (zonal)	5 *(4.1)*	12 *(10.2)*	3 *(4.3)*	0 *(1.4)*	20
W (zonal)	8 *(4.9)*	12 *(12.3)*	4 *(5.2)*	0 *(1.7)*	24
HSE (blocking)	9 *(5.7)*	15 *(14.3)*	3 *(6.0)*	1 *(1.9)*	28
HE (blocking)	5 *(6.1)*	18 *(15.3)*	7 *(6.5)*	0 *(2.1)*	30
NE (blocking)	5 *(2.0)*	5 *(5.1)*	0 *(2.1)*	0 *(0.7)*	10
HW (blocking)	0 *(1.4)*	4 *(3.6)*	3 *(1.5)*	0 *(0.5)*	7
R (blocking)	2 *(2.2)*	6 *(5.6)*	3 *(2.4)*	0 *(0.8)*	11
count	56	140	59	19	274

Using the Chi-square (χ^2) test a null hypothesis for the distribution of data would be that "there is no significant difference between the expected and observed occurrence of a particular combination of Kidson type and category of σ T_{min}". In this case, the value of (χ^2) was calculated as 48.4 and using 33 degrees of freedom, the Chi-squared distribution table gives a 'p' value (probability that the difference between observed and predicted values is due to chance) of between 0.025 and 0.01. In this case, there is a 1 – 2.5% probability that the difference between the observed and expected frequencies is due to chance. Therefore, it is reasonable to assume that climatic processes or mechanisms are effectively producing a statistically significant relationship between the frequency of Kidson types and σ T_{min}.

A convenient method of comparing σ T_{min} with Kidson synoptic type is by way of box and whisker plot (Figure 5.2). The plot reveals that while the Kidson types associated with the trough weather group (T, SW TNW and TSW) have some of the greatest ranges of σ T_{min}, the Kidson type NE (from the blocking group) is more likely to be associated with smaller σ T_{min}, and a reduced spatial variation of minimum near-surface temperature. The highest mean σ T_{min} of 2.05°C was recorded during Kidson synoptic type H, and it is closely followed by Kidson types TNW (1.95°C) and T (1.90°C) respectively. Although Kidson type H is strongly associated with anticyclonic conditions and light ambient winds, the presence of cloud over the region is likely to reduce the spatial variation of near-surface temperatures on some occasions. The higher σ T_{min} during Kidson types H, TNW and T is believed to reflect local meteorological processes that develop within the region during cooling under a predominantly clear sky. These processes will become the focus of subsequent results chapters six and seven.

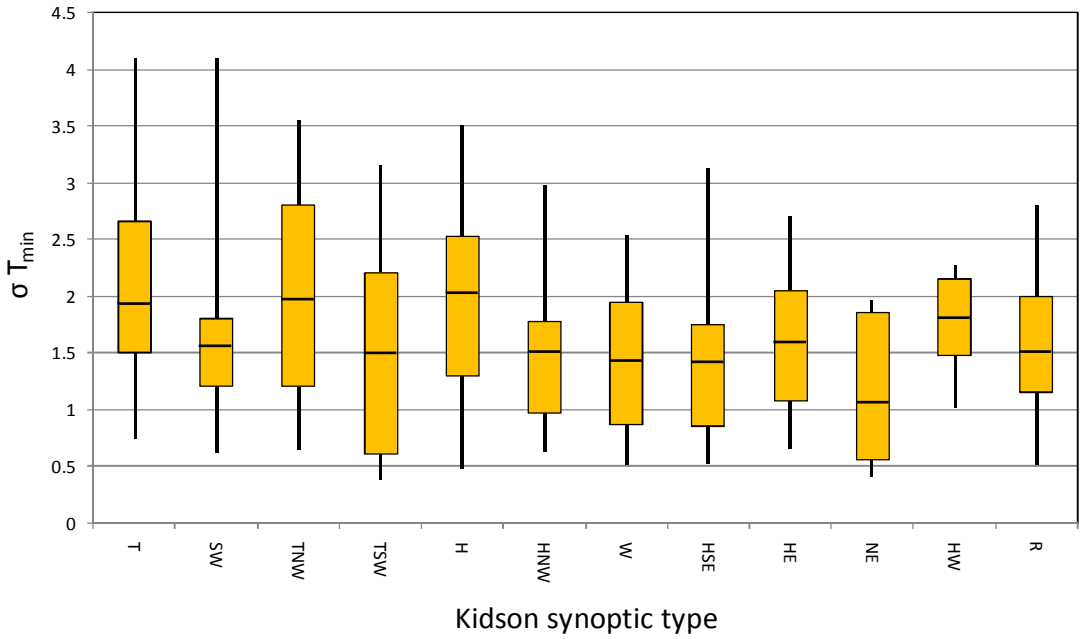

Figure 5.2 *Box and whisker plot of* σ T_{min} *in the Marlborough region calculated for each occasion of the Kidson type (2009 – 2011). The box represents the upper and lower quartiles, the whiskers the extreme high and low values, and the mean is indicated by the black line across each box.*

The analysis of Marlborough's spatial variation of T_{min} can be extended by comparing the mean minimum near-surface temperature at each AWS with Kidson type. Observations have shown that each synoptic type produces a different spatial pattern of near-surface minimum temperature around the region, and a change of synoptic type influences the minimum temperature more in some parts of the region than in others. Table 5.2 presents the average near-surface minimum temperature at each of the nine AWS for each Kidson type, and the standard deviation (σ) of the means for the spring periods (2009 – 2011).

Table 5.2 *The mean and standard deviation of near-surface minimum temperature (°C) at the network of AWS for each occurrence of Kidson type, for the spring periods (2009 – 2011) in Marlborough. (Southern Valleys has been abbreviated to S.V, and Wairau Valley Township to W.V)*

	Fairhall	**Rapaura**	**Wairau coast**	**S.V**	**Waihopai Valley**	**W.V**	**Seddon**	**Awatere Valley**	**Ward**	**Mean**	**σ**
T	6	7	7.2	6.1	5.4	5.6	6.7	5.6	6.8	6.3	0.63
SW	3.3	4.5	4.8	3	2.9	3.1	4.0	2.9	3.9	3.6	0.68
TNW	6.4	7.3	7.5	6.3	5.6	5.5	7.4	6.1	7.5	6.6	0.77
TSW	5.5	6.2	6.3	5.5	4.6	3.5	5.5	5.6	6.6	5.5	0.89
H	2.7	4.6	4.6	3	2.0	2.4	3.8	3.8	3.8	3.4	0.88
HNW	2.9	4.9	4.7	3.1	2.1	3.1	3.9	4.3	3.5	3.6	0.86
W	6.3	7.3	8.3	6.4	4.8	5.1	7.5	5.6	6.7	6.4	1.09
HSE	2.9	4.3	4.7	3.3	1.6	1.2	4.4	3.9	4.2	3.4	1.19
HE	5.5	7.4	7.6	5.8	4.4	4.3	7.8	6.3	8.4	6.4	1.41
NE	6	7	7.6	6.2	5.6	4.9	6.9	6.9	6.5	6.4	0.77
HW	-0.7	0.9	0.9	-0.6	-1.7	-1.9	2.1	1.6	2.1	0.3	1.47
R	4.1	4.7	5.1	4.1	3.3	2.0	5.0	4.4	5.0	4.2	0.95
Mean	4.3	5.7	5.9	4.4	3.5	3.5	5.5	4.7	5.5	4.8	0.87
σ	2.03	1.83	1.98	2.02	2.07	2.06	1.75	1.48	1.84	1.90	

The results presented in Table 5.2 show that for the region as a whole, the warmest mean near-surface minimum temperatures occur during TNW, although this Kidson type does not produce the warmest overnight minimum temperatures in all locations. The coolest overnight minimum temperatures occur region-wide during HW and this frequently resulted in frost. While a 'greater number' of frost events occur during Kidson type H in any given spring season, Kidson type HW (associated with cold southerly wind outbreaks) is 'more likely' to result in frost.

Waihopai Valley AWS recorded the coolest mean T_{min} of 3.5°C and also the greatest variability of minimum temperature (σ of 2.07°C), as a function of Kidson type. The result is followed very closely by Wairau Valley Township. The higher variations of T_{min} as a function of Kidson type at these locations, reflects the increased sheltering provided by

terrain during some Kidson types, whilst complete ventilation still occurs on other occasions. In contrast the upper Awatere Valley recorded the least variability of T_{min} as a function of Kidson type with σ of 1.48°C. The reduced variation of T_{min} at the Awatere AWS is believed to reflect a higher incidence of strong thermally-induced drainage winds that modify T_{min} under a wide range of Kidson types.

The results in Table 5.2 are more easily visualised by the sequence of maps in Figure 5.3 (a – l). Each map of the Marlborough region reflects the average T_{min} for the Kidson type indicated in the top right hand corner of the map.

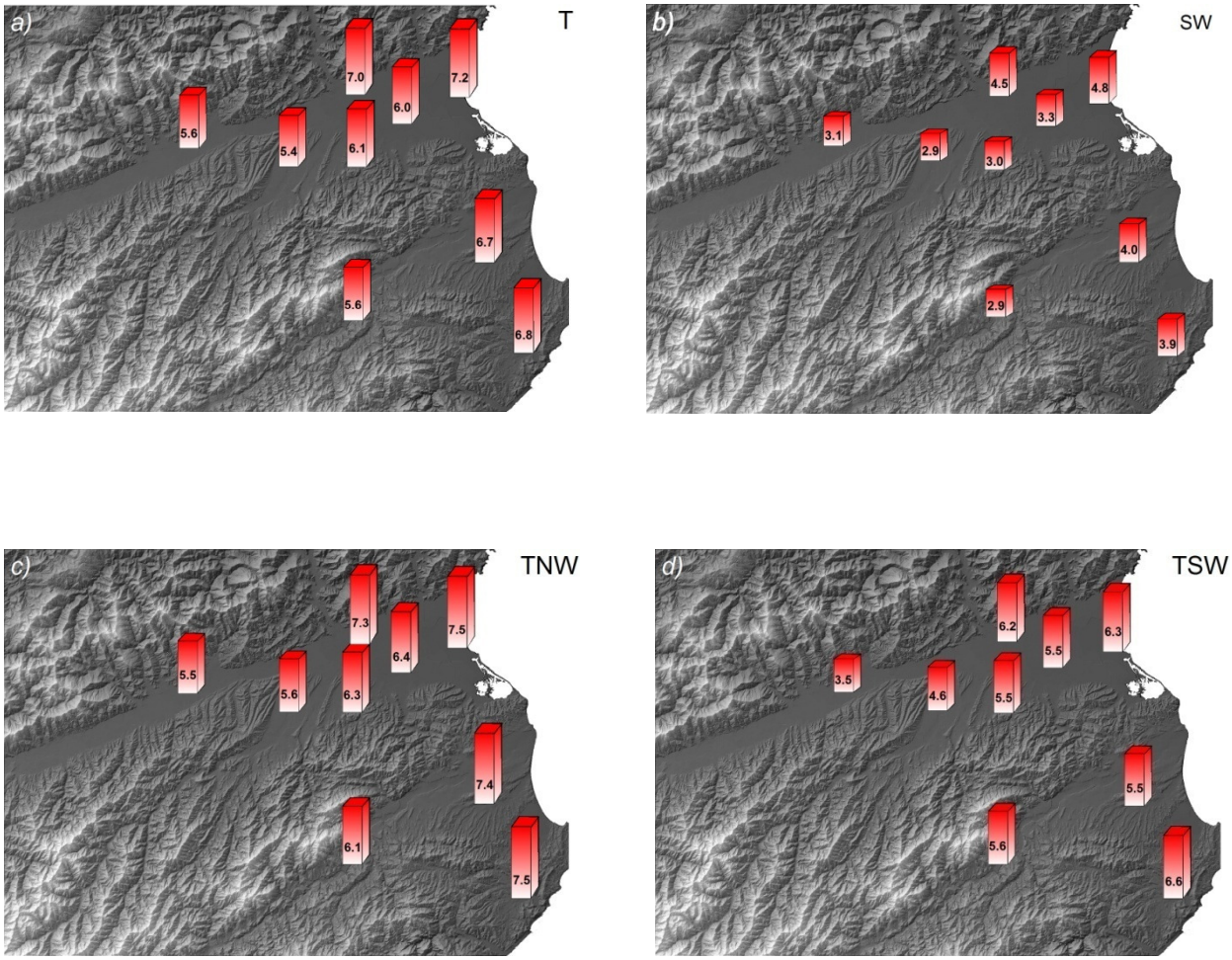

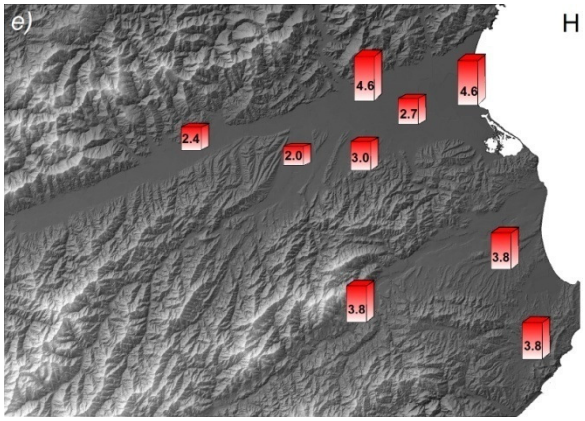
e)
H
4.6
4.6
2.7
2.4
2.0
3.0
3.8
3.8
3.8

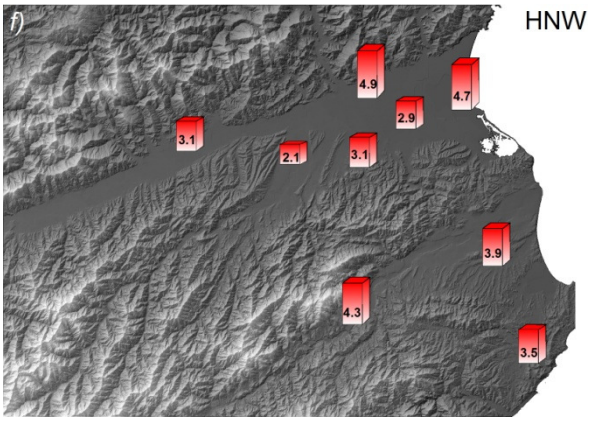
f)
HNW
4.9
4.7
2.9
3.1
2.1
3.1
3.9
4.3
3.5

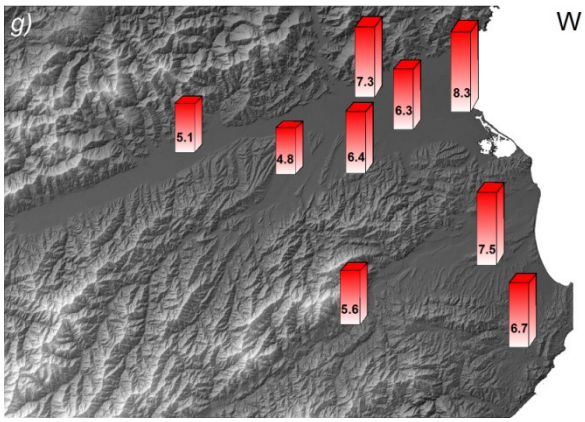
g)
W
7.3
8.3
6.3
5.1
4.8
6.4
7.5
5.6
6.7

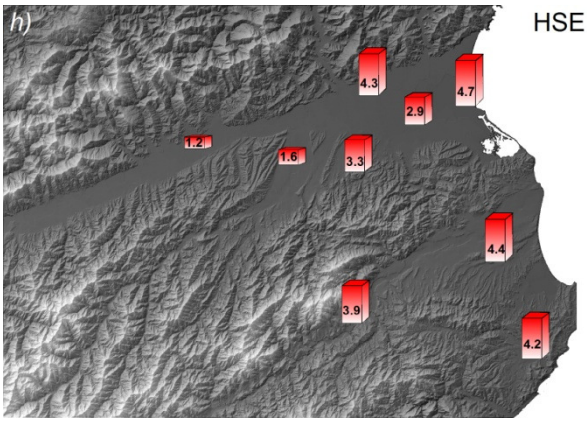
h)
HSE
4.3
4.7
2.9
1.2
1.6
3.3
4.4
3.9
4.2

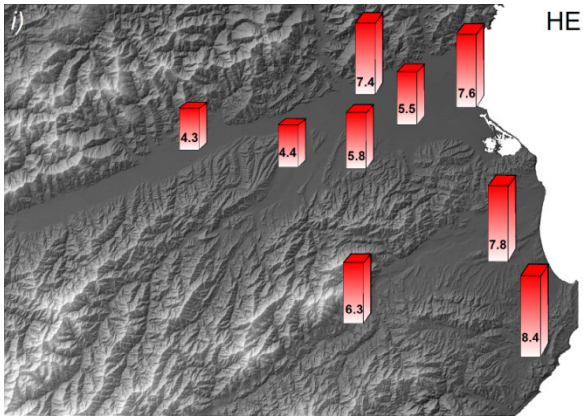
i)
HE
7.4
7.6
5.5
4.3
4.4
5.8
7.8
6.3
8.4

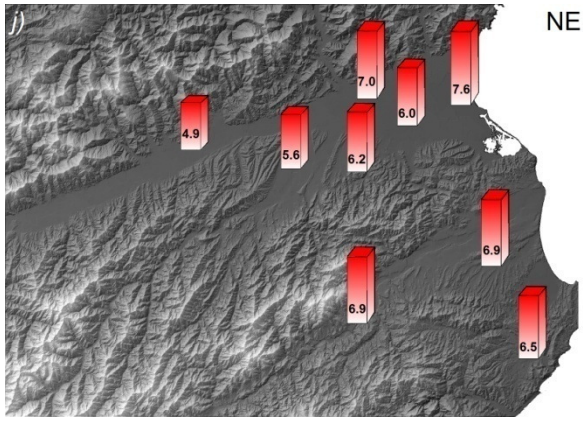
j)
NE
7.0
7.6
6.0
4.9
5.6
6.2
6.9
6.9
6.5

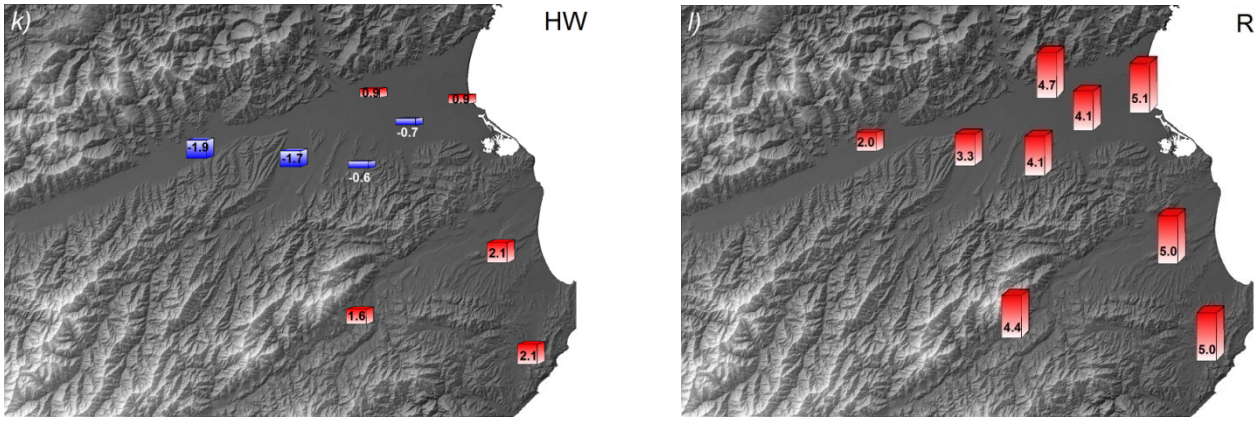

Figure 5.3 (a – l) *The mean near-surface minimum temperature recorded at each of the nine AWS for the twelve Kidson types, September – November 2009 - 2011. The average minimum temperature is represented by the height of the column, and the mean minimum temperature (°C) for the respective Kidson type is displayed on each column. The Kidson type for each map is located in the top right hand corner.*

5.4.1 Case study: Awatere Valley

To extend the analysis of Kidson type and spatial variability of T_{min}, the difference in T_{min} between Seddon and Welds Hill in the Awatere Valley are examined for the spring periods of 2009 – 2011. Seddon is located in the wider lower region of the valley, where adjacent hills are not only further away, but lower in height. Welds Hill is situated in the narrow upper section of the valley surrounded by steep mountainous terrain (Figure 3.5). The difference in T_{min} has been calculated by subtracting the minimum temperature at Welds Hill from the minimum temperature at Seddon. The temperature difference was then regressed with the adjacent ridge top wind speed for each of the twelve Kidson types, and results are summarised in Table 5.3 below.

Table 5.3 *Summary analysis of minimum temperature differential between Seddon and Welds Hill based on Kidson type. Frequency % describes the frequency of cooler temperatures at either Seddon or Welds Hill for the specific Kidson type, Ave temp diff °C is the mean temperature difference per occasion and Ridge ms^{-1} is the mean overnight wind speed at the ridge top AWS.*

	Seddon cooler			Welds Hill cooler		
Kidson type	Frequency %	Ave temp difference °C	Ridge m s^{-1}	Frequency %	Ave temp difference °C	Ridge m s^{-1}
H	51	2.0	5.2	49	1.9	8.5
HE	20	0.9	8.6	80	2.1	10.0
HNW	45	2.8	5.8	55	1.4	8.5
HSE	32	3.1	7.5	68	2.1	8.4
SW	26	0.8	5.6	74	1.7	8.7
T	26	1.6	8.2	74	2.0	9.7
TNW	14	1.6	9.2	86	1.4	8.5
W	21	0.9	8.1	79	2.7	10.5
HW	43	2.3	7.5	57	2.6	6.2
TSW	45	1.4	7.3	54	1.0	8.3
R	36	1.9	5.9	64	1.9	9.6
NE	40	1.4	5.6	60	1.0	8.0

The results in Table 5 .3 revealed a number of broader features about the evolution of T_{min} between the upper and lower Awatere Valley. Welds Hill in the upper Awatere Valley records cooler T_{min} most of the time, and the occurrence is more likely to be associated with stronger ridge top wind speeds. Cooler near-surface temperatures at Seddon are generally associated with reduced mean ridge top wind speeds. The only Kidson type that favours the development of lower T_{min} in Seddon, compared to Welds Hill in the upper Awatere Valley is type H (51%).

The results suggest that the Awatere Valley AWS is sheltered by the proximity of steep terrain from a range of synoptic air flows, in particular Kidson types W and HW, and that on these occasions near-surface cooling may continue in spite of simultaneous ventilation of the lower Awatere Valley at Seddon. Cooler temperatures that are often recorded at Seddon during lighter ridge top wind speeds are thought to be attributed to strong drainage winds that have been shown to modify T_{min} in the upper region of the Awatere Valley. The strong drainage winds are responsible for mixing warmer air to the surface during anticyclonic synoptic conditions.

5.5 Frost conditions and Kidson type

As indicated earlier in the chapter, a cold night during the spring months for the region is defined as a minimum temperature of +1.4°C or lower. This temperature threshold is important for the local grape industry and represents the point at which most frost protection systems are engaged to protect crops. An improved understanding of the broader synoptic situations and the meteorology that results in cold nights, will improve attempts at down-scaling the general forecasts that are often used for the derivation of local frost predictions.

In the following contingency table (Table 5.4), Kidson synoptic type has been analysed on the basis of producing frost conditions (< 1.4°C) at each of the nine AWS. The highest numbers of frost events have been highlighted in red bold font, and the second to most frequent occurrence of Kidson type is coloured red, but is normal font.

While Table 5.4 demonstrates that the highest number of frost conditions occurred with three Kidson types (H, HSE, and SW), the greatest likelihood of frost conditions occurred during Kidson type HW in most of the Wairau Valley, with the exception of Wairau Valley township. Waihopai Valley recorded frost conditions on every occasion of Kidson type HW. Kidson type HW also produces the highest σT_{min} and this supports the association

between the occurrence of frost and a high spatial variation of T_{min}. The cool southerly winds that accompany the HW Kidosn type are often associated with a clear, dry atmosphere, in the lee of the Seaward and Inland Kaikoura Ranges.

Table 5.4 *The frequency (%) of frost conditions as a function of Kidson synoptic type for the privately owned network of AWS in Marlborough, September – November 2009 – 2011. The actual number of frost events for each Kidson type is indicated in brackets. Highest occurrences of frost conditions at each AWS as a function of Kidson type are highlighted in red.*

Kidson type	Fairhall	Rapaura	Wairau coast	Southern Valleys	Waihopai Valley	Wairau Valley	Seddon	Awatere	Ward
T	7.4 *(2)*	3.7*(1)*	3.7*(1)*	7.4*(2)*	11.1*(3)*	14.8*(4)*	7.4*(2)*	7.4*(2)*	7.4*(2)*
SW	19.0 *(8)*	16.7*(7)*	14.3*(6)*	33.3*(14)*	28.6*(12)*	30.9*(13)*	16.7*(7)*	28.6*(12)*	26.2*(11)*
TNW	9.5 *(2)*	0*(0)*	4.8*(1)*	9.5*(2)*	14.3*(3)*	14.3*(3)*	4.8*(1)*	0*(0)*	4.8*(1)*
TSW	7.7 *(1)*	0*(0)*	0*(0)*	7.7*(1)*	23.0*(3)*	30.7*(4)*	7.7*(1)*	7.7*(1)*	7.7*(1)*
H	41.5 *(17)*	24.3*(10)*	19.5*(8)*	34.1*(14)*	46.3*(19)*	41.5*(17)*	26.8*(11)*	19.5*(8)*	31.7*(13)*
HNW	40.0*(8)*	25.0*(5)*	20.0*(4)*	40*(8)*	50.0*(10)*	55.0*(11)*	25.0*(5)*	25.0*(5)*	**45.0*(9)***
W	16.7*(4)*	0*(0)*	4.2*(1)*	4.2*(1)*	16.7*(4)*	12.5*(3)*	8.4*(2)*	12.5*(3)*	25.0*(6)*
HSE	39.2*(11)*	42.9*(12)*	32.1*(9)*	46.4*(13)*	46.4*(13)*	**60.7*(17)***	**39.2*(11)***	28.6*(8)*	35.7*(10)*
HE	6.7*(2)*	3.3*(1)*	6.7*(2)*	10.0*(3)*	16.7*(5)*	16.7*(5)*	6.7*(2)*	10.0*(3)*	6.7*(2)*
NE	30.0*(3)*	0*(0)*	0 (0)	30.0*(3)*	20.0*(2)*	30.0*(3)*	30.0*(3)*	20.0*(2)*	30.0*(3)*
HW	**71.4*(5)***	**71.4*(5)***	**71.4*(5)***	**85.7*(6)***	**100.0 *(7)***	57.1*(4)*	28.5*(2)*	**42.8*(3)***	42.8*(3)*
R	45.5*(5)*	27.2*(3)*	18.2*(2)*	36.4*(4)*	36.4*(4)*	54.5*(6)*	18.2*(2)*	18.2*(2)*	18.2*(2)*
total	68	44	39	71	85	90	49	49	63

The greatest likelihood of frost conditions in the Awatere Valley and at Ward is more variable, with the highest incidence of frost conditions spread between Kidson types HW, HSE and HNW. Although higher in actual number, Kidson types H, HSE and SW do not always produce frost conditions, as meteorological factors such as the presence of cloud or strong synoptic pressure gradients may prevent decoupling of the airstream from near the surface.

Rapaura recorded among the least number of frost conditions during the three spring seasons with 44 events. These events were recorded on 8 of a possible 12 Kidson types as frost conditions were not observed during TNW, TSW, W and NE. By comparison, Wairau Valley and Waihopai Valley recorded over twice the number of frosts, and they were spread over each of the 12 Kidson types.

Using the Chi-square (χ^2) test to examine the relationship between the frequency of frost events and Kidson type at each AWS, the null hypothesis would be that "there is no significant difference between the expected and observed number of frost events for a particular Kidson type. In this case, the value of $(\chi)^2$was calculated as 40.5 and using 88 degrees of freedom, the Chi-squared distribution table gives a 'p' value (probability that the difference between observed and predicted values is due to chance) of > 0.995. In this case, there is greater than a 99.5% probability that the difference between the observed and expected frequencies is due to chance, and any variability does not reflect the effect of a particular climatic process.

5.5.1 Frost conditions, Kidson type and ridge top winds

It is commonly purported in the literature that light winds are a requirement for radiative frost conditions. While analysis has shown that H, HSE and SW are most often linked with radiative frost conditions in Marlborough, these Kidson types are not always associated with light winds, particularly at surrounding ridge top level. In stable atmospheric conditions, however, stronger ridge top winds may decouple from the surface, especially in areas of complex terrain where shelter is provided by mountainous topography to surrounding areas. The extent of shelter provided within the valleys of Marlborough from surrounding terrain has been explored by plotting ridge top wind speed and direction as a function of frost conditions at each AWS using wind rose software in Figure 5.4.

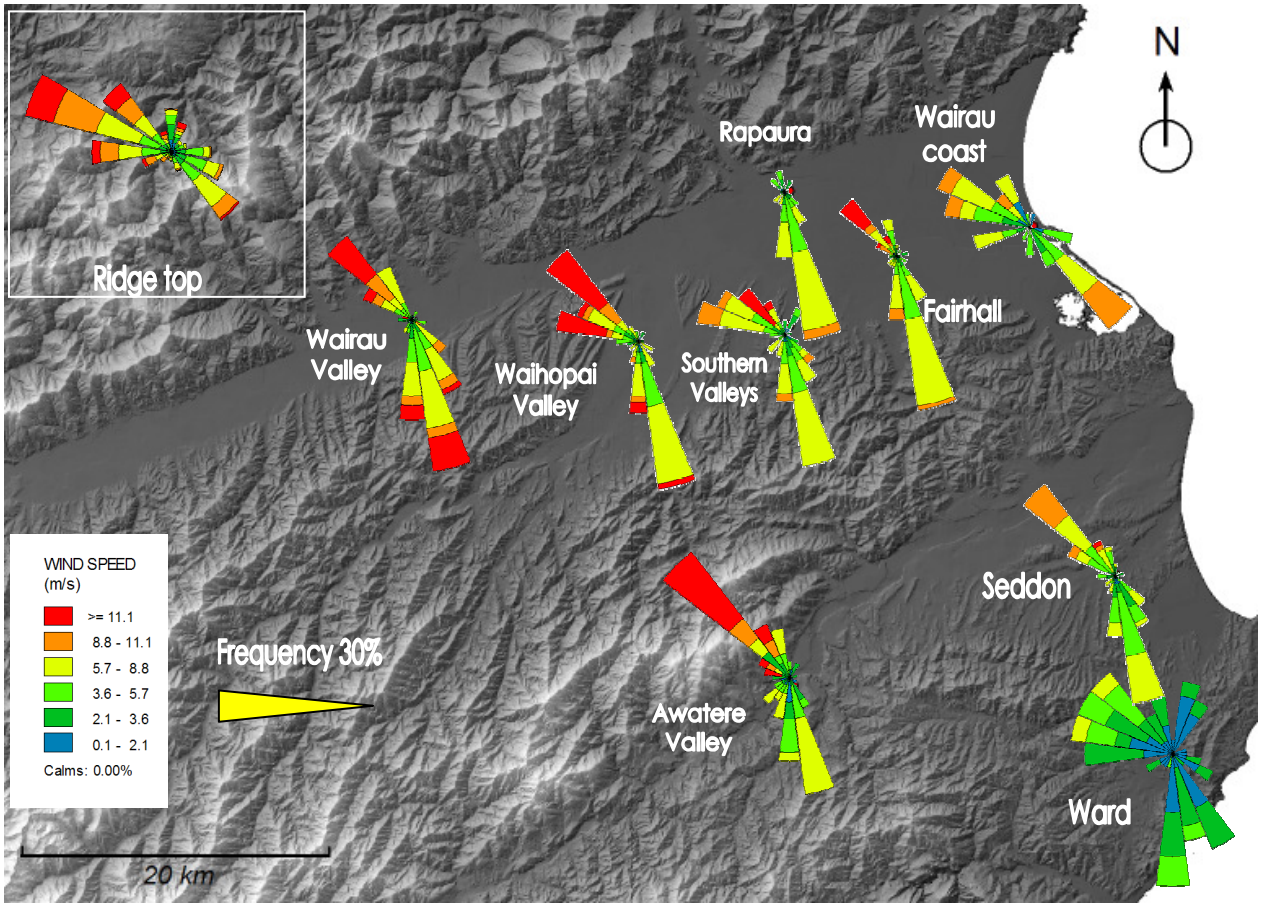

Figure 5.4 *WRPLOT rose plots illustrate the frequency of wind speed and direction at the ridge top AWS during frost conditions(< 1°C) at each of the nine AWS (2009 – 2011). Data are logged at 5 minute intervals by each AWS during frost conditions. Inset wind rose displays all overnight data from the ridge top AWS.*

The main features of the wind rose plots are summarised as follows:

1. Each of the AWS sites has a specific signature of ridge top wind conditions that are associated with the local formation of frost conditions. This reflects the shelter provided to that area by the region's topography.
2. In all areas except Ward, cold nights are more commonly recorded when mean ridge top wind speeds are moderate to strong (> 5 m s^{-1}). Cold nights around the region are infrequent or rare during light ridge top winds (< 5 m s^{-1}), in spite of these wind speeds comprising 34% of all the nocturnal winds at the ridge top AWS.

3. The peculiarity of ridge top wind conditions that are associated with the development of frost at Ward reflects the site's increased distance from the region's highest terrain. The location of Ward near Cook Strait predisposes the area to ventilation from moderate ridge top winds from any direction, when other parts of the Marlborough region are experiencing frost conditions.
4. Coldest nights are recorded in many areas (except Ward) during moderate to strong south to south-south-easterly and north-westerly ridge top wind directions. The finding is interesting, particularly as the actual occurrence of winds between directions of south-south-east to south-west at the ridge top AWS is very low. The low incidence of these winds at the ridge top AWS reflects the topographical alignment of these wind directions as they become funnelled through Cook Strait (Figure 5.5a). In a similar fashion, west or west-south-westerly synoptic winds (associated with Kidson type H, HNW and W), are topographically re-aligned more north-westerly, after traversing the Southern Alps and funnelling through Cook Strait (Figure 5.5b).
5. Rapaura is located close to the confluence of the Kaituna and Wairau Valley, and is clearly exposed to winds from the north-west that are channelled down the Kaituna Valley. While relatively light to moderate ridge top winds from this direction will ventilate the area, Rapaura is also ventilated by strong drainage winds that are more likely to be impeded during strong southerly ridge top winds.
6. The occurrence of stronger ridge top winds during frost conditions increases with distance inland and proximity to the region's mountainous terrain. This observation is supported by the increased number of frosts at Waihopai and Wairau Valley, which have been recorded in all of the twelve Kidson types.

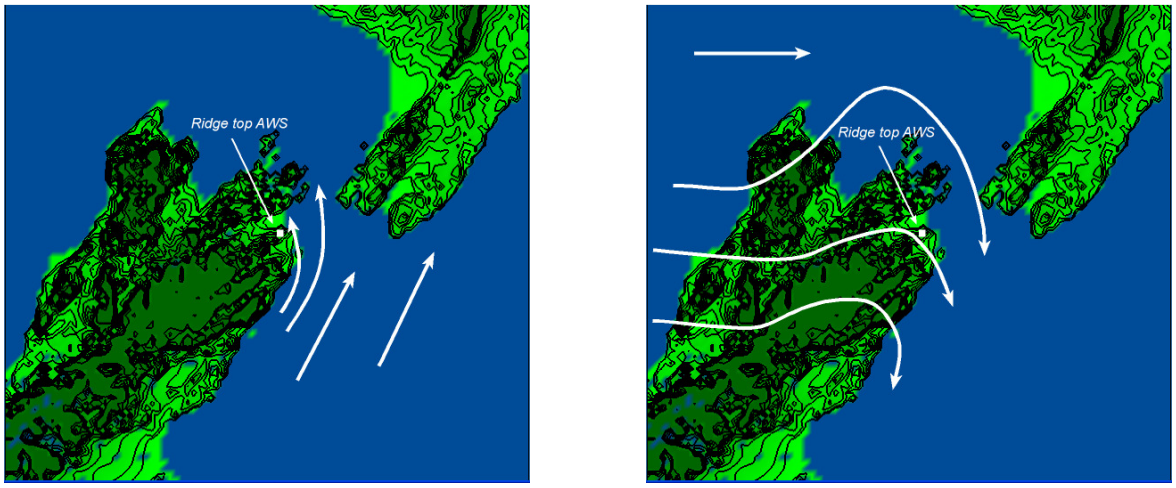

a) *b)*

Figure 5.5 *Wind flow from the south-west (a) is modified by Cook Strait and recorded as south-south-easterly at the ridge top AWS. Winds from the west (b) are also re-aligned and recorded as north-westerly at the ridge top AWS. White arrows indicate direction of ridge top airflow.*

5.6 Ridge top wind speed and minimum near-surface temperature variation

Ridge top wind speed has been recognised for some time as one of the leading predictors of near-surface minimum temperature (Laughlin and Kalma 1987), through various interactions with surrounding terrain and underlying thermally-induced wind flows (Nappo and Snodgrass 1981; Sturman et al 1985; Barr and Orgill 1989; Sturman et al. 2003; Poulos and Zhong 2008 and Schmidli et al 2009). In this section, σT_{min} is regressed with the average overnight wind speed (2000NZST – 0800NZST) from the exposed ridge top AWS for the spring periods of 2009 – 2011 and the results are presented in Figure 5.6. A key finding from the previous section implied that many of the largest σT_{min} occurred during Kidson type H, which is generally associated with anticyclonic conditions and lighter ridge top winds across the region.

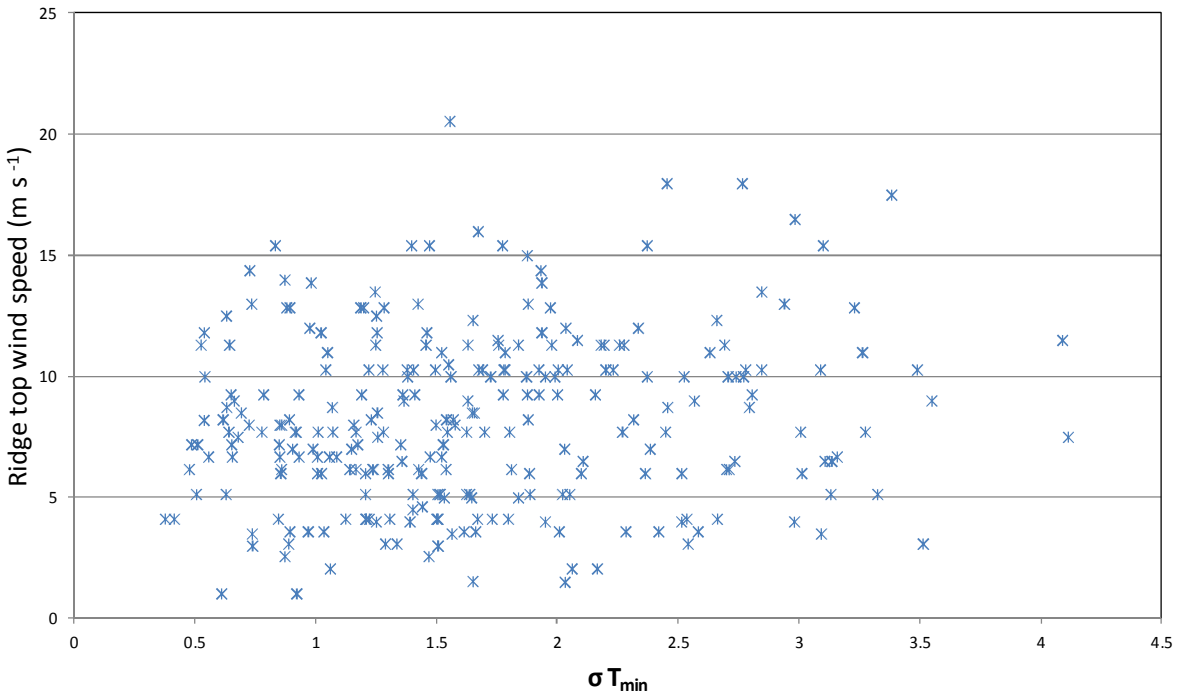

Figure 5.6 *Scatter plot of* σ T_{min} *around the Marlborough region and ridge top wind velocity for the spring periods of (2009 – 2011).*

The regression plot of σ T_{min} and mean overnight ridge top wind speed does not reveal any significant relationship. The plot reveals that there is as much likelihood of a low σ T_{min} during light ridge top winds as there are during stronger wind conditions. Similarly, high values of σ T_{min} (σ T_{min} > 3°C) have been recorded for a wide range of wind speeds, from as little as 3 m s^{-1} to 17 m s^{-1}.

The absence of any obvious relationship between σ T_{min} and ridge top wind speed on a daily basis could be attributed to several factors. Firstly, it was not possible to exclude cloudy nights from the data set. As the presence of cloud cover reduces near-surface cooling processes, any local variations in near-surface temperature that occur as a result of this process, would be minimised, regardless of ridge top wind speed. Secondly, topographic-induced sheltering from strong ridge top winds may result in cool near-surface temperatures at only one AWS. This occurrence will be masked by the standard deviation calculation used to measure the spatial variation of minimum temperatures. A

relationship may exist between T_{min} at one particular AWS for a critical range of ridge top wind speeds, but it will not be revealed by regressing σ T_{min} with ridge top wind speed. Thirdly, if other meteorological processes, such as the development of strong drainage winds occur during light ridge top winds (e.g with Kidson type H), then the mixing of near-surface air layers induced by these winds as described by Pinto et al (2006), would raise near-surface temperatures in some parts of the region, while stagnation may continue in areas that are less exposed to the drainage winds and this would result in high σ T_{min}. This phenomenon would distort any linear relationship that might otherwise exist between σ T_{min} and ridge top wind speed, and will be the focus of the subsequent chapter (Chapter 6) of this thesis. Finally, averaging ridge top wind speeds over the course of the night provides a very crude estimation of the dynamic nature of wind. In many cases wind conditions change dramatically through the course of the night and this influences the evolution of near-surface minimum temperatures. Lighter wind speeds may facilitate a large σ T_{min} for a short period overnight, while the average overnight wind speed could be considerably stronger. In this respect, a regression of ridge top wind speed at the time of T_{min} at each AWS may provide stronger relationships.

5.7 Discussion

Synoptic climatological techniques have been used for interpretations of New Zealand's climate and climate change scenarios since the early 1980's. Recent investigations by Sturman and Quénol (2013) have focused on the Marlborough region and linked changes in the three broader Kidson weather groups to changes in the region's mean daily maximum and minimum temperatures. Results from this chapter have not only shown a relationship between Kidson types and the spatial variation of minimum temperature, but that specific Kidson types have a significant influence on the occurrence of frost. In this respect the use of synoptic climatological techniques in New Zealand have more than just a qualitative value, as suggested by Kidson (2000).

Although the mean daily σ T_{min} between the nine AWS sites was found to be 1.7°C, the Kidson types H, TNW and T were associated with some of the highest σ T_{min} at 2.05, 1.95 and 1.90 respectively. As the analysis has been conducted for three spring periods (2009 – 2011), it is not clear how the summer, autumn or winter periods, might affect the mean σ T_{min}. In addition, it would be interesting to examine how representative analysis from the years 2009 – 2011 are when compared with longer-term data sets or other regions of complex terrain. International studies by Gustavsson et al. (1998) recorded (single event) temperature variations of up to 15°C in moderately undulating terrain in Sweden and Smith et al. (2010) observed 7.5°C variations using an instrumented vehicle in south-west England. The high proportion of nights that have σ T_{min} > 2.0°C in Marlborough emphasises the extent of the forecast dilemma faced by local grape growers who may receive one predicted temperature from the national weather provider "MetService" and must then attempt to modify this prediction for their location of interest.

Nights that recorded the lowest σ $T_{min,}$ such as, during Kidson types NE and HSE, could have been expected. They are associated with onshore winds that are more likely to push cloud into the region. Similarly, relatively low σ T_{min} associated with Kidson types W and TSW are more likely to be linked with stronger ridge top winds that ventilate many parts of the region. A surprising finding, however, was the large variability in σ T_{min} associated with Kidson types T and TNW from the trough group. In spite of the increased likelihood of cloud and the unstable atmosphere that is linked with these Kidson types, on some occasions, large spatial variations of near-surface minimum temperature can occur. The phenomenon is thought to be attributed to areas of simultaneous ventilation and stagnation of near-surface airflow, as a result of terrain-induced sheltering, and this will become the focus of further analysis in the following two results chapters using numerical weather prediction modelling.

Visualisation of the effect of Kidson type on the spatial variation of minimum temperature (Figure 5.3 a – l) reveals a great deal more about the interactions of

synoptic airflow patterns with local topography. Some Kidson types favour the ventilation of coastal locations, such as SW, H, HE, HNW, W, HSE and R, whilst other Kidson types appear to affect the region more evenly, such as T, TNW, TSW and NE. The simultaneous ventilation of inland areas and stagnation of coastal areas is more unusual and difficult to reveal through the averaging of temperature data. However, it has been observed on several occasions during Kidson type SW.

In the case study examining T_{min} between Welds Hill and Seddon, analysis indicated that Welds Hill recorded cooler T_{min} for most of the time, and during all Kidson synoptic types except type H. Analysis also shows that cooler T_{min} at Welds Hill is more likely to be associated with stronger winds on surrounding ridge tops. It is not possible to predict whether Seddon or Welds Hill will record the coolest T_{min} on any one given night based exclusively from Kidson type, as fluctuations of ridge top wind speed may become more important in determining which part of the valley becomes subject to ventilation or stagnation. Although the greatest variations in T_{min} between Welds Hill and Seddon occur during Kidson types HNW, HSE, W and H, there is no clear relationship with ridge top wind speed on these occasions. The results point towards the development of local meteorological processes that can affect the variation of T_{min} (between Welds Hill and Seddon) independent of ridge top wind speed. These phenomena will become the focus of further analysis in Chapters 6 and 7.

There is some overlap between the Kidson types that favour the greatest σ T_{min} (T, TNW and H) and those associated with the highest numbers of frost conditions (H, HSE, SW). However, results have also shown that Kidson types H, HSE and SW, only produce high numbers of frost conditions because they occur more often. Kidson type HW is most likely to produce frost conditions, in spite of it occurring less often. It is most likely to be associated with cooler ridge top temperatures, and a clear dry atmosphere in the lee of the Kaikoura Ranges. Kidson type HSE is second most likely to produce frost conditions. The proximity of the anticyclone to the Marlborough region gives rise to east or south-

easterly winds, which can accentuate cloud development on some occasions and reduce the incidence of frost.

The amalgamation of local ridge top wind data together with the analysis of Kidson type and frost conditions, has demonstrated an effect that is believed to be the topographic channelling of wind through Cook Strait. The higher frequency of frost conditions during Kidson type HSE and SW, are generally linked with higher incidence of south-south-easterly ridge top winds, and in a similar manner, winds that originate from the west or west-south-west, such as Kidson type H, are forced over the ridge top AWS from the north-west. Local terrain then provides varying amounts of shelter to the region's grape growing areas from these winds. Provided that other atmospheric conditions conducive to cold near-surface temperatures are also present, frost conditions may result.

Finally, no obvious relationship was found between ridge top wind speed and σT_{min}. As mentioned in the previous section, this could have been expected for a number of reasons, but is primarily due to the inability to accurately eliminate nights with cloud cover from the (2009 – 2011) data set. While the use of σ as a measure of regional minimum temperature variability works well, alternative statistical approaches would be required for identifying site-specific relationships between near-surface temperatures and other climate phenomena, such as ridge top wind speed. For example, if one AWS records a significantly lower minimum temperature than all remaining AWS, then σT_{min} would be classified as a moderate variation. If three AWS record significantly lower temperatures, then the σT_{min} is classified as having a high variation. In this respect, a number of days may have been classified as having a moderate σT_{min}, in spite of the occurrence of strong relationships between ridge top wind speed and near-surface temperatures at one or two locations. The weak relationship between ridge top wind speed and σT_{min} is further distorted by the use of an 'average' overnight wind speed, which does not reflect the true dynamic nature of ridge top wind speed that has a continuous effect on the cooling processes that take place near the surface. Finally, σT_{min}

is believed to be affected by the development of local meteorological cooling processes during light ridge top wind conditions. This may significantly increase σ T_{min} on some occasions due to a locations susceptibility to cold air drainage.

5.8 Summary

This chapter has established that relationships exist between the spatial variability of near-surface minimum temperature, frost conditions and Kidson type. The strength of ridge top winds has an effect on the spatial variability of near-surface minimum temperatures in the Awatere Valley, but no significant relationship can be found elsewhere. The analysis has raised a number of questions that the following chapter will attempt to answer using numerical weather prediction modelling.

Numerical modelling will attempt to establish how well the spatial variability of near-surface temperature in Marlborough's complex terrain is represented, and help identify the atmospheric boundary layer processes that influence near0-surface temperature patterns.

Chapter 6

The application of numerical weather prediction modelling to minimum temperature variation

6.1 Introduction

In the preceding chapter, Kidson weather regimes were used to explore the broader weather patterns that account for spatial variation of minimum temperature and frost conditions around the Marlborough region. Results demonstrated a relationship between specific Kidson types and an increase in σ T_{min}. While large region-wide variations in near-surface minimum temperature were found to be associated with Kidson type H, further analysis revealed large σ T_{min} in the Awatere Valley between Seddon and Welds Hill were associated with Kidson type W when the Welds Hill location is often considerably cooler. A relationship was also revealed between a high incidence of spring frost conditions (T_{min} <1.4°C) and Kidson type HW, increasing the interest in exploring interactions between the region's terrain and local meteorology, in these conditions. The application of NWP modelling to the evolution of near-surface minimum temperature provides an opportunity to evaluate the models ability to resolve interactions between synoptic scale weather, and the region's topography during specific Kidson types of interest.

There are two broader questions to be addressed in this chapter:

- Identify how well NWP models represent the spatial variability of near-surface temperature in the complex terrain of the Marlborough region.
- Determine whether NWP models help identify the atmospheric boundary layer processes that influence near-surface temperature patterns.

For the purpose of this chapter the NWP models The Air Pollution Model (TAPM) and Weather Research and Forecasting (WRF) have been used as heuristic tools as described by Oreskes et al. (1994), to explore relationships between the region's complex terrain and local meteorology under a range of quiescent and more dynamic conditions. While the heuristic approach to the evolution of minimum temperature using WRF and TAPM in complex terrain is uncommon in the literature, many studies have examined the suitability of other NWP models, including the evaluation of physics schemes within the same model, to predict near-surface climate variables.

Hanna and Yang (2001) evaluated four NWP models [Fifth-Generation Pennsylvania State University–National Center for Atmospheric Research Mesoscale Model (MM5), Regional Atmospheric Modeling System (RAMS), Coupled Ocean–Atmosphere Mesoscale Prediction System (COAMPS), and Operational Multiscale Environmental Model with Grid Adaptivity], to predict near-surface wind velocity and temperature. Each of the models tested revealed large errors in wind speed and direction, and underestimated the vertical temperature gradients in the lowest 100 m of the atmosphere at night. It was thought much of the discrepancy between observation and prediction were due to sub-grid variations in terrain and land use, and that better simulation of inversion conditions could be achieved if model vertical grid sizes were smaller. Zhang and Zheng (2004) investigated five different planetary boundary layer (PBL) schemes using the MM5 model and found that both near-surface temperature and wind velocity were highly sensitive to PBL physics, but interestingly strong relationships between observed and predicted near-surface temperatures were not necessarily linked with strong relationships between observed and predicted near-surface wind velocity. Steeneveld et al. (2008) compared three NWP models (MM5), (COAMPS), and the High-Resolution Limited-Area Model (HIRLAM)] to predict the diurnal cycle of the atmospheric boundary layer focusing on stable boundary layer conditions, however, model simulations over a 72 hour period were not specifically focused on the evolution of near-surface minimum temperature.

The following sections of this chapter provide a brief introduction to the TAPM and WRF models and their respective configurations for the modelling process. The results section then presents a series of idealised simulations using TAPM, where the synoptic file has been modified to provide a constant wind direction with height during clear, stable conditions. This configuration provides a broad indication of the shelter afforded by the region's complex terrain in creating areas of local ventilation and stagnation. This is followed by an exploration of the spatial variation of near-surface wind and temperature for two case studies using the WRF model. The chapter concludes with a discussion of the results, in particular the usefulness of the models in explaining local meteorological processes that account for spatial and temporal variability in near-surface observations of wind and temperature.

6.2 The TAPM and WRF numerical models

Numerical weather prediction models describe the weather mathematically, using computers to solve 'primitive equations' that describe how the atmosphere will evolve over time (http://blog.metservice.com/2011/04/metservice%E2%80%99s-investment-in-forecasting). While global models cover the entire globe and are run at large international agencies such as the US National Weather Service or the UK Met Office, Limited Area Models (LAM's) cover smaller areas of specific interest and take their boundary conditions from the larger global models. These models may be run more cost-effectively using less computational power at higher resolution and reveal greater detail by incorporating effects of local topography. In some cases, local climate observations can be assimilated into the model predictions, in an attempt to fine tune the models predictive ability as it is running. Both TAPM and WRF are LAM's that may be run at high resolution (< 1 km) to predict local climate variables such as wind, rain and near-surface temperature.

The NWP models TAPM and WRF are quite different in design. The differences extend across a range of aspects that include physical process-based parameterisations, the level of

user control over land and atmospheric physics schemes, and the graphical user interface (GUI) available for analysis of data output. These differences in model characteristics have a profound impact on the level of computing power required for simulations, so that TAPM can be run easily on most personal computers, whereas WRF ideally requires access to high-powered computing facilities.

Both TAPM and WRF were available for use through the University of Canterbury's computing facilities with a high level of user support. The contrast of model design and computing requirements was one of many reasons that lead to selection of the models.

6.2.1 TAPM

The Air Pollution Model (TAPM Version 4.0.3), first developed by Australia's Commonwealth Scientific and Research Organisation (CSIRO) in 1997, is a coupled meteorological and air pollution model designed to run on a standard laptop or personal computer, and is routinely used by many atmospheric consultants around the world. The model predicts flows important to local-scale air pollution, such as sea breezes and terrain-induced flows, against a background of larger-scale meteorology provided by synoptic analysis (Hurley 2008). For the purposes of this research, only the meteorological component of TAPM has been evaluated.

The meteorological component of TAPM is an incompressible, optionally non-hydrostatic, primitive equation model with terrain-following vertical co-ordinates for three dimensional simulations. It includes parameterization schemes for cloud, rain and snow, microphysical processes, turbulence closure, urban/vegetation canopy, as well as soil and radiative fluxes (Hurley 2008). The model design allows for a telescopic nested configuration where higher resolution gridded domains are placed inside coarser resolution grids. The model solution for each domain is one-way interacting, where synoptic and boundary layer information is passed from low to higher resolution domains.

The attractive features of TAPM include its quick and efficient simulation time, with two or more simulations able to be run simultaneously on a dual-core processor computer. TAPM is well suited to users who have no prior modeling experience, as it is driven by a user friendly graphical user interface (GUI) which allows the model to be configured using a Windows-based operating system for a variety of applications. Output from the model is also displayed through the GUI, providing easy to interpret animation of results. The TAPM model is supplied with a number of data sets, including gridded global terrain height, vegetation and soil type, Leaf Area Index (LAI), sea surface temperature and synoptic scale meteorology. User-defined databases of terrain, vegetation, soil, LAI and synoptic analysis can be used by the model (Hurley 2008).

A complete description of model microphysics schemes, as well as calculation of turbulence and diffusion, can be found in the TAPM model user's guide (Hurley 2008). The user guide includes a review of some verification studies, and more recent studies were conducted by Thatcher and Hurley (2010). In most of these studies pollution forecasting was the main objective for the research and comparisons between modelled and observed meteorological parameters used large data sets over a wide range of meteorological conditions, from which it is easy to demonstrate broad model skill. Exceptions to these studies include two Masters theses prepared by Leishman (2005) and Hirdman (2006), who investigated TAPM's ability to predict wind and near-surface temperature over Australia's Queensland coast and the Canterbury Plains, New Zealand, respectively. Both of these studies focussed on shorter model simulations, and compared the diurnal fluctuations of near-surface wind speed and temperature with local observations.

6.2.2 WRF

The Weather Research and Forecasting model is the product of a multi-agency effort to build a next generation mesoscale forecast model (Skamarock et al. 2008). It is expected to advance the understanding and prediction of mesoscale weather and accelerate the transfer of research into operational forecasting. It has been specifically designed for use

with a range of forecasting applications, from the microscale to the mesoscale, and is efficient in a range of computing environments.

At the time of this study, the current version of WRF V3 (version 3) is a collection of several NWP models in a single software architecture. It includes two popular weather forecasting models, the non-hydrostatic Mesoscale Model (NMM) and the Advanced Research WRF model (ARW). The ARW is adaptable to very high resolutions (1 km or less) by zooming into an area of interest with the aid of telescopic nested domains. Ultimately, resolution is governed by available computing power, initialisation data, resolution of terrain elevation, land use and soil data, and skill in adapting accurate parameterisations of physical processes in specific forecast areas. The model integrates the equations for atmospheric motion and uses physical parameterisations for the unresolved, complex, non-linear processes to predict temperature, pressure, wind fields and water vapour for three-dimensional domains. The WRF V3 model simulations are continually evaluated by a host of independent researchers, mainly in the United States, including a specific test-bed centre developed jointly by the National Oceanic and Atmospheric Administration (NOAA), the National Centre for Atmospheric Research (NCAR), and the United States Department of Defence (DOD).

Evaluation of the WRF model through sensitivity studies continues on a frequent basis, particularly in relation to physics schemes and improved model performance following data assimilation. The WRF user's web page provides an extensive resource for review of these evaluations (*http://www.mmm.ucar.edu/wrf/users/wrfv3.5/phys_references.html*). Studies that pertain more specifically to near-surface temperature, wind regimes and frost are less frequent, although the evaluation of WRF for frost warning and consequences of cold air pooling in Georgia (Prabhakaran et al. 2007) and simulation of a morning air temperature inversion break-up in complex terrain (Hole and Hauge 2003) are two examples. Prabha and Hoogenboom (2008) evaluated the WRF model for two frost events in south-eastern United States and, more recently, a study by Ngan et al. (2013) used WRF to predict the nocturnal

wind speeds and temperatures in south-eastern Texas, and found that nocturnal wind speeds and temperatures are over-predicted.

Zhang et al. (2013) examined the ability of WRF to predict near-surface temperature and wind conditions in complex terrain under a variety of weather conditions. It was found that WRF predicted the weather events reasonably well, however, the models inability to reproduce near-surface atmospheric conditions in complex terrain was a complicating issue. They concluded that increasing the number of model vertical layers does not necessarily improve prediction of near-surface variables and that forecast errors in near-surface variables depend strongly on the diurnal variation in surface conditions, especially when synoptic forcing is weak. These findings are strongly supported by early sensitivity studies and the subsequent modelling of case studies in this research.

6.3 Model configurations

The model configurations that were adopted for the analysis were the product of extensive sensitivity analysis. While each model presents hundreds (possibly thousands) of potential configurations that yield different outcomes, only a handful of model configurations provide realistic simulations when compared with observations for a particular area of interest. The configuration selection process was protracted, hampered by the Marlborough region's complex terrain and surrounding mountainous topography which can lead to model instability, erroneous output, or a simulation crash during higher resolution simulations. While the range of sensitivity studies performed using TAPM and WRF were extensive, analysis focused on events that predisposed the region to wide spatial variation of overnight minimum temperatures and at times, frost. TAPM provided an easier platform from which to perform sensitivity studies. It was possible to run several simulations using the Windows-based model, while user demand on the University's high-powered computing facilities could leave a WRF simulation waiting in a queue for days before starting.

As mentioned earlier, each model provides the user with a range of settings and parameterisation schemes for optimising the model for use in a range of environments. Where parameterisation schemes were recommended they were not adjusted, so the remaining parameters relating to soil moisture, soil temperature, number of vertical layers, grid spacing, number of grid points and grid centre co-ordinates provided the basis for sensitivity analysis.

6.3.1 TAPM

TAPM was only used to run idealised simulations. In these cases the synoptic file was modified to exclude the development of cloud, to mimic near-surface cooling at night under clear sky conditions. The wind velocity was set to follow a standard wind speed profile above the surface, (except in the case when all synoptic wind influence was eliminated) but direction remained constant. The model was initiated using 25 vertical layers in a 3 domain set up of 90 x 90 grid cells. The 3rd (highest) domain resolution of 1800 m encompassed the entire Marlborough region, as well as Cook Strait, and covered an area of 26,244 km^2. The areas covered by each domain are very similar to domains 1 – 3 of the WRF set up (Figure 6.1). In each simulation, synoptic conditions varied with 3-D space and time and boundary conditions on the outer grid were obtained from synoptic analysis files. A version 4 land-surface scheme was implemented, as well as the TKE-EPS turbulence (prognostic TKE and eddy dissipation rate) and eddy-diffusivity/mass flux (EDMF) schemes. Extensive sensitivity analysis (over 150 simulations) revealed that model performance was greatly affected by model configuration and choice of default settings. The sensitivity analysis was crucial in determining which model inputs made the greatest changes to predicted near-surface wind speeds and directions. The relative ease of TAPM file manipulation and the quick simulation time rendered the model well suited for assessing the effects of topography on near-surface winds. At the time of this research no published material was available on the use of TAPM in idealised simulations.

6.3.2 WRF model

The final model configuration for the WRF simulations was selected on the basis of the models ability to reproduce the spatial and temporal evolution of near-surface temperature and wind observations. The model used 28 vertical layers in a 4 domain set up, with each domain using 112 x 112 grid cells (Figure 6.1). The 4^{th} (highest) domain resolution of 500 m encompassed most of the areas used for grape growing in Marlborough and covered an area of 3,136 km^2.

In the literature, Wang et al. (2009) suggested that the most successful microphysics parameterisation scheme for prediction of near-surface temperature is the WRF single moment 6-class scheme (WSM6), engaging ice, snow and graupel processes for high resolution simulations. This was combined with the Rapid Radiative Transfer Model (RRTM) for calculation of longwave radiation, the Dudhia shortwave radiation scheme, the Eta similarity for surface physics, the Rapid Update Cycle (RUC) for land surface physics, and the Mellor-Yamada-Janjic (MYJ) scheme for planetary boundary layer physics.

The RRTM scheme was the preferred long-wave physics option in a study of frost warning and cold air pooling by Prabhakaran et al. (2007), while Borge et al. (2008) and Baker and Dolwick (2009) concluded that the MM5 (Dudhia) scheme revealed less systematic bias in longer term temperature predictions when compared to other short-wave radiation schemes. The scheme has been used by a number of other researchers in the prediction of near-surface temperature, such as Prabhakaran et al. (2007) and Baker et al. (2011), who concluded that the Dudhia scheme was the most suitable for temperature prediction. Although three alternative surface layer physics schemes were tested in the analysis, the preferred Pleim-Xiu scheme as recommended by Borge et al. (2008) and Chigullapalli and Mölders (2008), did not appear significantly better for Marlborough. The Rapid Update Cycle (RUC) was tested and later preferred, despite higher RMSE's and lower cooling rates, as reported by Prabhakaran et al. (2007). A new land surface scheme called WRF-CLM3 was

selectable at the time of analysis but no literature was available on its application to temperatures. Jin et al (2012) have since evaluated this scheme and claimed improved temperature predictions, and the scheme has been further updated to CLM4. Finally, several researchers reported that the selection of planetary boundary layer (PBL) scheme has a significant influence on near-surface temperature prediction (Baker et al. 2011, Borge 2008, Mao et al. 2006), although they were all reluctant to identify the most successful scheme. In eight simulations the local Mellor-Yamanda-Janjic scheme proved equally as robust in predicting near-surface temperature as two alternative schemes for Marlborough, although in the final model configuration predictions of near-surface wind speed and direction were consistently more accurate than predictions of near-surface temperature.

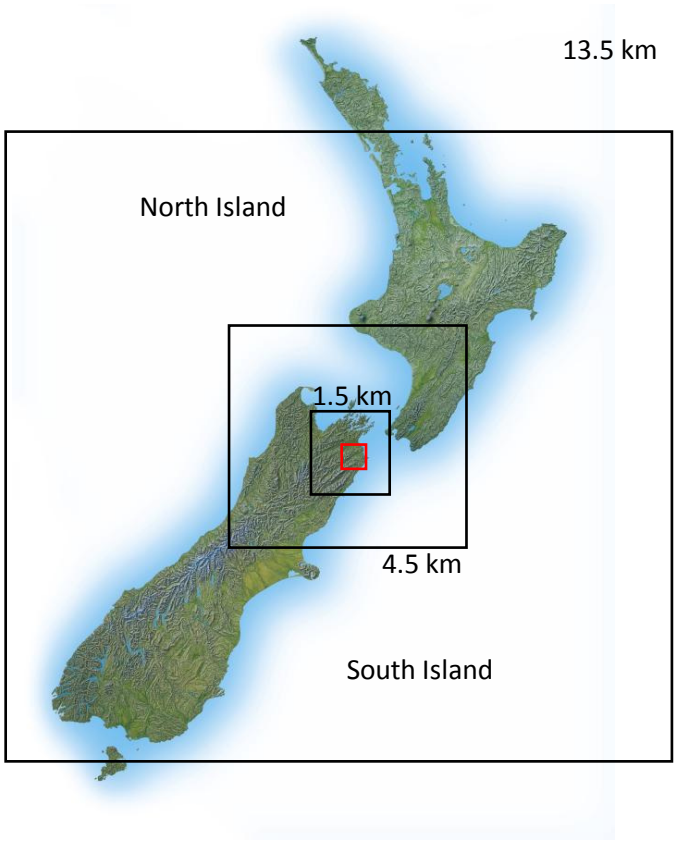

Figure 6.1 *The four domain 112x112 grid cell configuration of the WRF model. The highest resolution domain illustrated in red is an area of 56x56 km and encompasses most of the grape growing areas in the Marlborough region.*

6.4 Results

In the preceding chapters, analysis has shown that the incidence of frost conditions shows a strong regional variation, as a function of ridge top wind speed and direction. This is believed to reflect interactions between ambient weather and the shelter provided by the region's complex terrain. Furthermore, the greatest spatial variations of minimum temperature are associated with the Kidson synoptic types H and TNW. In these conditions, topography that surrounds the most highly valued agricultural land in Marlborough simultaneously creates areas of both ventilation and stagnation, leading to very variable near-surface temperatures. Numerical weather prediction models provide an opportunity to compare predicted results with observations, and allow the researcher to examine local meteorological processes that generate observed near-surface phenomena.

6.4.1 The effects of local topography on near-surface wind flow

The effects of Marlborough's complex mountainous topography on modifying the near-surface climate are well recognised by local agricultural and wine industries, but not so well documented, apart from the summary provided by Pascoe (1983), who analysed data from a sparse network of local observation sites. His technical publication adequately described the influence of many weather systems that affect the Marlborough region, but no link was made between local meteorological processes and the generation of temperature variability or the incidence of frost. The shelter afforded by the region's topography is of prime interest to this research as it allows the development of meteorological phenomena such as katabatic drift, which has been observed to influence the evolution of minimum temperature around the region.

In the first results section, TAPM has been used to generate a series of idealised simulations where the wind direction above the region has been set to a constant direction. As the simulation shown in Figure 6.2 assumed no synoptic wind, the predicted light to moderate

winds in some parts of the region at 6 am local time (especially the Awatere and Waihopai Valleys) are assumed to be thermally generated winds (e.g. cold air drainage). While this simulation could serve as a reference situation, it is recognised that even under the strongest anticyclonic conditions there is always air movement at ridge top level and that even when other physical mechanisms are not considered, this may impact near-surface wind observations. A number of simulations were then completed with a 10 m s^{-1} synoptic wind at ridge top height for each of the cardinal and intercardinal wind directions, as shown in Figure 6.3. A snapshot of each simulation has been illustrated next to the image of a compass that shows the wind direction of the idealised simulation. Lightest near-surface wind speeds are indicated by the deeper blue colours, while higher wind speeds are indicated by the colours yellow, orange or pink. Small white arrows on each plot illustrate wind direction. The areas of lightest winds are more likely to be associated with local stagnation and increased cooling under clear sky conditions.

Although the series of simulations are hypothetical, they do reveal a number of important features about Marlborough's nocturnal climate, especially influences from the region's mountainous terrain. It is of no surprise that when moderate wind is present above the region, significantly lighter winds are indicated in the region's valleys and on the leeward side of mountain ranges. Interestingly, the modelling exercise suggests that the greatest extent of light winds in the two main valley systems occurs during south and south-westerly conditions rather than in the absence of any synoptic wind (Figure 6.2). The model also suggests that a greater spatial variation of surface wind speeds occurs when there is a synoptic wind component in the simulation from any direction (except south-west) above the region. This adds further weight to the perception that synoptic wind interaction with the region's surrounding terrain can lead to simultaneous areas of ventilation and stagnation, causing a high σT_{min}. The large areas of very light near-surface winds across much of the region during south-westerly flow suggests that topographic sheltering from synoptic wind reaches its greatest regional extent under these conditions.

In Figure 6.3, a large variation of near-surface wind speeds is portrayed by the westerly wind simulation (typical of Kidson type W). Synoptic winds appear to ventilate areas of inland Wairau Valley (Wairau Valley Township), while at the same time areas in the upper Awatere Valley and along the eastern coast, including Ward remain under very light winds. The southerly simulation (typical of Kidson type HW) reveals the influence of synoptic winds on Ward, the lower Awatere Valley (Seddon) and the lower Wairau Valley coast, while remaining parts of the region are projected to have very light winds. In spite of the shelter provided to the region from the Kaikoura Ranges, the model suggests that near-surface winds are reduced to speeds below those indicated in the absence of any synoptic wind (Figure 6.2). This supports the idea that synoptic flow interacts with more local terrain to cancel or reduce the development of thermally generated winds. As synoptic winds approach south-easterly, the entire Awatere Valley becomes susceptible to ventilation, as do the coastal margins of the lower Wairau Valley. Inland areas of Wairau Valley, including the Waihopai Valley remain particularly sheltered behind the higher terrain of the Black Birch range and strong radiational cooling may therefore continue unabated.

The topographic channelling of wind through Cook Strait is apparent under southerly and south-easterly synoptic conditions, which is shown to cause local acceleration of near-surface winds in eastern coastal areas (Figure 6.3). This is likely to reduce the incidence of frost conditions to Seddon and Ward (Figure 3.5). Further channelling of winds through Cook Strait in westerly conditions does not appear to affect the variation of near-surface wind speeds in Marlborough to the same extent.

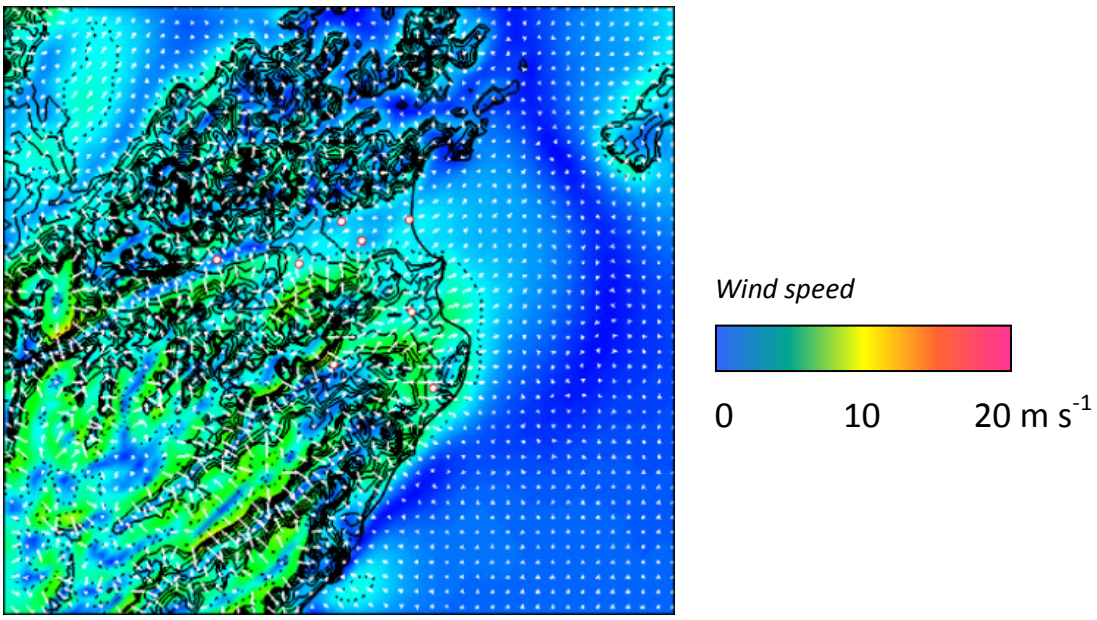

Figure 6.2 *Idealised TAPM simulation of near-surface winds at 6 am local time with zero synoptic wind. Strong drainage winds are indicated by the turquoise and green colours that extend some distance off the coast (grid resolution 1800 m).*

6.4.2 Case study 1: Light wind conditions

The two case studies that follow have been modelled using WRF Version 3.2.1. Although the principal climate variables of interest are near-surface wind speed and temperature, the Integrated Data Viewer (IDV) (*http://www.unidata.ucar.edu/software/idv*) display allows broader flexibility of simultaneously plotting additional climate variables, such as vertical wind profiles, and ridge top wind velocity. Each case study depicts four diagrams that include a streamline plan view with upper level (925 hPa) wind barbs, and contour plan views of near-surface wind speed and temperature, and a vertical profile of wind speed at the upper Awatere Valley AWS. The streamline function is a useful method of presenting a plan display of vector-based data, such as wind. The density of streamlines provides a relative indication of wind speed, while the directions of the streamlines are indicative of near-surface wind direction. The vertical profile of wind speed has a low resolution, as only

a handful of data points represented by model vertical layers are available from the valley surface to surrounding ridge top height.

In the first case study near-surface temperature and wind conditions are examined for 6 am 3rd October 2010, in the presence of light ridge top winds (<5 m s^{-1}) and anticyclonic conditions, characteristic of Kidson type H. Results from the preceding Chapter 5 suggested that Kidson type H were associated with a high spatial variability of minimum temperature, and a relatively high incidence of spring frost. The observed and predicted 6 am temperatures and wind velocities for 3rd October 2010 for nine AWS are given in Table 6.1 below, followed by a streamline plot with upper level winds (Figure 6.4), a contour plan view of near-surface wind speed (Figure 6.5), near-surface temperature (Figure 6.6), and a vertical profile of wind speed at the Awatere AWS (Figure 6.7).

Table 6.1 *Observed and WRF predicted near-surface temperatures and wind velocities for nine AWS in Marlborough, 6am 3rd October 2010, under light ridge top winds.*

AWS location	Observed 6am temperature	Predicted 6 am temperature	Observed 6 am wind velocity	Predicted 6 am wind velocity
Fairhall	3.6°C	6.5°C	1.3 m s^{-1} W	0.9 m s^{-1} W
Rapaura	5.8°C	7.7°C	4.1 m s^{-1} WSW	1.6 m s^{-1} NW
Wairau Valley coast	5.7°C	10.3°C	4.6 m s^{-1} W	3.8 m s^{-1} NW
Waihopai Valley	2.6°C	6.2°C	1.1 m s^{-1} SSW	1.8 m s^{-1} W
Southern Valleys	3.5°C	7.0°C	1.8 m s^{-1} SW	0.8 m s^{-1} S
Wairau Valley Town	2.8°C	7.2°C	1.0 m s^{-1} SE	1.1 m s^{-1} N
Upper Awatere Valley	7.2°C	7.3°C	6.1 m s^{-1} S	3.3 m s^{-1} SW
Seddon	4.2°C	6.8°C	2.0 m s^{-1} WNW	3.8 m s^{-1} NNW
Ward	4.5°C	7.7°C	0.8 m s^{-1} W	4.5 m s^{-1} N

While it is apparent from the Table 6.1 that there are considerable discrepancies between the observed and predicted near-surface temperature and wind speed values, the means of the observed and predicted parameters can be assessed using a t-test. This determines whether the observed and predicted values are statistically different from one another. The null hypothesis for testing the two groups of data will be “that there is no statistical difference between the observed and predicted values”, and the alpha level (level of risk) has been determined as 0.05. At this confidence level, there is 5% chance that the

conclusions from the calculations could be wrong. As wind direction uses cardinal values, only the speed component is assessed. The calculated and critical t-values are shown for the observed and predicted near-surface temperature and wind speeds in Table 6.2.

Table 6.2 *Calculated and observed t-values for assessing the means of near-surface temperature and wind speed from 9 AWS, 6am 3rd October 2010.*

	Calculated-t	Critical-t
Temperature	6.5	1.86
Wind speed	0.2	1.86

If the calculated t-values are greater than the critical-t, then the null hypothesis may be rejected. In this case, the null hypothesis is rejected for temperature but accepted for wind speed. In other words, there is a statistically significant difference between the observed and predicted mean temperatures, although there is no statistically significant difference between the observed and predicted mean wind speeds.

The 6 am near-surface σ T has been calculated from Table 6.1 of 1.53°C. Analysis from the preceding Chapter 4 suggests this magnitude of variation is typical of clear settled weather during Kidson type H. The table also reveals that warmer 6am temperatures at Rapaura, Wairau Valley coast and the upper Awatere Valley are observed in conjunction with higher near-surface wind speeds. These observations are partly supported in Figure 6.4 with a higher density of streamlines within close proximity to Rapaura and Wairau Valley coast, but it is difficult to reconcile the higher near-surface wind speeds at the upper Awatere location with increased streamline density, and this reflects the limitations of the model resolution. Upper level winds, as indicated by the red wind barbs, show light winds above the region from the south to south-east.

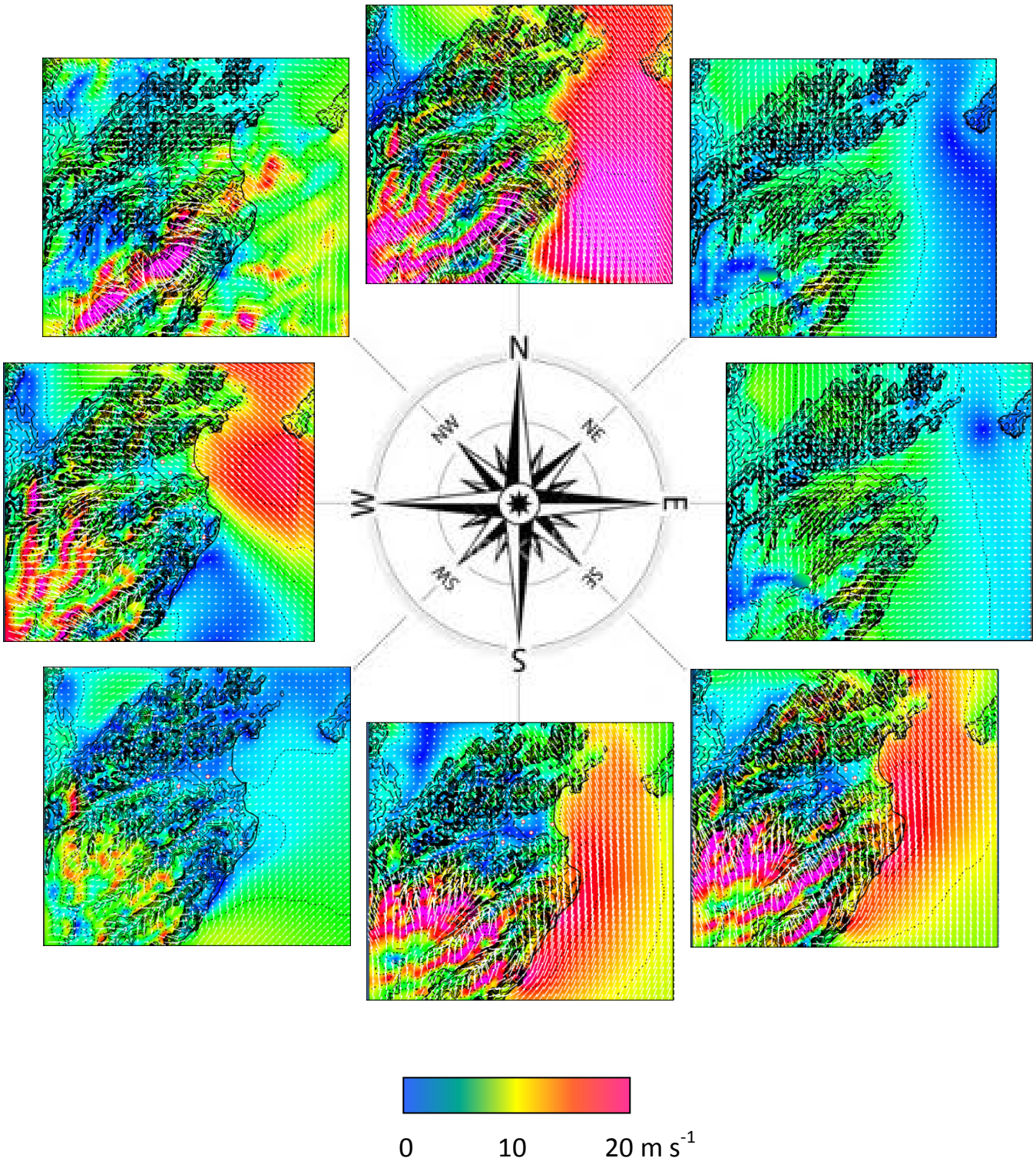

Figure 6.3 *Idealised TAPM simulations of near-surface winds with winds above the region from the cardinal and intercardinal directions. Areas of stagnation, which are associated with increased cooling are indicated by the deeper blue colours (grid resolution 1800 m).*

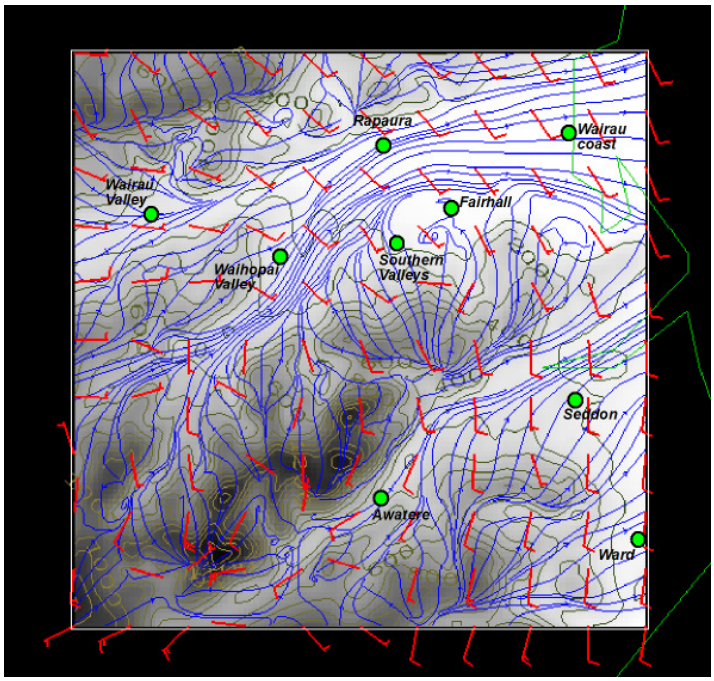

Figure 6.4 *WRF simulation illustrating streamline plan view of near-surface winds (blue) and upper level (925 hPa) winds illustrated using red barbs, 6am 3rd October 2010. Stronger surface winds are indicated by a higher density of streamlines for a cross sectional area. Model grid resolution 500 m.*

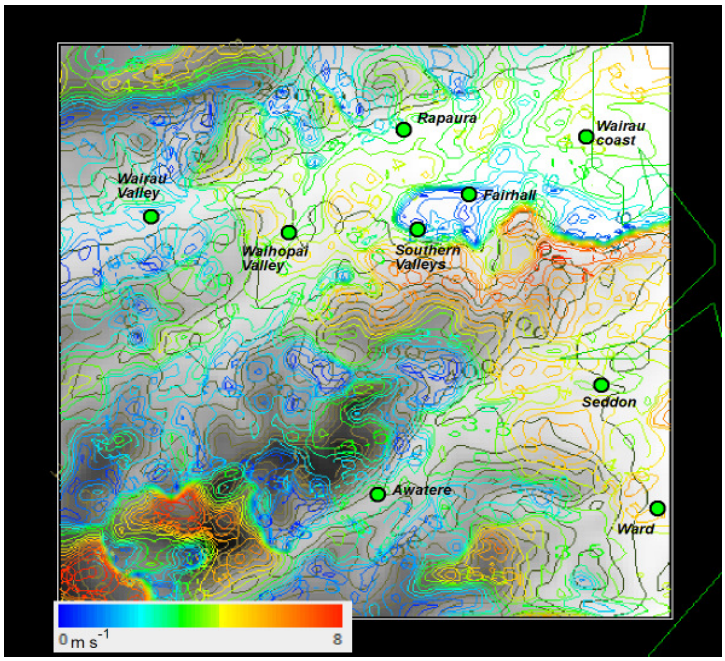

Figure 6.5 *WRF simulation showing plan view of near-surface wind speed isotachs 6 am 3rd October 2010. Areas of lightest winds are indicated by a deeper blue coloured contour. Grid resolution 500 m.*

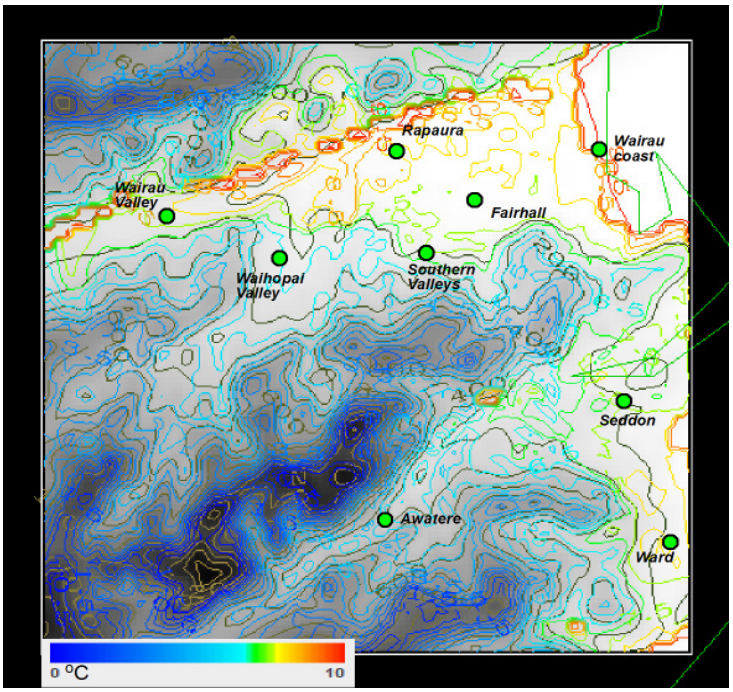

Figure 6.6 *WRF simulation showing plan view of near-surface air temperature isotherms 6 am 3rd October 2010. Cooler temperatures are indicated by a deeper blue contours. Grid resolution 500 m.*

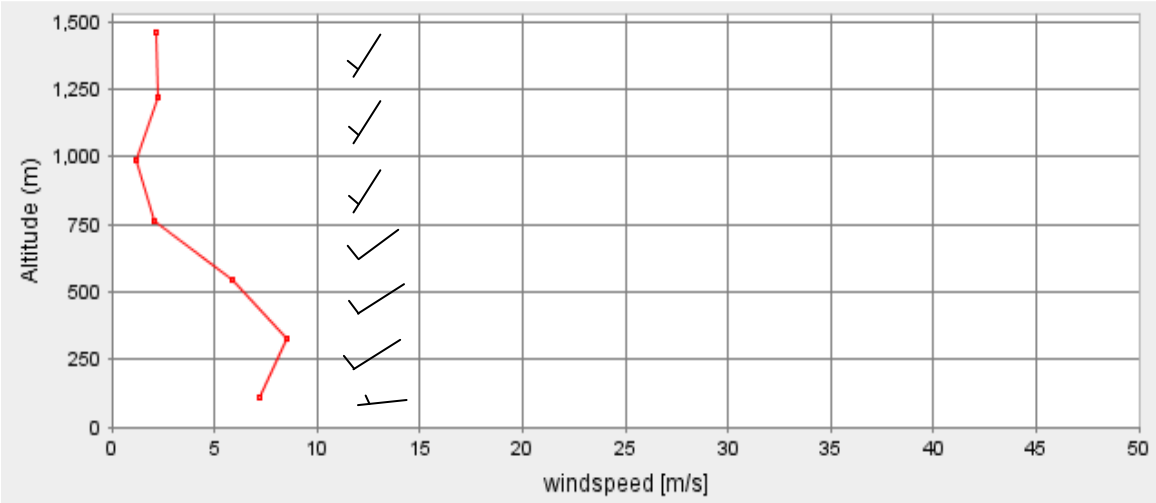

Figure 6.7 *WRF simulation showing vertical profile of wind speed only (red line) and wind speed and direction (wind barbs) 6 am 3rd October 2010. Each whole wind barb is approximately 5 m s^{-1}.*

The general tendencies of the streamlines reveal a strong signature of drainage winds that are concentrated down the Waihopai Valley, as well as the lower Wairau and Awatere

Valleys. Observations from the lower Wairau and upper Awatere AWS (Table 6.1) reflect this simulation with both elevated wind speeds and higher temperatures. Lighter drainage winds in the lower Awatere Valley at Seddon coincide with cooler temperatures, some 3°C lower than the upper Awatere AWS. The Waihopai AWS is located closer to a range of hills to the west and does not record the strong drainage winds that are projected (and have been observed) to blow down the centre of the valley closer to the river. Although the density of streamlines (Figure 6.4) and the contour plot of near-surface wind speeds (Figure 6.5) agree reasonably well, areas of lightest wind speeds are not supported by areas of projected cooler temperatures in the corresponding Figure 6.6. Lighter surface winds would normally facilitate a greater rate of cooling under clear skies, as demonstrated by the cooler temperatures observed at Wairau Valley Township and Fairhall.

The simulated 6 am vertical profile of wind speed and direction at the Awatere Valley AWS suggests a zone of elevated, down-valley wind speeds between 250 and 500 m above the valley floor. The first data point which represents the lowest vertical level of the WRF model indicates wind speeds of 7 m s^{-1}, and this is very similar to the observed 6 am observation of 6.1 m s^{-1}.

6.4.3 Case study two: Moderate to strong westerly synoptic winds

In the second case study, near-surface temperature and wind conditions are described for a period of moderate to strong west to west-south-west ridge top wind conditions at 6 am 10th October 2010. The synoptic situation is typical of Kidson type W. Results from Chapter 5 suggest that the stronger ridge top winds are associated with increased spatial variability of minimum temperature in the Awatere Valley, between Seddon and Welds Hill, as the region is subject to simultaneous ventilation and stagnation of near-surface winds. The observed and predicted 6 am temperatures and wind velocities for 10th October 2010 for nine AWS are given in Table 6.3 below, followed by a streamline plot with upper level winds (Figure 6.8), contour plan views of near-surface wind speed (Figure 6.9), temperature

(Figure 6.10) and a vertical profile of wind speed and direction at the Awatere AWS (Figure 6.11). The observed and predicted means of temperature and wind speed are assessed using the t-test, and the results are listed in Table 6.4.

Table 6.3 *Observed and WRF predicted near-surface temperatures and wind velocities for nine AWS in Marlborough, 6 am 10th October 2010, under moderate to strong westerly synoptic winds.*

AWS location	Observed 6am temperature	Predicted 6 am temperature	Observed 6 am wind velocity	Predicted 6 am wind velocity
Fairhall	5.1°C	5.1°C	0.5 m s^{-1} W	3.0 m s^{-1} NW
Rapaura	5.9°C	6.2°C	3.1 m s^{-1} W	4.1 m s^{-1} NW
Wairau Valley coast	5.8°C	8.3°C	2.6 m s^{-1} WNW	5.5 m s^{-1} WNW
Waihopai Valley	3.0°C	5.6°C	1.3 m s^{-1} W	2.9 m s^{-1} W
Southern Valleys	4.2°C	6.5°C	1.0 m s^{-1} SSW	1.5 m s^{-1} SW
Wairau Valley Town	2.5°C	1.7°C	Calm	4.1 m s^{-1} WSW
Upper Awatere Valley	1.4°C	5.9°C	Calm	2.5 m s^{-1} WNW
Seddon	7.9°C	5.8°C	5.1 m s^{-1} NNW	5.9 m s^{-1} NW
Ward	6.6°C	7.8°C	2.8 m s^{-1} N	5.5 m s^{-1} NW

The observed and predicted values of near-surface temperature show some variation, but the most noteworthy discrepancy is in the upper Awatere Valley, where there is a 3.5°C difference. Observed near-surface temperatures are considerably cooler than predicted. Wind speeds were over-predicted at each of the AWS locations, particularly at the Wairau Valley Township and Upper Awatere AWS, and this may have had an influence on predicted near-surface temperatures.

Calculations of the mean near-surface temperatures and wind speeds using the t-test are summarised in Table 6.4. For near-surface temperature, the null hypothesis is accepted, but only just, which suggests there is no significant difference between the observed and predicted mean values. As the calculated t-value for assessing wind speeds is significantly higher than the critical t-value, the null hypothesis is rejected. In this case there is a significant statistical different between observed and predicted values.

Table 6.4 *Calculated and observed t-values for assessing the means of near-surface temperature and wind speed from 9 AWS, 6am 10th October 2010.*

t-test	Calculated-t	Critical-t
Temperature	1.72	1.86
Wind speed	5.28	1.86

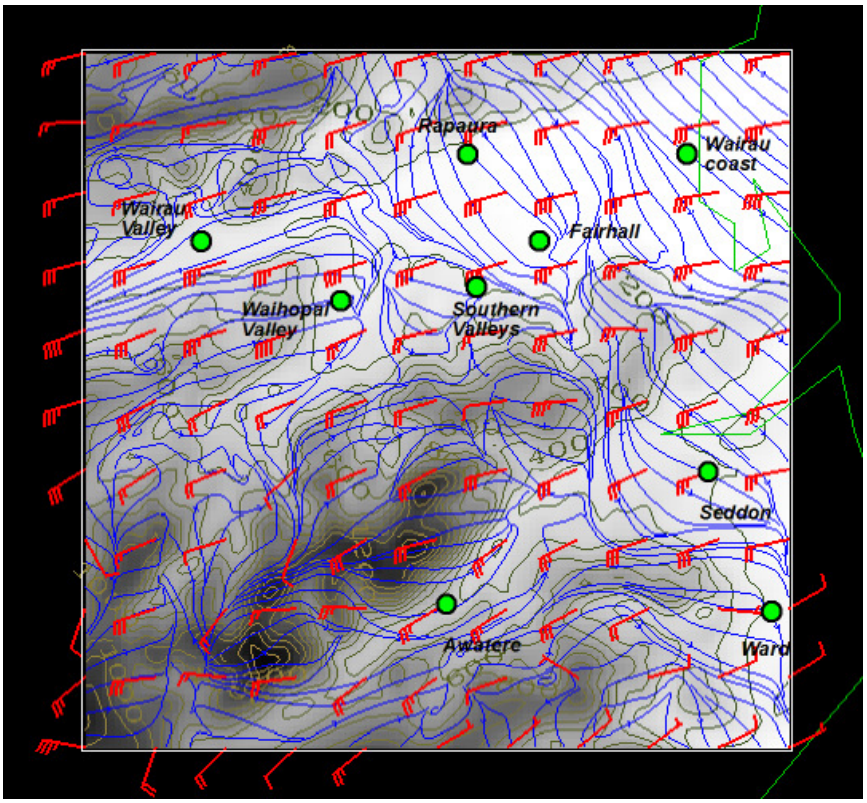

Figure 6.8 *WRF simulation of streamline plan view with near-surface winds (blue) and upper level (925 hPa) winds illustrated using red barbs, 6 am 10th October 2010. Stronger surface winds are indicated by a higher density of streamlines for a cross sectional area. Grid resolution 500 m.*

In Table 6.3 local observations reveal the extent to which shelter is provided to the region from surrounding topography. The spatial variation of 6 am near-surface temperatures was 6.5°C, with the largest temperature variation observed between the upper Awatere Valley

at Welds Hill and Seddon. Once again a relationship is evident between observed lighter near-surface winds and cooler near-surface temperatures. In Figure 6.8 the close proximity of streamlines are in areas where winds are predicted to be topographically channelled through some of the region's mountain passes and over exposed hilly terrain. This is in contrast to wider spaced and disorganised alignment of the streamlines near Fairhall, Wairau Valley Township, and parts of the upper Awatere Valley, which is supported by the spatial arrangement of blue isotachs in Figure 6.9 indicating light winds in these areas. Moderate winds are predicted through Rapaura, Wairau Valley coast, Seddon and Ward with associated warmer temperatures.

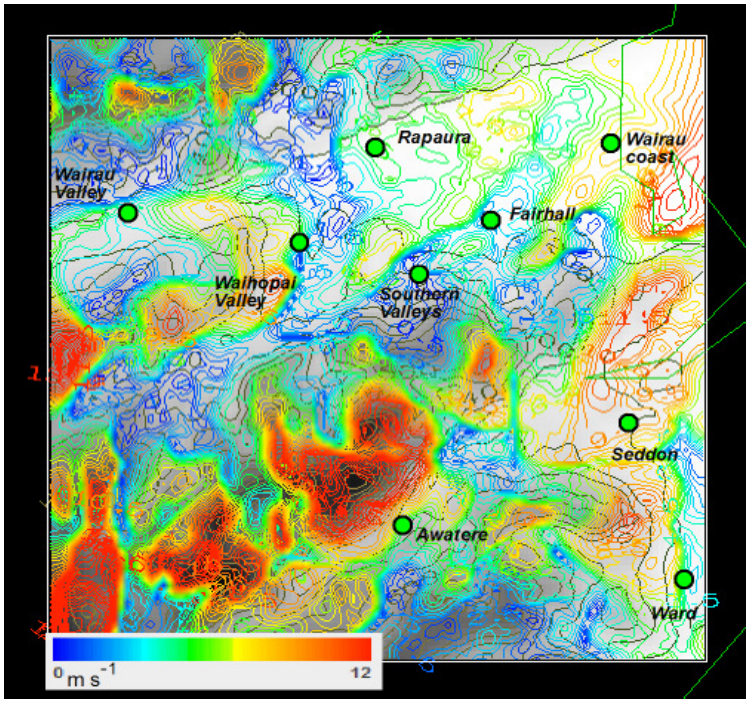

Figure 6.9 *WRF plan view of near-surface wind speed isotachs 6 am 10th October 2010. Areas of lightest winds are indicated by a deeper blue coloured contour. Grid resolution 500 m.*

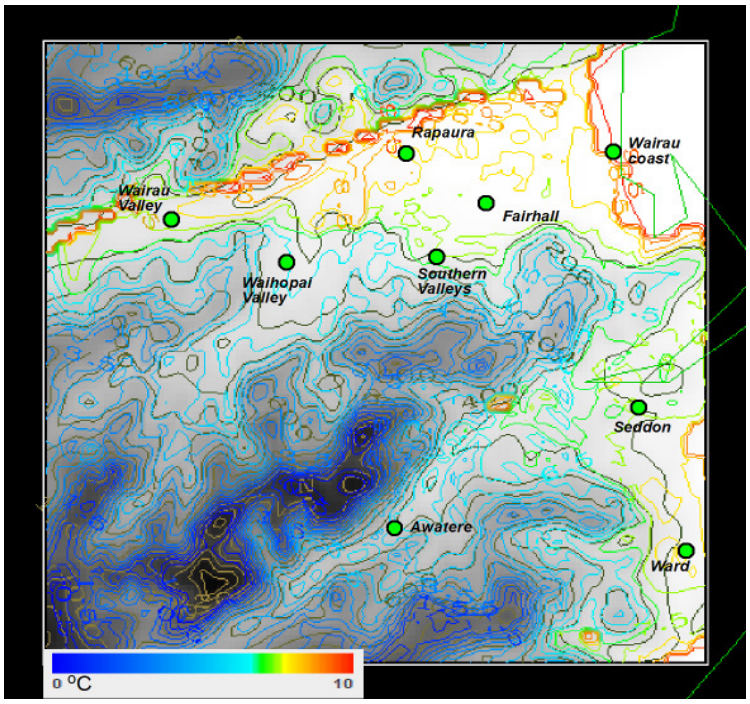

Figure 6.10 *WRF plan view of near-surface air temperature isotherms 6 am 10th October 2010. Areas of cooler temperatures are indicated by a deeper blue coloured contour. Grid resolution 500 m.*

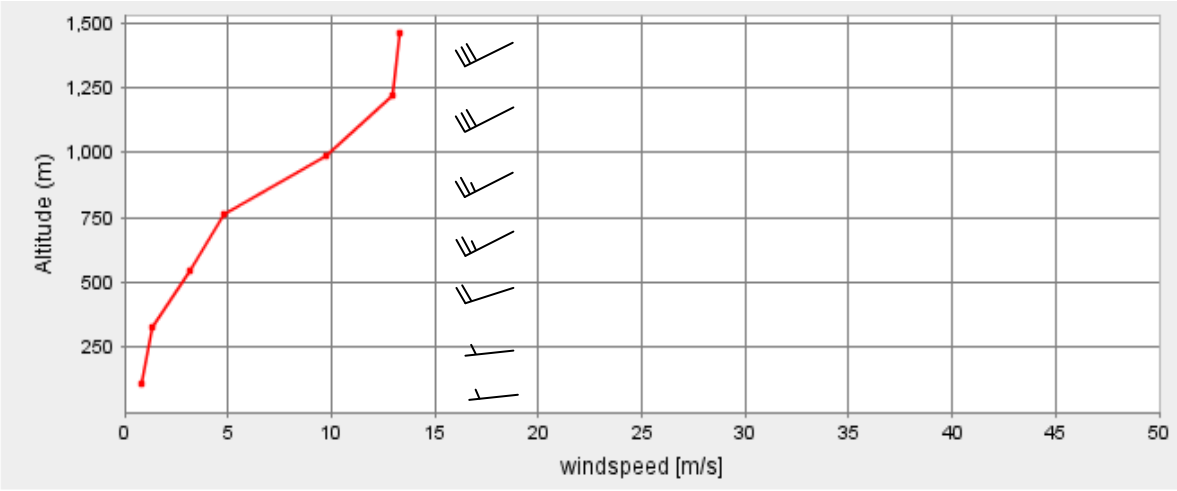

Figure 6.11 *WRF simulation showing vertical profile of wind speed only (red line) and wind speed and direction (wind barbs) 6 am 10th October 2010. Each whole wind barb is approximately 2.5 m s^{-1}.*

Although there is a moderate to good relationship between model generated wind speeds in Figure 6.9 and observations, predicted wind speeds are exaggerated. The simulated near-surface temperatures in Figure 6.10 show some resemblance to observations, particularly in the Awatere Valley, but as in the preceding case, warmer or cooler temperatures in the mid and lower sections of the Wairau Valley do not correlate with areas of increased or decreased wind speed.

The WRF generated vertical profile of wind speed and direction at the Awatere AWS (Figure 6.11) shows a very different profile compared to case study 1. The profile shows that wind speeds increase quickly above surrounding ridge top height (750 m) while at lower elevations, much lighter winds are predicted. The simulation of vertical wind speed suggests the steep topography surrounding the Awatere AWS provides considerable shelter from the strong west-south-west synoptic airflow, while strong winds are observed in many other areas of the Awatere Valley including Seddon. In some situations the synoptic winds above the terrain surrounding the upper Awatere AWS reach a critical speed so as to suppress the development of thermally generated winds, but are not strong enough to flush cold air from the valley floor. In these situations in-situ cooling will dominate in the near-calm conditions and may lead to localised lower minimum temperatures. This theory is explored using the University of Canterbury SODAR in Chapter 6.

6.5 Discussion

Idealised simulations where one or more model variables are held constant provide a method of investigating the strength of the relationship between that variable and the phenomenon of interest. Idealised simulations are common in the literature, particularly in studies involving pollution transport inside idealised terrain, (Lehner and Gohm 2010, Soltanzadeh et al. 2011 and Sabatino et al. 2007). In other cases, both terrain and synoptic influences can been modified, such as a study by Maja Telišman Prtenjak (2002) on sea breeze penetration across ground with a step change in surface roughness. For the

Marlborough region wind speed and direction were deemed critical predictors for the ventilation and stagnation of near-surface air layers, and these meteorological variables could be relatively easily manipulated inside the TAPM reanalysis data files.

As local observations suggest a relationship between near-surface wind speed and near-surface temperature, the idealised TAPM simulations provide a method of quantifying changes in the spatial variability of near-surface winds and near-surface temperature as a function of synoptic wind velocity. Simulations have shown that the least spatial variation of near-surface winds occurs during a complete absence of synoptic pressure gradients and during south-westerly synoptic conditions, as these conditions allow for the development of strong drainage winds in many parts of the region. These results are partially supported by Chapter 5, where the smallest spatial variation of minimum temperatures was found to occur during Kidson type SW. Simulations show that terrain-induced shelter to the region is at the greatest extent during south-westerly synoptic wind conditions when the 6 am simulation is remarkably similar to the zero synoptic simulation. If terrain-induced shelter during south-westerly conditions extended to the height of surrounding ridge tops, this would allow for the widespread unhindered development of katabatic and drainage winds, which would reduce the intensity of local stagnation and reduce the spatial variation of near-surface temperatures. It is also well recognised that katabatic flows are associated with warm air advection (Bodine et al. 2009) through the downward turbulent flux of warmer air from within an inversion layer (Smith et al. 2009). These theories are tested by the two case studies.

As the first case study encompassed light ridge top winds and Kidson type H, the streamline plot indicates the presence of strong drainage winds in parts of the region, including the Waihopai Valley, Rapaura and lower Wairau Valley. The vertical profile of wind speed at the Awatere AWS shows a zone of elevated wind speeds above the valley floor, and below the height of surrounding ridge tops. This provides some resemblance to the presence of a LLJ and this will be explored further using the University of Canterbury's SODAR in the following

chapter. In areas where near-surface drainage winds were predicted to be stronger, this generally coincided with elevated near-surface temperatures, except in Waihopai Valley. Cooler near-surface temperatures recorded by the Waihopai AWS are believed to reflect the sheltered location of this site, rather than the absence of strong drainage winds in the valley. In a private study completed for a large Marlborough winery in December 2013, wind velocity from the Waihopai AWS was compared with two privately owned AWS located centrally within the Waihopai Valley. In the seven month period from May to November 2013, the average wind speed during frost conditions was 1.1 m s^{-1} at the Waihopai AWS, compared with 2.6 m s^{-1} and 3.4 m s^{-1} recorded at the two privately owned AWS, respectively.

The strong drainage winds and elevated temperatures recorded in the upper Awatere Valley were not well resolved by the model, although this could be attributed to the low (100 m) resolution of the WRF digital elevation model and the narrow steep-sided valley walls of the upper Awatere Valley. There is clear agreement between the streamline and contour plots of near-surface wind speed as they are derived from the same model output, but there is a disconnect between near-surface wind speed and near-surface temperature plots which remains a problem. The projected near-surface temperatures do not correlate well with observations or reflect areas of lighter near-surface wind speeds, as would be expected in clear settled weather. Zhang and Zheng (2004) found similar problems when investigating the performance of planetary boundary layer schemes, and they concluded that a perfect simulation of the diurnal near-surface temperature did not guarantee the reproduction of associated diurnal cycles in near-surface wind speed. In a recent study by Ngan et al (2013) that examined the over-prediction of wind speed by the WRF model, it was concluded that warm near-surface temperature bias is a result of an over-prediction of downward sensible heat flux by the model, and that sensitivity studies revealed that it could be minimised by implementation of either the National Oceanic and Atmospheric Administration (NOAA) or the PX (Pleim-Xiu) Land Surface Models. Both of these Land Surface Models were tested in WRF sensitivity studies in Marlborough, but the RUC scheme

provided the best combination of near-surface wind speed and temperature predictions for the cases tested.

In the second case study the interaction of a moderate to strong westerly synoptic flow (Kidson type W) with Marlborough's topography, resulted in simultaneous areas of ventilation and stagnation, particularly in the Awatere Valley. In Chapter 5, analysis revealed that Kidson type W was more likely to produce a high spatial variation of minimum near-surface temperature in this part of the region. In spite of the 6.5°C spatial variation of near-surface temperature observed on this occasion, variations in excess of 12°C have been observed at other times, particularly during Kidson synoptic types that belong to the blocking group such as synoptic type HE.

The impact of ambient meteorology, especially strengthening of synoptic winds on the development of local katabatic and drainage flows is well established (Nappo and Snodgrass 1981; Gudiksen et al. 1992; Orgill et al. 1992). Increased wind speeds at ridge top have been shown to reduce the total drainage wind budget from a catchment, as well as reduce drainage wind speeds. Clements et al. (1989) extrapolated data from Colorado's Brush Creek Valley and suggested that ridge top wind speeds of 10 – 15 m s^{-1} with an up-valley component might prevent the establishment of nocturnal drainage flow. The complete elimination of drainage winds from the upper Awatere Valley AWS in the second case study was well simulated in the vertical profile of wind speed (Figure 6.11), resulting in an area of local stagnation with considerably cooler temperatures than was recorded in the first case study, where strong drainage winds elevated the near-surface temperature. The cooler temperatures could be attributed to a greatly reduced downward transfer of warmer air from above the valley floor by turbulent mixing, allowing a greater component of in-situ cooling to take place close to the point of observation.

Upon comparing the streamline and contour plots of wind speed (Figures 6.8 and 6.9) the model suggests that many of the areas of lightest near-surface winds are associated with

areas of convergence, where katabatic flows meet the synoptic wind. In the second case study the phenomenon is located about the mid sections of both the Wairau and Awatere Valleys at 6 am, but the size, shape and horizontal extent of the light wind zone is transient and moves about the mid sections of the Wairau Valley through the night. It is not clear from the analysis whether the zone of lightest winds is attributed to the interaction of thermally-induced flow and synoptic wind, or a result of the shelter provided in the valley by the interaction of synoptic winds with the surrounding terrain, but it is likely to be associated with periods of local strong in-situ cooling, giving rise to large spatial variations of minimum temperature.

Results from the two modelled case studies support the findings from Chapter 5 that pointed toward the occurrence of a high spatial variation of minimum temperature across several Kidson types, and that high spatial variations of near-surface minimum temperature occur as a result of simultaneous ventilation and stagnation. The two case studies presented in this chapter have shown that simultaneous ventilation and stagnation can occur during both light and strong ridge top winds around the region however, in each case different meteorological processes are involved. In stable weather, simultaneous ventilation and stagnation can occur irrespective of a locations relative exposure to strong thermally-induced drainage winds, whereas during stronger ridge top winds, simultaneous ventilation and stagnation may occur as result of grounding of the synoptic flow and sheltering provided to some (upper valley) locations from the close proximity of steep terrain. The implications of this finding are crucial for the generation of local frost forecasts, where the fleeting passage of a light wind zone can plunge isolated parts of the region into unexpected frost.

6.6 Summary

The idealised numerical modelling simulations have supported ideas developed in Chapter 5 where relationships were identified between Kidson type, sheltering provided by terrain,

and the spatial variation of minimum temperature. The ideas were investigated further in two case studies where light and strong ridge top wind speeds were present above the region, respectively. The WRF NWP model has revealed the development of strong drainage winds during light synoptic wind scenarios, although areas predicted to have stronger drainage winds were less well correlated with increased near-surface temperature. Model simulations have also shown that the interaction of stronger synoptic winds with surrounding complex terrain generated areas of simultaneous ventilation and stagnation, but once again the near-surface wind predictions were not well supported by predicted variations of near-surface temperature. Nevertheless, the NWP models have been useful in identifying local atmospheric boundary layer processes, such as extent of strong drainage winds that strongly influence near-surface temperatures.

This chapter closes by proposing two further questions that arise from the modelling exercise: If strong drainage winds are responsible for modifying the spatial variation of minimum temperatures in light wind conditions, what are the physical mechanisms that deliver the warmer air to surface? Secondly, what prevents air from mixing inside zones of stagnation during stronger synoptic wind conditions? In the final results chapter, these questions are addressed through analysis of vertical soundings collected by the University of Canterbury's SODAR from separate locations in the Awatere and Wairau Valley. Data from the SODAR are complemented by fixed and temporary AWS's in these areas.

Chapter 7

The influence of boundary-layer vertical structure on near-surface temperature variation.

7.1 Introduction

In the preceding chapter, NWP models helped to identify the highly complex nature of the thermal wind regime in Marlborough. In particular, they revealed the strong topographical channeling of drainage winds in parts of the Awatere and Wairau Valleys under clear, settled atmospheric conditions. Subsequent analysis then linked the areas of stronger near-surface wind speeds with higher near-surface temperatures, suggesting a mechanism of mixing, as a result of higher wind speeds, where warmer air within the core valley atmosphere is transferred to the surface.

Banta (2008) suggested that roughly half of the diurnal (temperature) cycle over land surfaces in mid-latitude areas is dominated by a stable boundary layer (SBL) regime. Analysis of local climate data from Marlborough for the winter and spring of 2010 revealed that nocturnal drainage winds were recorded on 26% and 31% of nights in the Awatere and Wairau Valleys, respectively. These values not only suggest that thermally generated wind regimes make up a significant proportion of Marlborough's nocturnal climate, but that the frequency is sufficient to affect the distribution of mean temperatures and have profound impacts on the region's agriculture.

In this chapter, data obtained from the University of Canterbury's SODAR are used to examine the vertical structure of drainage winds at Welds Hill in the Awatere Valley and at the Rapaura AWS. These areas are renowned for higher nocturnal surface wind speeds during clear stable weather and frequently remain frost-free in these conditions. It was

thought that observations from the SODAR would reveal the presence of LLJ above these points of interest and that through closer analysis, a mechanism for mixing warmer air to the surface would become clear. To confirm this hypothesis three cases have been selected to show that changes in ridge top wind conditions exert an influence on LLJ structure and how this ultimately affects near-surface temperature.

7.2 The stable nocturnal boundary layer (NBL)

According to Whiteman (1990) early research such as Defant (1951) focused on conceptually isolated local circulation systems that operated independently from ambient meteorology. It is now well documented that local thermally generated wind regimes seldom completely decouple from the ambient atmosphere above ridge tops in complex terrain (Barr and Orgill 1989, Kaufmann and Weber 1996, Nappo and Snodgrass 1981, Schmidli et al. 2009, Bossert and Poulos 1995, Sturman and Tyson 1981). The larger scale atmospheric processes have been described as exerting a continuum of influence on the near-surface climate, with the smallest influence observed during stable, anticyclonic conditions and greatest influence during episodes of strong synoptic flow. In stable weather, thermally generated wind regimes dominate the near-surface wind patterns, while under strong synoptic forcing, strong winds and turbulence overpower local circulations and may ventilate an entire complex terrain environment. However, between these two ends of the spectrum ambient meteorology may exert a more subdued influence on a thermally generated wind regime. When the overlying synoptic flow opposes the drainage wind, Barr and Orgill (1989) suggested the presence of a transition layer, characterized by light winds of variable direction. Earlier research by Sturman et al. (1985) in the Chilton Valley of the Southern Alps, New Zealand, also recognised an 'intermediate layer' between the underlying drainage flow and synoptic wind loft.

Barr and Orgill (1989) defined the base height of a transition layer as the height where wind speed (of the drainage layer) decreases to a minimum, and simultaneously, the wind

direction changes by more than 50% of the difference between the down-valley direction and ridge top wind direction. Their schematic diagram showing the relationship of the transition layer to observed wind and temperature profiles is reproduced in Figure 7.1, but with a modification to better represent conditions in the Marlborough region. Red arrows have been added to the base height of the transition layer to indicate its dynamic nature as a function of synoptic wind strength and atmospheric stability. Stull (1988) proposed that the peak velocity in drainage flow over sloping terrain is typically well below the inversion top.

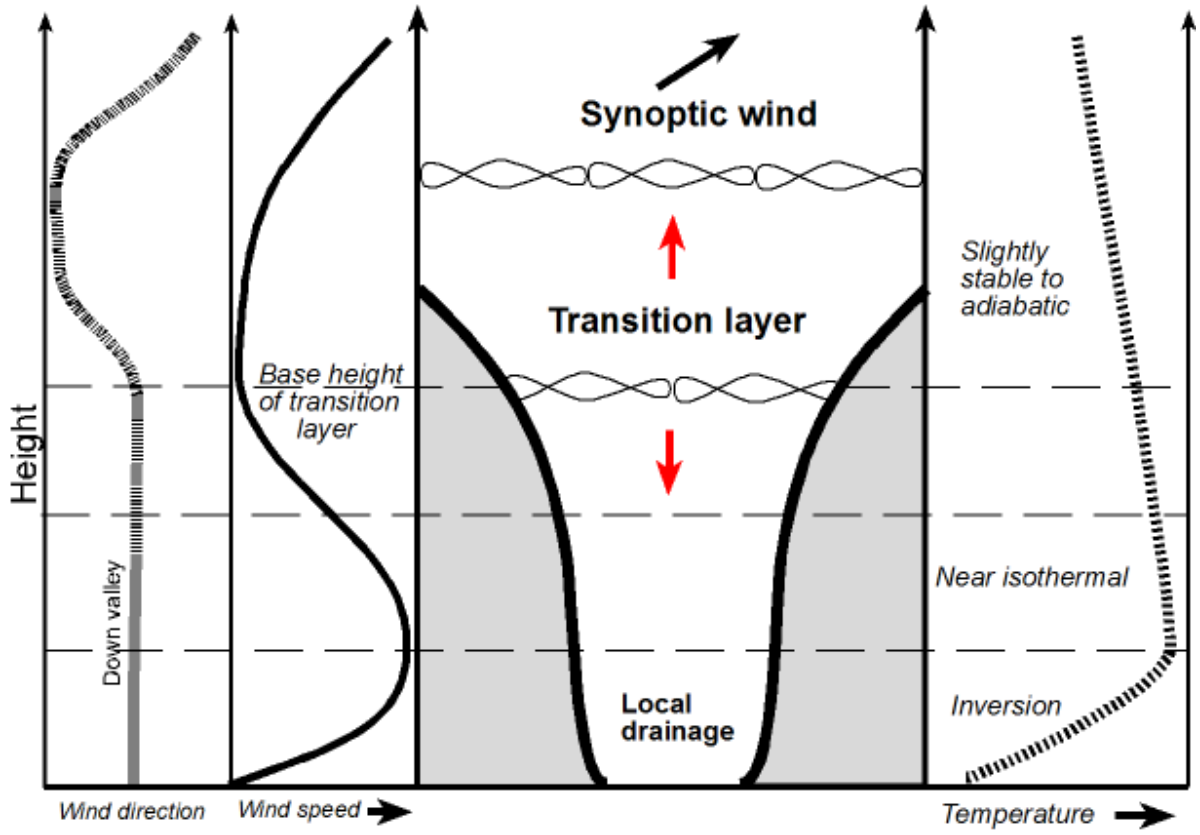

Figure 7.1 *Model of NBL structure based on observations over predominantly flat terrain (Barr & Orgill 1989). The original model has been modified by introducing red arrows to indicate a dynamic transition layer that is transient in height, in response to changes in synoptic wind velocity.*

Observed fluctuations in the near-surface strength of drainage winds have been attributed to changes in overlying synoptic wind in the literature (Gudiksen et al. 1992, Barr and Orgill 1989, Clements et al. 1989, Doran 1991, and Whiteman and Doran 1993). Gudiksen et al. (1992) devised a classification scheme for drainage flows based on the extent of interruption from external meteorology. Four categories of drainage wind were described as: A – well established slope flows with minimal interruptions from external influences; B – well established slope flows with major interruptions by external influences; C – weak slope flows with major interruptions by external influences; and D – minor or no drainage winds. The classification scheme devised by Gudiksen et al. (1992) is particularly important for the Marlborough region because of the strong relationship established in the preceding chapter between surface wind velocity and temperature.

7.3 Stable atmospheric conditions

For the purposes of this section, stable atmospheric conditions are encountered under anticyclonic conditions when mean ridge top wind velocities are below 5 m s^{-1}. Assuming predominantly clear skies, katabatic winds develop unhindered within the multitude of tributary valleys in Marlborough and merge into larger scale drainage flows (Figure 7.2) that dominate the region's larger river valleys. The schematic illustration portrays the observed mean drainage pattern based on observations of wind speed (Figure 4.12) from the network of privately owned AWS with the wider, longer arrows depicting observations of stronger drainage winds.

The first case study was selected to illustrate the development of the NBL at the upper Awatere Valley AWS location during a period of stable anticyclonic conditions. The observation period is described as a type "A" category of drainage flow, according to the classification scheme by Gudiksen et al. (1992). The vertical wind profile from this location was limited at times by the resolution of the SODAR, but provides a good indication of wind velocity and direction to a height of 4 – 500 m above ground level (AGL). SODAR data were

complemented by a temporary AWS located on Scrub Rough Spur (Figure 3.5), approximately 220 m above the height of the SODAR.

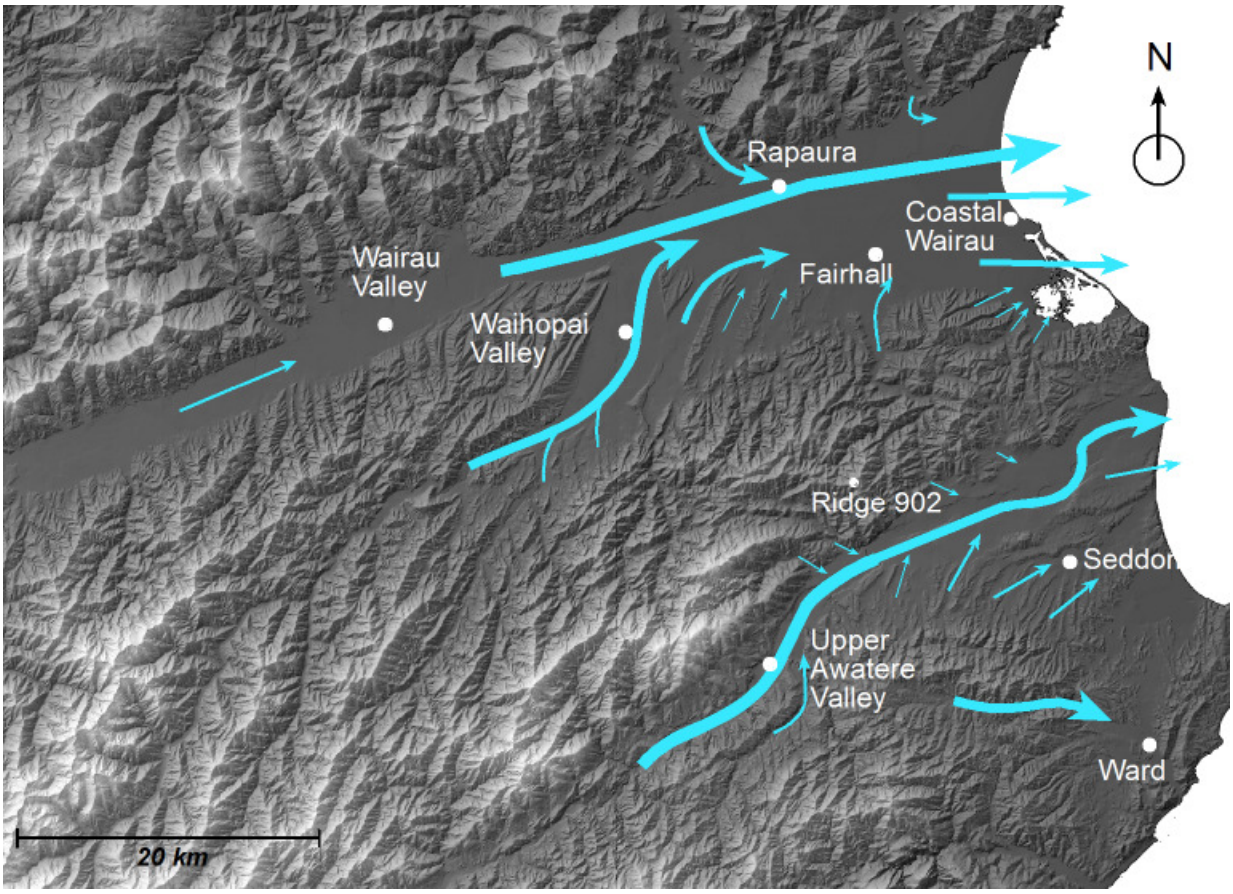

Figure 7.2 *A typical spatial pattern of the drainage wind field under settled atmospheric conditions.*

7.3.1 Case study 1

Case study 1 explores the evolution and vertical structure of drainage winds above the Awatere AWS for the 18 hour period from 1800 NZST 2nd October to 1200 NZST 3rd October. It was a period of anticyclonic weather with clear skies and light ridge top winds from the south-south-east of 2 – 5 m s^{-1}. Surface based observations recorded the onset of down-valley drainage winds at the Awatere AWS (Figure 7.3a) from 2230 NZST, with wind velocities of 3.5 m s^{-1} attained after just 20 minutes. However, it was almost 2 hours before similar wind velocities were attained at the elevated Scrub Rough Spur AWS (Figure 7.3b),

220 m above the height of the Awatere AWS. Wind velocity continued to increase at both locations until 0700 NZST, when speeds of 7 m s^{-1} and 11.3 m s^{-1} were attained at each site respectively. While the increase in velocity was steady at the well exposed Scrub Rough Spur AWS, it was erratic at the Awatere AWS, which is expected to be the result of near-surface winds being affected by interaction with undulating terrain and vegetation.

a) Awatere Valley AWS

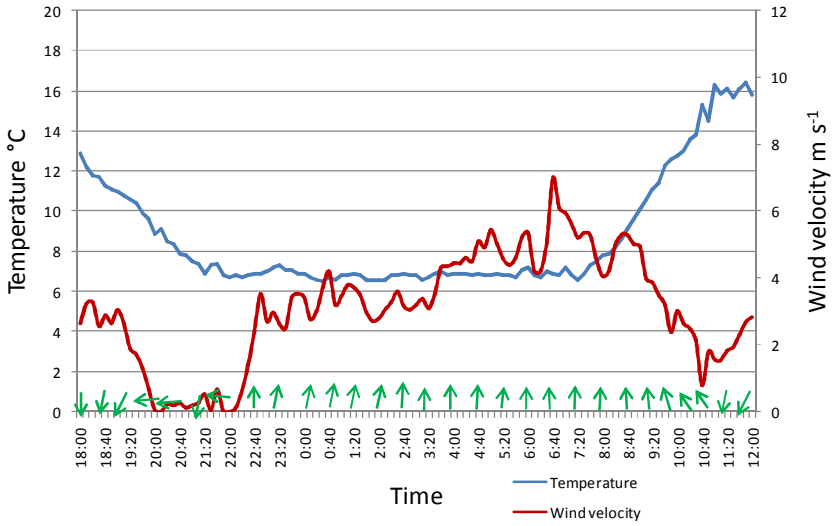

b) Scrub Rough Spur AWS

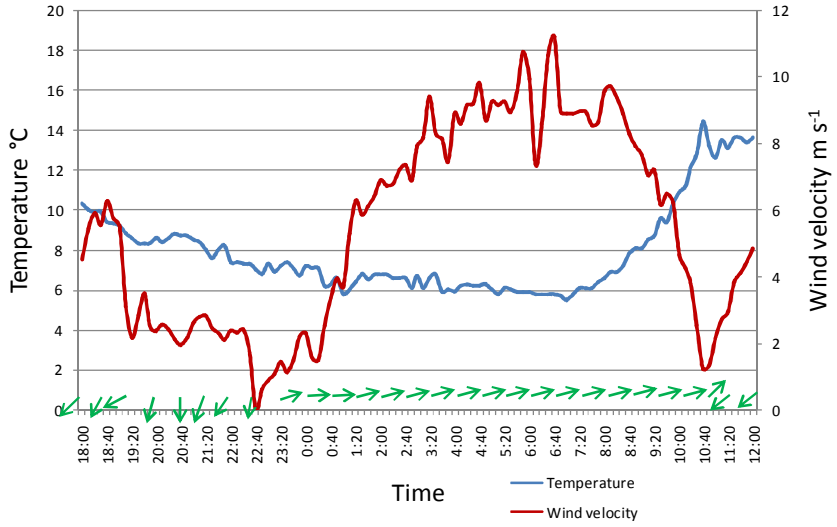

Figure 7.3 *Temperature, wind speed and direction at a) Awatere Valley AWS and b) Scrub Rough Spur AWS 2 – 3 October 2010.*

Observations from the Awatere and Scrub Rough Spur AWS show that the drainage wind grew in both height and velocity with time, as ambient meteorology remained stable. The higher down-valley wind velocities recorded on Scrub Rough Spur initially demonstrated the possibility of a LLJ, which was subsequently confirmed by analysis of SODAR data.

A time-height cross-section of SODAR data (Figure 7.4) indicates the onset of drainage winds near the valley surface from a south-south-westerly direction (down-valley) shortly after 2200 NZST. From 0000 NZST the down-valley flow grew quickly in both height and speed, extending beyond the range of the SODAR (480 m AGL) by 0100 NZST. The cross-section shows that wind direction veered to the west with height as winds were realigned by the orientation of side walls of the Awatere Valley. It also reveals that down-valley drainage winds increased quickly above the valley floor, reaching maximum speeds at a height range of 140 – 220 m AGL, similar to those reported by Pinto et al. (2006) in the Great Salt Lake Valley, Utah. Winds then showed a reduction in velocity with further height and in this manner exhibit the features of a LLJ, as described by many researchers (Whiteman 1982, Kraus et al. 1985, Post and Neff 1986, Banta et al. 1992, Whiteman et al. 1997, Banta et al. 2004, Sturman et al. 2003 and Darby et al. 2006).

The definition of a low-level jet has varied from study to study depending on the situation and the limitations of the available data set (Banta 2008). However, in this study a nocturnal low-level jet is considered to be a fast moving stream of air in the low levels of the atmosphere that forms overnight in the lowest few hundred meters AGL, often reaching maximum development early in the morning. The wind-speed maximum is is required to have a peak speed of at least 2 m s^{-1} greater than winds at levels both above and below the maximum (nose).

While the vertical extent of the LLJ in this case is not known, it is assumed to be contained below the height of surrounding ridge tops (700 m AGL). An interesting feature of the SODAR plot is the rapid increase in horizontal wind velocity within the first 20-40 m above

the ground. The increase in horizontal wind velocity beneath the LLJ reflects strong wind shear (Banta 2008) which has been linked with increased near-surface temperatures as a result of enhanced vertical mixing (Banta et al. 2004 and Pinto et al. 2006). A time-height cross-section of wind shear calculated from the SODAR data is presented in Figure 7.5. The red colours are indicative of horizontal wind velocity that increases with height, while the blue colours indicate a decrease. Clearly some of the most intense colours are observed very close to the surface signifying strong wind shear.

While LLJ's have been observed to exhibit meandering and helical flow in larger river valleys (Van de Wiel et al 2010) the relatively narrow, steep sided Wairau and Awatere Valleys may not experience such features. If they did exist, the implications of a meandering drainage flow on near-surface minimum temperatures include periods of reduced near-surface wind speed associated with horizontal displacement of the LLJ allowing for increased cooling and lower near-surface minimum temperatures. In this respect, the case described here may have limited applicability to areas of complex terrain that have significantly wider river valleys.

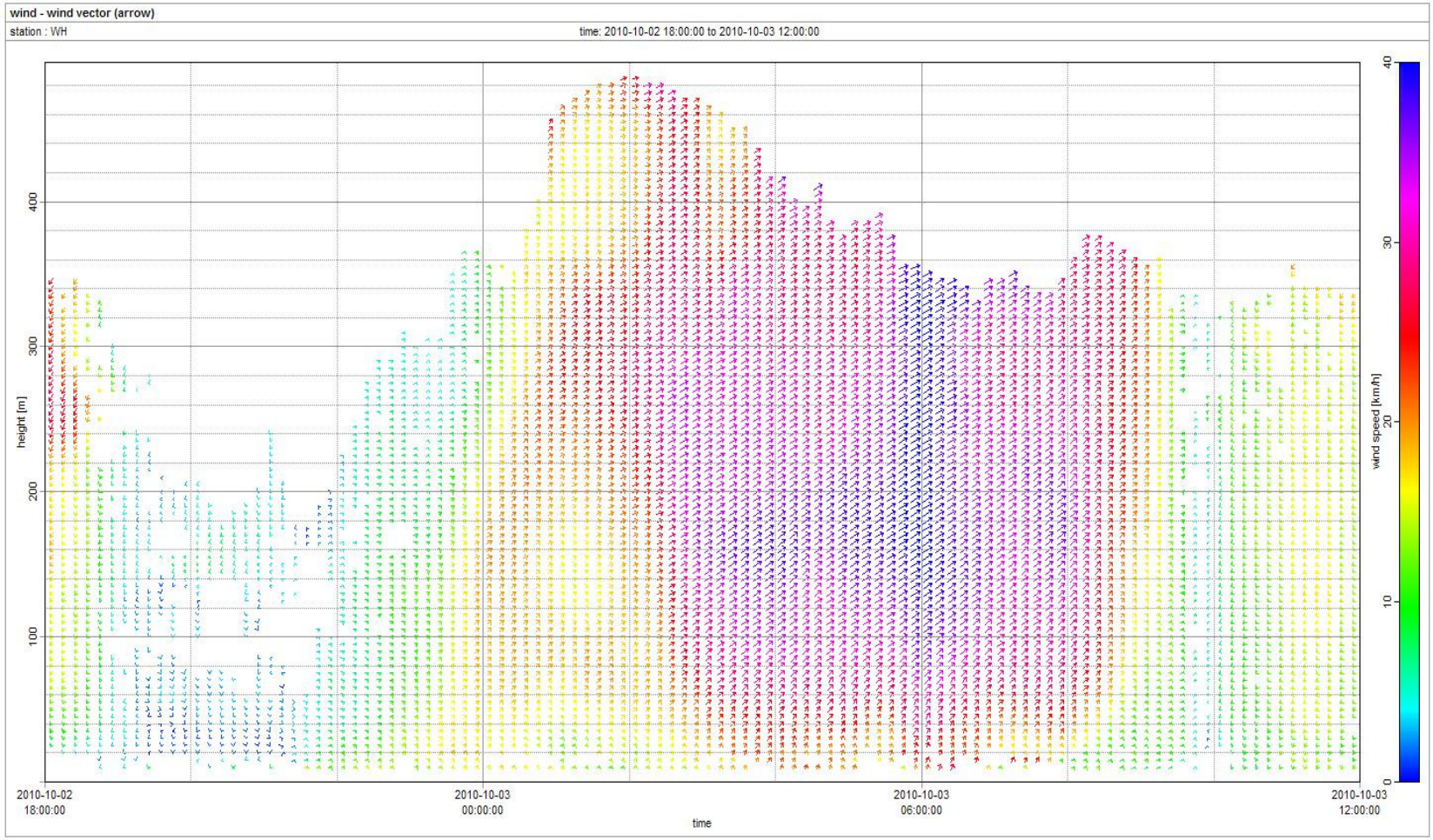

Figure 7.4 *Vertical time-section of wind speed and direction from the SODAR at the Awatere AWS, 2 – 3 October 2010. Strong down-valley drainage flow was recorded from 2240 NZST until mid-morning on 3rd October.*

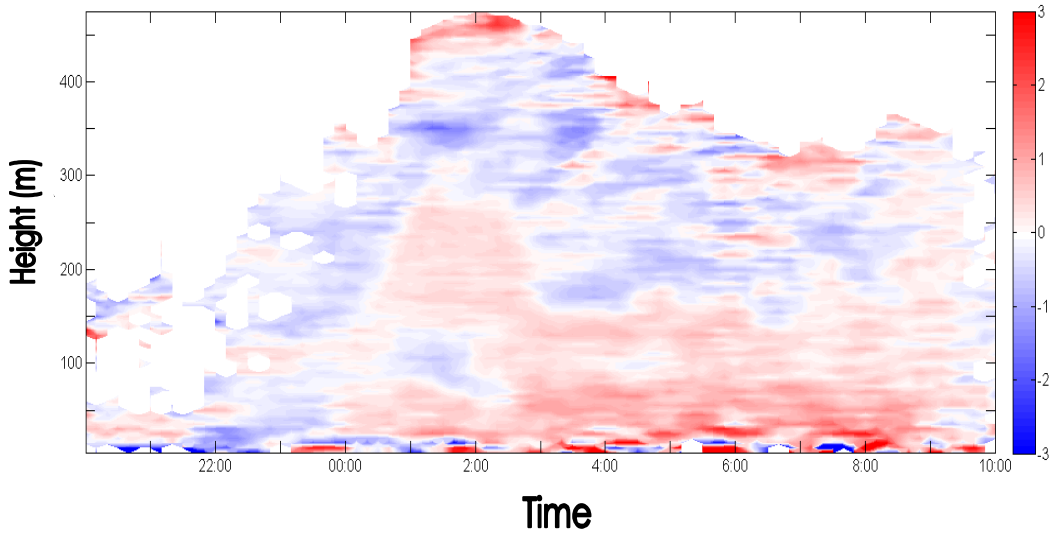

Figure 7.5 *A time-height cross-section of wind shear derived from the SODAR, 2 – 3 October 2010. Higher shear values are observed near the surface and these are thought to have a significant influence on modifying near-surface temperatures beneath the LLJ.*

Whilst it is not possible to distinguish the mode of air mixing between the LLJ and the near-surface layer from this data set, Pinto et al. (2006) described how pulses in the strength of a LLJ may create localized areas of low-level convergence, gravity waves and Kevin-Helmholtz waves, all of which contribute to vertical mixing and warming of air layers closest to the surface. Given the 0400 NZST temperature of the drainage wind on Scrub Rough Spur of 6.0°C and the temperature at the Awatere AWS on the valley floor is 7.2°C, it is fair to conclude that air within the LLJ was being mixed to the surface. (The slightly higher temperature at the Awatere AWS can be attributed to adiabatic warming of near-surface air). Although the entire air layer associated with the LLJ appears to gradually cool, as reported by Pinto et al. (2006), this is not entirely reflected by temperatures at the Awatere AWS. The vertical mixing of air associated with the LLJ appears to limit the near-surface minimum temperature at the Awatere AWS to values well above those that would have occurred through unhindered radiational cooling. Similar results were reported again by Pinto et al. (2006), as part of the Vertical Transport and Mixing (VTMX) research programme in the Great Salt Lake Valley.

7.4 Moderate ridge top winds

In the second and third case studies, moderate winds were recorded on ridge tops above Marlborough. These cases present just two examples out of hundreds of possible scenarios where synoptic winds exert an influence on the development of thermally-induced wind and temperature regimes. For the purpose of these two cases, moderate winds are defined as having mean ridge top speeds of between 5 to 10 m s^{-1}. Clements et al. (1989) ascribed the speed of ridge top winds as the main determinant of drainage wind velocity on surrounding slopes and valleys. Assuming predominantly clear skies, research has shown that ridge top wind conditions may weaken, intermittently interrupt, or completely cancel the development of local thermally-induced wind regimes (Doran and Horst 1990, Gudiksen et al. 1992, Barr and Orgill 1989, and Banta et al. 2004). The degree to which a local valley wind regime is affected is a function of not only ridge top wind velocity, but the angle of the overlying wind direction to valley side-walls (Doran and Horst 1990) and valley atmospheric stability.

The effect of weakened or interrupted drainage wind regimes in Marlborough is captured vividly by near-surface temperatures on numerous occasions each season. Temperature variations in excess of 12°C have been observed between AWS sites in some instances. Figure 7.6 attempts to show the effects of a strengthening synoptic wind on cold air drainage over the Marlborough region. The thinner arrows depict historic observations of lighter drainage winds that are recorded in these situations, whilst in some locations (such as the lower Awatere Valley) synoptic ventilation over-powers the thermally-induced winds.

Case study 2 is described as a “B” type category of drainage flow, according to the classification scheme by Gudiksen et al. (1992), although interruptions at the surface from external meteorology are slight rather than major. Once again, observations of the vertical extent of the wind profile were limited by the vertical range of the SODAR, but a good indication is provided to heights of 400 – 500 m AGL.

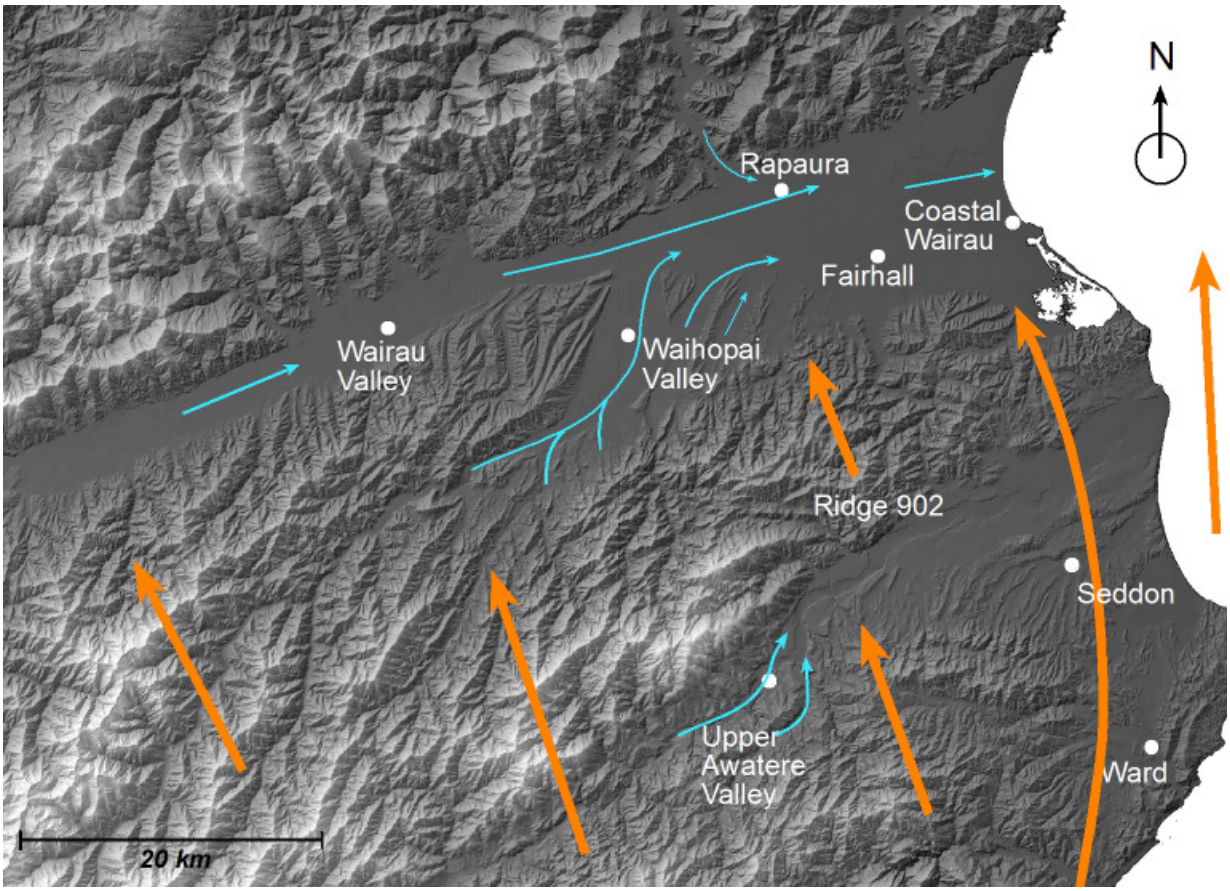

Figure 7.6 *A schematic illustration of case 2 showing diminished drainage winds under moderate (south-easterly) synoptic flow. The orange arrows are indicative of synoptic flow, whilst the weakened thermally-induced wind regime is depicted by smaller blue arrows.*

7.4.1 Case study 2

Case study two explores the vertical structure of the NBL from the Rapaura data set for the overnight period of 29 – 30 April 2011, when moderate south-easterly winds (6 – 7 m s^{-1}) were observed at ridge top level. The case was selected from the data set as it demonstrates several phenomena of interest to this chapter, in particular a transition zone that is identified in between the overlying synoptic flow and LLJ.

The onset of down-valley drainage winds is identified from the Rapaura AWS (Figure 7.7) as a west-south-west breeze from 1930 NZST. The quick drop of near-surface temperature

from 1800 – 1900 NZST slowed following onset of the drainage winds. Observations show that a near-surface drainage wind velocity of about 3 m s^{-1} was sustained well into the following morning, although brief disturbances to the flow were recorded at 2230 and 0230 NZST, and these are reflected by small decreases in temperature of around 1 - 2°C.

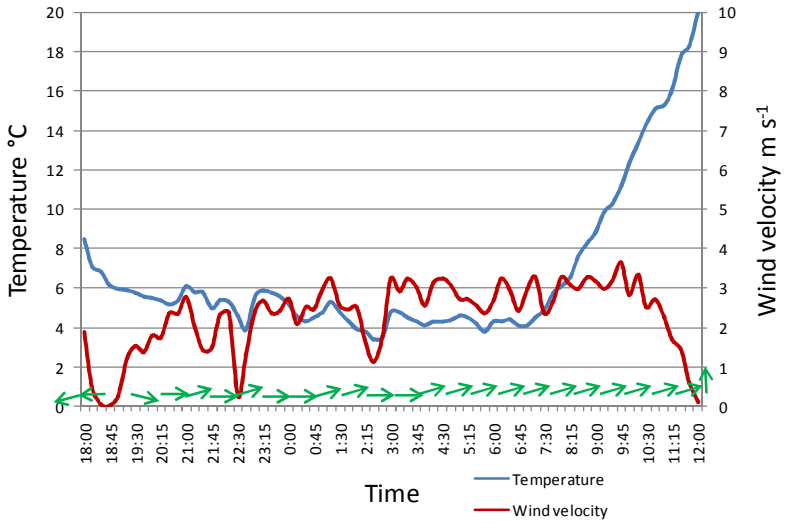

Figure 7.7 *Temperature, wind speed and direction at Rapaura AWS, 29 – 30 April 2011. Temperatures decreased slowly following the onset of drainage winds at 1845 NZST.*

A time-height cross-section from the SODAR is presented in Figure 7.8. The onset of drainage winds is shown by the west to west-north-west wind direction after 1900 NZST. The drainage wind steadily grew in depth, similar to results found by Pinto et al. (2006) and developed a wind speed maximum that varied in height from 40 to 140 m AGL. The location of an elevated wind velocity maximum is strongly characteristic of a LLJ, with mean wind velocities in the centre of the jet in excess of 8 m s^{-1} (28 km hr^{-1}).

Of particular interest to this case is the way in which south-easterly winds at ridge top, tend north-easterly at lower elevations (4 – 500 m) and suppress the vertical extent of the LLJ from aloft after 0400 NZST. Although the data from the SODAR were lost above 400 m after 0600 NZST, the north-easterly winds were clearly evident above 260 m at this time. A transition layer, characterized by light and variable winds is unmistakable between the LLJ

and the synoptic wind. The depth of the transition layer is relatively constant with the zone of lightest winds and is only 20 - 40 m thick. Transition layers of similar nature have been observed by many researchers and are well described by Sorbjan (1988), Mahrt (1985), Sturman et al. (1984), Barr and Orgill (1989) and Orgill et al. (1992). While the north-easterly winds were strong enough to reduce the vertical extent of the LLJ by almost 200 m after 0400 NZST, no significant effect to drainage wind speed was observed at the Rapaura AWS. Earlier disturbances to the drainage wind at Rapaura AWS were likely to be caused by a partial decoupling of the drainage flow from the surface, and this is confirmed by subtle lifting of the jet about 2245 and 230 NZST in Figure 7.8.

The plot of wind shear (Figure 7.9) once again demonstrates that higher values were recorded within 25 m of the surface, reflecting the increase in horizontal wind velocity to the height of the jet maximum (40 – 140 m AGL), particularly the rapid increase near the surface. Wind shear values were smallest near the top of the LLJ but increase again within the narrow transition zone. A zone of increased shear above 200 m after 0400 NZST reflects the intrusion of synoptic winds into the LLJ. No significant changes are detectable in the near-surface wind shear at the times of disturbance to drainage flow at Rapaura AWS, and this is believed to explain the small decrease in near-surface temperature. Although near-surface wind velocities were briefly reduced, shear above the surface was still sufficient to mix some warmer air downwards and prevent larger decreases in surface temperature.

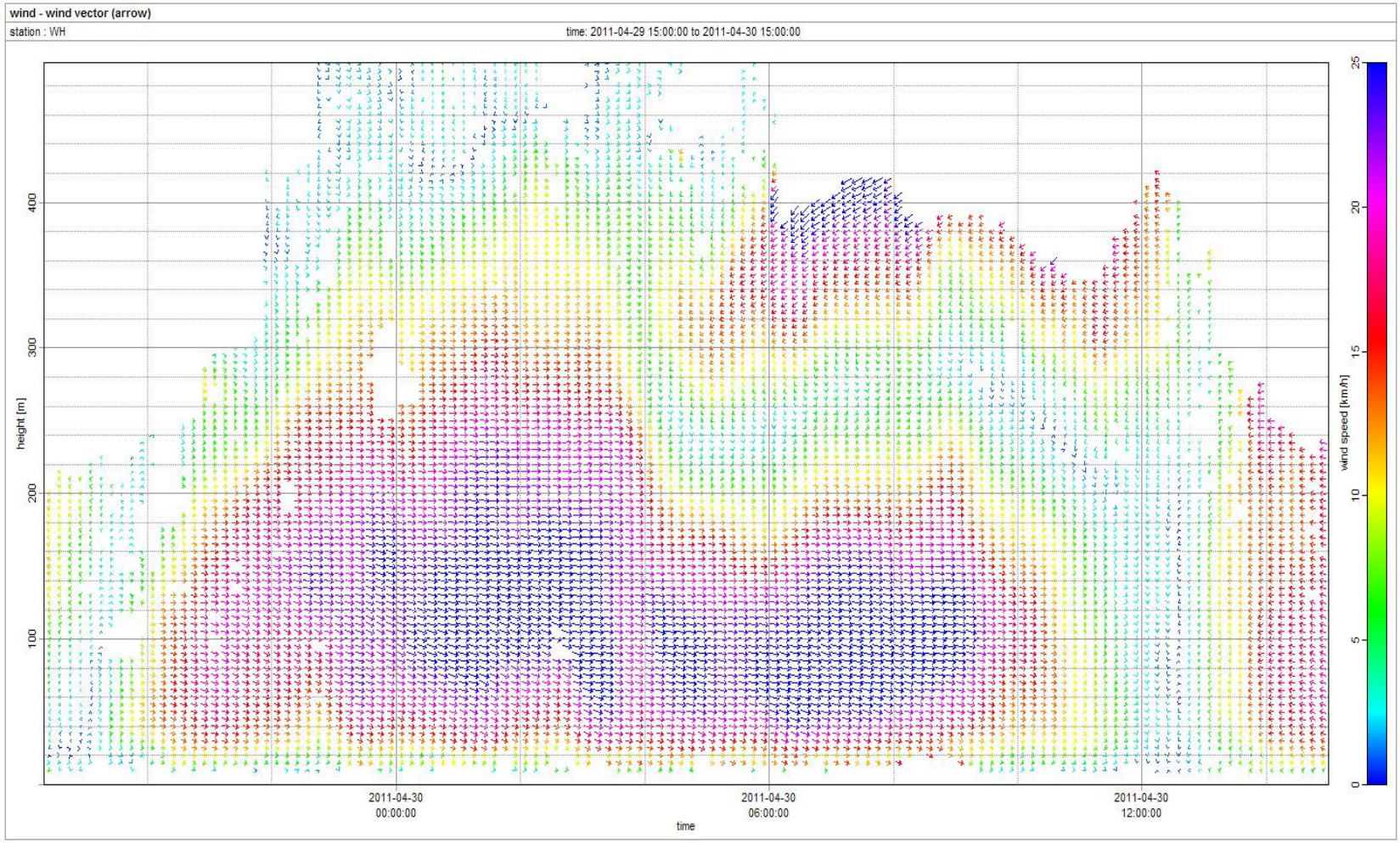

Figure 7.8 *Vertical soundings of wind velocity from the SODAR at Rapaura, 29 – 30 April 2011. A transition layer is present above the LLJ from 0400 NZST as the synoptic wind erodes the drainage flow from aloft.*

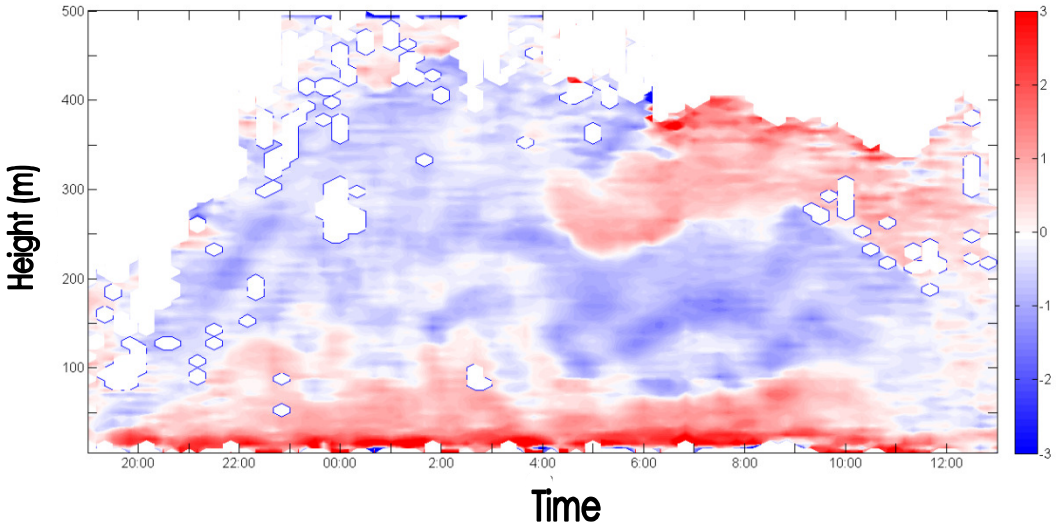

Figure 7.9 *A time-height cross-section of wind shear derived from the SODAR at Rapaura, 29-30 April 2011. Higher shear values are observed very near the surface and these are thought to induce turbulence which mixes warmer air from the LLJ to the surface.*

7.4.2 Case study 3

The third case study entails the overnight period of 26 – 27 July 2010 and data were obtained from the Awatere AWS site. Strong west-north-westerly winds of 7 – 10 m s^{-1} prevailed across surrounding ridge tops throughout this period, but despite the stronger ridge top winds skies remained clear and provided an opportunity for strong radiational cooling in areas sheltered from the wind. Frost was recorded at the Awatere AWS, an uncommon occurrence even during winter months due to the consistent development of a thermally-induced drainage wind. Frost is only recorded at this site when strong down-valley drainage is interrupted or weakened.

In the absence of any significant near-surface wind, temperatures steadily decreased at the Awatere AWS, reaching 0°C before midnight (Figure 7.10). Although temperatures rose above 0°C for a short time prior to 0400 NZST, the AWS did not record any significant changes to wind velocity at this time. Overnight drainage winds recorded at the AWS were

weak, disorganised and intermittent, and in this respect the drainage wind fits a class of C or D according to the descriptions given by Gudiksen et al. (1992).

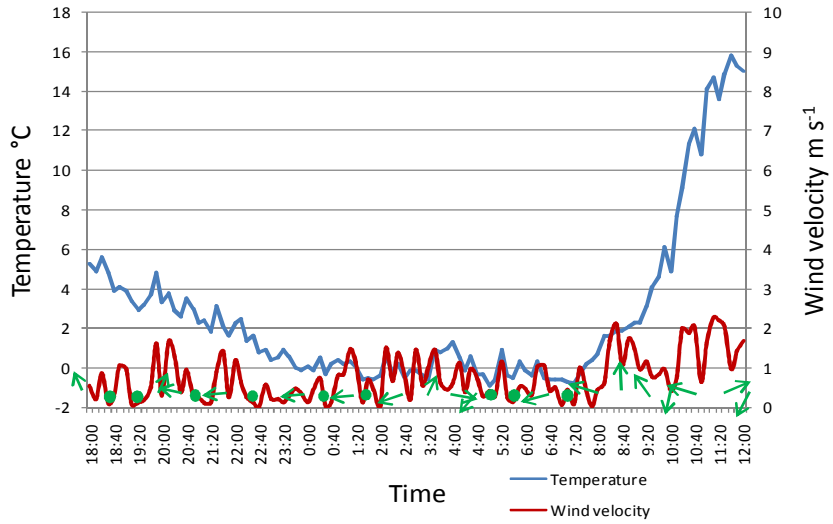

Figure 7.10 *Temperature, wind speed and direction from Awatere AWS, 26 - 27 July 2010. Frost is recorded in the absence of any organized down-valley flow (green dots represent 30 minute periods of mean wind speeds less than 1 m s^{-1}).*

The SODAR time-height cross-section (Figure 7.11) reveals the extent of synoptic wind intrusion into the Awatere Valley, sufficiently strong to suppress the development of any thermally generated winds. The SODAR reveals that synoptic winds in excess of 5 m s^{-1} frequently descended to within 80 m of the valley surface during this period, with the lengthiest intrusion occurring at 0345 NZST. The increase in surface temperature recorded at this time is thought to be associated with some increased mixing of warmer air from the synoptic airstream, and to some extent this is verified by the brief increased presence of near-surface shear, as illustrated in Figure 7.12.

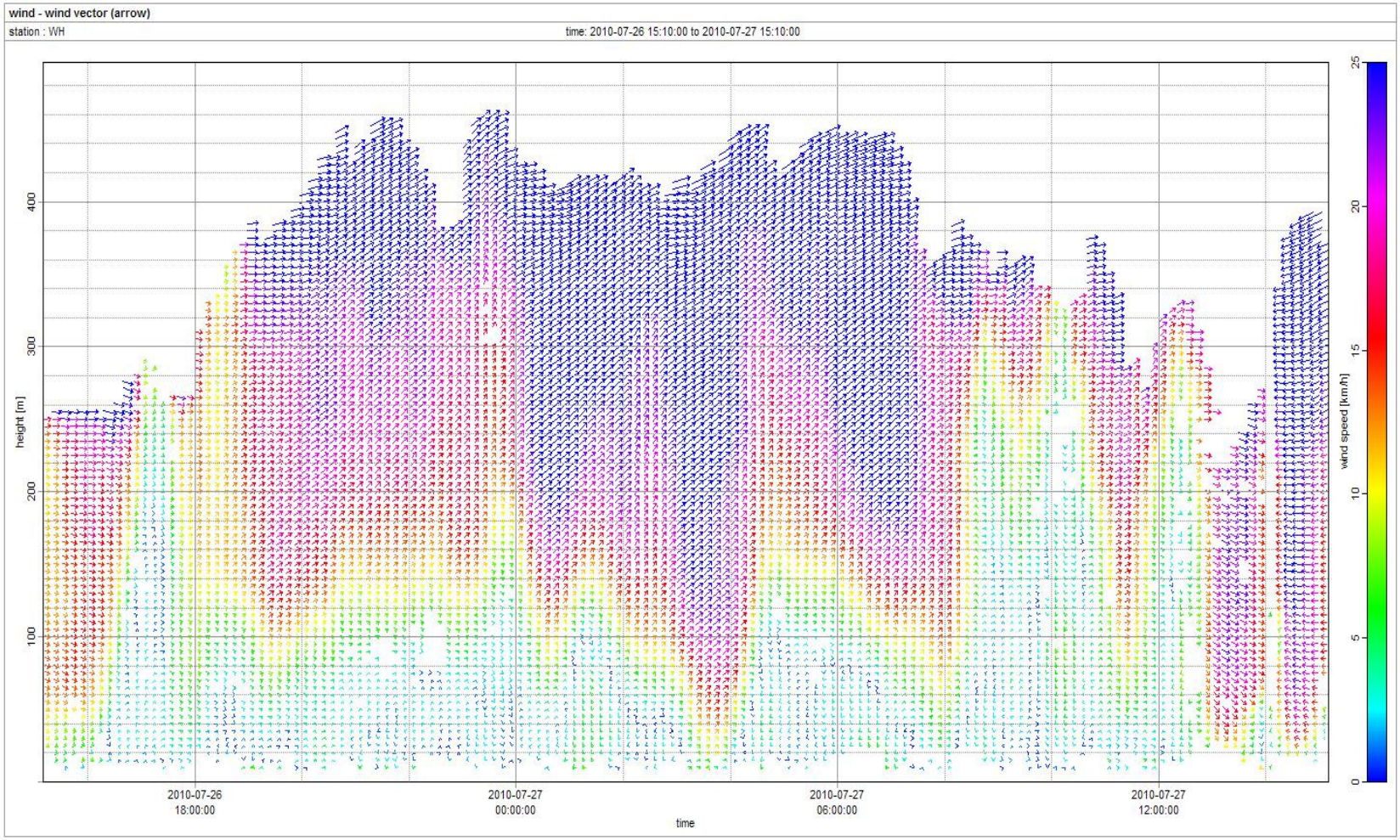

Figure 7.11 *Vertical soundings of wind speed and direction from the SODAR at Awatere Valley AWS, 26 – 27 July 2010. Synoptic winds descend to within 20 m of the valley floor at 0345 NZST. A synoptic wind change can be seen just after 1400 NZST, as wind direction changes from down-valley to up-valley.*

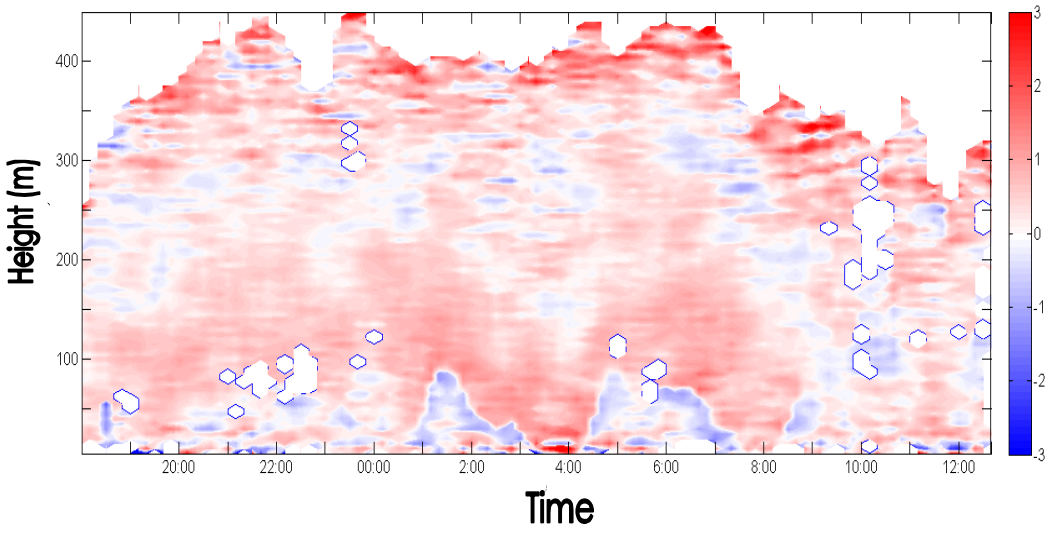

Figure 7.12 *Time-height cross section of wind shear derived from the SODAR at Awatere Valley AWS, 26 – 27 July 2010. Intense near-surface shear values are not present in this case which suggests minimal mixing of air to the valley surface. A brief period of increased shear at 0345 NZST is discernible and is associated with a near-surface temperature increase of almost 2°C.*

The shallow layer of very light winds above the valley surface is believed to represent a grounding of the transition layer, beneath the synoptic winds aloft. The absence of higher wind shear values near the surface allowed increased radiational cooling.

7.5 Discussion

While the data collected by surface-based AWS indicate that warmer air currents affected particular areas within the region under certain weather conditions, little was known of their vertical structure or extent. It is also recognised that fixed point observations give only a partial picture of near-surface flow structure. The first indication of a LLJ in the Awatere Valley was portrayed by the WRF simulation in Chapter 6, where the vertical profile of wind speed above the Awatere AWS during light ridge top wind conditions, revealed a zone of stronger down-valley winds, some distance above the valley surface, yet below the level of surrounding ridge tops. Subsequent examination of this data comprises the first case study in

this chapter, and this has provided further evidence in support of LLJ occurrence, including the gradual onset and vertical development of an elevated core of stronger winds that blow down segments of the upper Awatere Valley. Further analysis of SODAR data during clear, settled conditions following deployment at the Rapaura AWS, revealed the existence of a second LLJ in the Wairau Valley. The discovery of these LLJ's is a key factor in helping to understand the spatial variation of minimum temperatures across Marlborough. The higher shear values found beneath the LLJ's in cases 1 and 2 from this chapter, offer a mechanism for increased turbulence that has been reported to transport warmer, well mixed air to the surface (Banta 2008).

It was not possible to discern a transition layer from the SODAR data in case 1 from the Awatere Valley, although earlier work by Nappo and Snodgrass (1981) found that during light ridge-top wind conditions (2 – 3 m s^{-1}) the transition height was close to ridge top height. During stronger ambient winds (5 – 7 m s^{-1}), they suggested that transition height was more variable and more likely to be within several hundred metres of the ground. Onset of the drainage wind (and subsequent development of the LLJ) in case 1 did not cause sudden increases in near-surface temperature as reported by Banta et al. (1992), but temperatures were observed to plateau and remained constant for the duration of the down-valley drainage flow.

While a transition layer was identified at 2 – 300 m AGL in case 2, this height was governed primarily by ridge-top wind velocity, which throughout this case was perpendicular to the drainage wind. It is not clear from the literature what effect cross-valley synoptic wind has on the depth of the transition layer, or underlying drainage wind when compared with an opposing up-valley synoptic wind. The angle of the ambient wind, however, does have an effect on ventilation of areas closer to the windward valley side wall and there is suggestion that in a model simulation of cross-valley flow, turbulent exchange between the valley and ambient air is increased (Doran and Horst 1990). A strengthening of synoptic winds perpendicular to underlying drainage flows will be the most common interaction over the

Marlborough region, following periods of stable conditions. Results from this case have shown that cross-valley ridge top winds can be separated from a drainage flow by a transition layer and that ridge top winds have to become strong to erode and disrupt the drainage flow near the surface. Clements et al. (1989) suggested that ridge-top winds of 10 – 15 m s^{-1} (with an up-valley component) might prevent the establishment of a nocturnal drainage flow in Brush Creek Valley, Western Colorado. Ridge top wind speeds of 7 – 10 m s^{-1} were effective in preventing drainage winds from developing within the upper Awatere Valley region during case study 3.

The WRF simulated vertical wind profile from the second case study in Chapter 6 represents a very similar observation period to the third case study in this chapter. The model predicted very light winds at the Awatere AWS below ridge top height, as shelter from the close proximity of steep terrain prevented the strong west–south-westerly winds from mixing to the valley surface, and the development of drainage flows. The third case study in this chapter demonstrated the increased near-surface cooling that can take place within the Awatere Valley, without the presence of significant drainage flows or strong near-surface wind shear. More importantly, it illustrated the effect of briefly increased wind shear on temperature, without any significant change to near-surface wind velocity. In this instance shear-induced turbulence was the dominant mechanism by which warmer air was mixed to the surface.

While the cases presented in this chapter were selected to illustrate typical examples of atmospheric vertical structure and its effects on near-surface temperature, it must be stressed that the near-surface vertical structure, including the presence of drainage winds, is dynamic and constantly trying to reach equilibrium with the ambient meteorology. Many examples from the entire SODAR data set show a range of development of the LLJ, with various effects on local temperatures. The drainage wind, or indeed a LLJ, has only to be disrupted briefly by the strengthening or veering of a synoptic wind, resulting from interaction with local terrain, to subsequently affect near-surface wind shear and

temperature. The key to understanding the spatial and temporal variability of near-surface temperature in Marlborough, as well as improved temperature prediction, will require a better understanding of interactions between synoptic flow and thermally-induced wind regimes. The spatial and temporal variation in the height of the transition layer is one such interaction.

It is recognized that data sets from both Awatere Valley and Rapaura identified a number of occasions when LLJ formation was likely to have been a response to topographic realignment of synoptic flow, rather than being thermally-generated, and the cause is often not possible to differentiate based on surface-based AWS. For example, southerly synoptic flow in the Awatere Valley was observed to be channeled along the windward side of the Blackbirch Range, raising near-surface temperatures at some vineyard AWS, while cooler temperatures were recorded in southern parts of the valley, away from any regular influence of the LLJ.

Unfortunately, wind and temperature observations are not available from the Scrub Rough Spur AWS for (the earlier) case study 3, due to damage by animals. Data might have shown episodes of north-westerly synoptic disturbance at low levels within the Awatere Valley and resulting fluctuations in temperature. It would have been interesting to observe the length of time that increases in temperature persisted, before in-situ cooling or the effects of weakened down-valley drainage flow resulted in cooler air returning to the AWS. The nearest AWS monitored as part of the network for this research, located in the lower Awatere at Seddon, recorded synoptic wind ventilation and temperatures as high as 9°C throughout case study 3.

The use of tethered balloon systems was not an option in either study area during the data collection periods. The nights of greatest interest to this research were also potential frost nights on vineyards and the use of helicopters for fighting frost took precedence over meteorological research.

Finally, as mentioned in Banta et al. (2004), it is hoped that the findings of this chapter can be used to help evaluate future NWP modeling studies, in particular to assess whether models properly mimic the response of the near-surface boundary layer in complex terrain to changes in ambient meteorology. It is thought, however, that international attempts at parameterizing the effects of drainage flows on mesoscale turbulence fluxes (e.g., Noppel and Fieldler 2002, Weigel et al. 2007, Rotach and Zardi 2007) and modeling of the topographic and ambient wind effects upon drainage flows (Bossert and Poulos 1995), would not impart significant help in understanding the interactions of drainage flows in Marlborough, as valleys dimensions are considerably shorter and narrower.

7.6 Summary

The formation of LLJ's plays an important role in modifying the spatial and temporal variation of temperatures under settled weather conditions in Marlborough. Shear-induced turbulence beneath the jets is believed to be a key mechanism for transferring warmer, well-mixed air within the LLJ to the surface. The presence, structure and height of a transition layer between a synoptic wind and drainage wind layer is believed to influence the structure and velocity of the LLJ and affect near-surface temperatures on many occasions.

Deployment of multiple SODARs together with RASS for extended data collection periods would contribute significantly to our present understanding of topographic interactions with thermally-induced and synoptic winds.

Chapter 8 Summary and further research

8.1 Introduction

This thesis has engaged observational, synoptic, and numerical analysis to investigate the spatial variation of minimum temperature and conditions conducive to spring frost in Marlborough. Observations of near-surface wind velocity and temperature were substantiated with a high density of local AWS and complemented by measurements with the University of Canterbury SODAR. The area of greatest interest is highly valued agricultural land that is primarily occupied by vineyards and is surrounded by complex mountainous terrain. This research has demonstrated that interactions between several synoptic weather types and complex terrain, facilitates the simultaneous ventilation and stagnation of the near-surface valley atmospheres, and this generates a wide variation of near-surface temperature and at times frost.

Before summarising the key results from the thesis, it is useful to reiterate the broader research aim "to account for the spatial variation of minimum temperatures in stable boundary layer conditions" and the following three research objectives:

1. To identify relationships between synoptic weather patterns and spatial variability of near-surface minimum temperature, including frost.
2. An exploration of the relationship between regional airflow patterns and spatial variation of near-surface minimum temperature, including frost.
3. An investigation of the influence of the vertical structure of the nocturnal boundary layer on near-surface temperature variations.

8.2 Summary of results

The first objective was achieved using the Kidson synoptic classification scheme. Higher spatial variations of near-surface minimum temperature were found to be associated with Kidson types H, TNW and T, however, these Kidson types encompass a wide range of synoptic weather, from stable anticyclonic conditions (Kidson type H), to the comparatively unsettled weather (Kidson types TNW and T). Further examination of these relationships found that specific Kidson types influenced the spatial variation of near-surface temperature in the Awatere Valley. In approximately 50% of the most stable conditions (Kidson type H), Seddon in the lower Awatere Valley would record cooler near-surface temperatures than the upper Awatere Valley at Welds Hill, yet for the majority of other occasions Welds Hill recorded cooler near-surface temperatures.

Analysis then demonstrated that frost conditions were much more likely to occur during Kidson type HW. This synoptic weather type is associated with colder southerly wind outbreaks, from which most of the region is sheltered behind the Kaikoura Ranges. In the clear, dry, and cool conditions, frost conditions are common at six of the nine AWS locations. The greatest numbers of frost conditions during the 2009 – 2011 spring periods were found to occur during Kidson types H, HSE and SW, as these synoptic types occurred more frequently through each spring season.

The second research objective was explored in two ways. Firstly, idealised TAPM simulations demonstrated the extent of shelter provided to the region from a range of synoptic conditions. These simulations suggested that the lightest near-surface winds would occur during moderate ridge top wind velocities, rather than a zero (calm) synoptic wind situation. The zero synoptic wind simulation revealed increased near-surface wind speeds across much of the region, which was believed to reflect the development of thermally-induced drainage winds. This finding is important as local observations point toward a relationship between increased near-surface minimum temperatures and increased near-

surface wind speeds. The idealised simulations also demonstrated large spatial variation of near-surface wind speed in some wind directions, and provided sky conditions are clear, could be related to spatial variations of near-surface cooling. When the idealised simulations are analysed in this manner, they provide a broad overview of which areas of the region could be expected to record cooler near-surface temperatures under specific synoptic wind directions.

Analysis for the second research objective was extended by using the WRF model on two case studies. In the first case study, light synoptic winds above the region (Kidson type H) revealed the development of strong drainage winds down the region's largest river valleys. These winds were observed by several of the private AWS network and were associated with warmer near-surface minimum temperatures. Remaining AWS that did not appear to be affected by the strong drainage winds recorded lower near-surface wind speeds and cooler near-surface temperatures. In this manner, the region was subject to simultaneous ventilation (by drainage winds) and stagnation (in areas not exposed to these winds), resulting in large spatial variations of near-surface minimum temperature. A vertical profile of wind speed from the Awatere AWS at Welds Hill illustrated an elevated zone of stronger down-valley winds. This core of stronger winds within the upper valley was thought to have an influence on warming near-surface minimum temperatures during weak synoptic gradients.

The second case study modelled a period of stronger synoptic winds (Kidson type W). Analysis revealed distinctive areas of lighter near-surface winds in the upper Awatere valley, and these were supported by observations from the Awatere AWS together with cooler near-surface temperatures. Stronger near-surface wind speeds and significantly warmer near-surface temperatures were observed at many other AWS locations, including Seddon in the lower Awatere Valley. This simulation provided further evidence of the simultaneous ventilation and stagnation of the near-surface air layers around the region, resulting in large spatial variations of near-surface temperature. A vertical profile of wind speed at the

Awatere AWS on this occasion indicated very light winds within the valley to the height of surrounding ridge tops, then winds rapidly increased from the direction of the westerly synoptic airstream. This suggests that the close proximity of steep terrain to the Awatere AWS provides considerably shelter from synoptic winds of this direction. A further interesting feature of this simulation was the depiction of lightest near-surface winds at the interface between synoptic and thermally-generated winds, which according to the literature is recognised as a transition zone. As increased near-surface cooling has been observed to occur in areas of lightest near-surface wind, this finding could help explain the anecdotal hap-hazard trail of early spring frost damage to vineyards, in the presence of moderate or strong ridge top winds. While further research could be focussed on identifying spatial patterns of lightest near-surface winds under a range of stable atmospheric conditions, the key finding from both modelled case studies was the high spatial variation of near-surface minimum temperature under contrasting ridge top wind conditions.

Predicted areas of lightest near-surface winds did not correlate well with coolest near-surface temperatures as results from both case studies indicated a warm near-surface temperature bias in spite of low surface wind speeds and clear skies. The problem is thought to be associated with the choice of land surface physics option, and the way in which complex biogeophysical processes are coupled with WRF. Recent studies comparing land surface schemes have shown significant improvements in prediction of near-surface temperature when combining the Community Land Model Version 3.5 (CLM3.5) with WRF, although studies so far have only used data sets consisting of extended time scales and covering large areas.

The third research objective was achieved using the University of Canterbury SODAR. This aspect of the research focussed on quantifying the extent of down-valley drainage winds during stable weather conditions in both the Awatere and Wairau Valleys, and identifying the mechanisms responsible for creating changes to near-surface temperature. The results

revealed a great deal more about the structure of the lower atmosphere above parts of the region than were first imagined. It confirmed the presence of an elevated zone of down-valley winds in both the Awatere and Wairau Valleys during light ridge top winds that are characteristic of a LLJ. Analysis then revealed that wind shear beneath the jets produced sufficient turbulence to mix warmer air towards the surface, and this was shown to account for increased near-surface temperatures beneath the jets. During moderate to strong ridge top winds, the SODAR established that synoptic winds could remain decoupled from the valley floor and that on these occasions, thermally generated drainage winds were either very light and disorganised or did not occur at all. In the absence of strong drainage winds, wind shear above the ground was significantly reduced and the light near-surface winds allowed strong in situ cooling to take place. The phenomenon was shown to be associated with frost conditions in upper valley locations during remarkably strong ridge top winds.

Observations from the SODAR also demonstrated the presence of an elevated transition zone between a synoptic and the thermally-induced wind. The transition zone appears to be dynamic in depth and height and is characterised by a zone of light variable winds and low wind shear. The presence of the transition zone underscores earlier studies that suggest the thermally driven wind is seldom fully decoupled from the ambient atmosphere and that its presence may influence near-surface temperatures on some occasions. In stronger ridge top wind speeds analysis suggests the transition zone can be pushed further towards the surface, and this is thought to influence the generation of thermally generated winds and subsequently affect near-surface temperature.

While achieving the first two objectives, it became clear that the greatest variability of near surface minimum temperature occurs as a result of simultaneous ventilation and stagnation of near-surface air flow and that this could occur for several Kidson synoptic types. Large variations of near-surface minimum temperature may occur in the presence of light ridge top winds, as a result of a locations susceptibility to shear-induced mixing of warmer air beneath strong thermally-induced drainage winds and LLJ's. Large variations of near-surface

minimum temperature may also occur as a result of terrain-induced shelter from stronger synoptic wind, which allows strong in situ cooling to commence in areas of lightest near-surface winds.

8.3 Research implications and future study

The implications of this research are of foremost interest to the prediction of minimum temperature in complex terrain, especially for improved warning against frost. Assuming clear skies and a cool atmosphere, determination of near-surface winds is crucial for an accurate prediction of near-surface temperature. Although the thermal or synoptic origin of near-surface winds are important, analysis has shown that the transient interface between these wind systems may determine local areas of most rapid near-surface cooling.

Given the relationship between increased near-surface wind speed and increased near-surface temperature, meteorologists need an improved understanding of the coupling between larger synoptic situations and local meteorological factors that drive near-surface winds. Accurate model predictions of the spatial and temporal evolution of near-surface winds will continue to provide an essential component of future high resolution forecasting of minimum temperature in complex terrain. In addition model resolution needs to be sufficient to resolve local meteorological phenomenon that modify the near-surface temperatures. Increasing our understanding of the physical processes that operate within a geographical region (such as the development of strong drainage winds or LLJ's, including further investigation into the spatial interactions of turbulence above the region), and the way these processes influence near-surface meteorology, will provide the foundations for accurate future predictions of near-surface minimum temperature. This could be achieved by an increased focus on short duration model simulations of near-surface climate parameters in areas of complex terrain.

While the focus of this thesis has accounted for spatial variations of near-surface temperature, including frost, at least two studies are being run concurrently to improve predictions of local climate. In a joint research venture by Pernod-Ricard New Zealand Ltd, MetService, and Harvest Electronics, data assimilation from the Brancott AWS into forecast models run by MetService aim to provide site specific tuned 7-day forecasts for near-surface temperature, wind velocity and rainfall. At time of writing this PhD the study is relatively infantile in its development and no results have been published. A larger two-year collaborative research project under the umbrella of the international TERVICLIM research program has engaged the University of Canterbury, Plant and Food Research, NIWA, and French Wine-Climate Scientists. The group have deployed many AWS and remote temperature data loggers throughout Marlborough to collect data that will be assimilated into atmospheric models for short and longer-term projections of climate change, specifically for the regions grape industry (Sturman et al. 2013). The project is expected to help New Zealand's wine-producing sector adapt to projected climate variability and take advantage of new opportunities arising from possible future climate trends and to reduce impacts of adverse events such as frost or high temperatures.

References

Adams, A. (2012), 'Midwest vineyards damaged by frost', Wines and Vines, 5 July 2012. **URL:** *http://www.winesandvines.com/template.cfm?section=news&content=100413*

Alpert, P., Tsidulko, M., Krichak, S. & Stein, U. (1996), 'A multi-stage evolution of an ALPEX cyclone' *Tellus* **48A**, 209 – 220.

Andre, J. C. & Mahrt, L. (1982), 'The nocturnal surface inversion and influences of clean-air radiative cooling', *Journal of Atmospheric Sciences* **39**(4), 864 – 878.

Baker, K.& Dolwick, P. (2009). *Meteorological Modeling Performance Evaluation for the Annual 2005 Eastern U. S. 12-km Domain Simulation* (EPA 2/2/09)

Baker, K. R., Simon, H. & Kelly, J. T. (2011), 'Challenges to modeling "cold pool" meteorology associated with high pollution episodes', *Environmental Science and Technology* **45**(17), 7118 – 7119.

Banta, R. M. (2008), 'Stable-boundary-layer regimes from the perspective of the low-level jet', *Acta Geophysica* **56**(1), 58 – 87.

Banta, R. M., Darby, L. S., Fast, J. D., Pinto, J. O, Whiteman, C. D., Shaw, W. J. & Orr, B. W. (2004), 'Nocturnal low-level jet in a mountain basin complex. Part 1: Evolution and effects on local flows', *Journal of Applied Meteorology* **43**(10), 1348 – 1365.

Banta, R. M., Newsom, R. K., Lundquist, J. K., Pichugina, Y. L., Coulter , R. L. & Mahrt, L. (2002), 'Nocturnal low-level jet characteristics over Kansas during CASES-99', *Boundary-layer Meteorology* **105**(2), 221 – 252.

Barr, S. & Orgill.M .M. (1989), 'Influence of external meteorology on nocturnal valley drainage winds', *Journal of Applied Meteorology* **28**(6), 497 – 517.

Barry, R. G. & Carleton, A. M. (2001), *Synoptic and Dynamic Climatology,* Routledge, London and New York, 620pp.

Barry, R. G. (2008), '*Mountain Weather and Climate'*, 3rd edn. Cambridge University Press, 506pp.

Basher, R. E. & Thompson, C. S. (1996), 'Relationship of air temperature in New Zealand to regional anomalies in sea surface temperature and atmospheric circulation', *International Journal of Climatology* **16**(4), 405 – 425.

Becker, N. J. (1984), 'Site selection for viticulture in cool climates using local climatic information' Proceedings of International Symposium on Cool Climate Viticulture and Enology, Oregon State University Agricultural Experiment Station, Technical Publication **7628**, 20 – 34.

Bodine, D., Klein, P. M., Arms, S. C. & Shapiro, A. (2009), 'Variability of surface air temperature over gently sloped terrain', *Journal of Applied Meteorology and Climatology* **48**(6), 1117 – 1141.

Borge, R., Alexandrov, V., del Vas, J. J., Lumbreras, J. & Rodriguez, E. (2008), 'A comprehensive sensitivity analysis of the WRF model for air quality applications over the Iberian Peninsular', *Atmospheric Environment* **42**(37), 8560 – 8574.

Bossert, J. E. & Polous, G. S. (1995), 'A numerical investigation of mechanisms affecting drainage flows in highly complex terrain', *Theoretical and Applied Climatology* **52**(1 – 2), 119 – 134.

Bridges, J. (2011), 'MetService's investment in forecasting, 8 April 2011. **URL:** *http://blog.metservice.com/2011/04/metservice%E2%80%99s-investment-in-forecasting*

Brooks, H. E., Cortinas, J. V. & Johns, R. H. (1996), 'Experimental winter hazards forecasting at the Storm Prediction Centre: Verification results for probabilistic freezing rain forecasts' 15th AMS Conference on Weather Analysis and Forecasting, Norfolk, Virginia, American Meteorological Society, 127 – 130.

Cellier, F. E. ed. (1982), '*Progress in modelling and simulation*' Academic Press, London, U.K.

Cellier, P. (1993), 'An operational model for predicting minimum temperatures near the soil surface under clear sky conditions', *Journal of Applied Meteorology and Climatology* **32**(5), 871 – 883.

Chigullapalli, S. & Mölders, N. (2008), 'Sensitivity studies using the Weather Research and Forecasting (WRF) model' ARSC Report pp 15.

Clements, C. B., Whiteman, C. D. & Horel, J. D. (2003), 'Cold-air-pool structure and evolution in a mountain basin: Peter Sinks, Utah', *Journal of Applied Meteorology and Climatology* **42**(6), 752 – 768.

Clements, W. E., Archuleta, J. A. & Hoard, D. E. (1989), 'Mean structure of the nocturnal drainage flow in a deep valley', *Journal of Applied Meteorology***28**(6), 457 – 462.

Clifo: (2013), NIWA's National Climate Database on the web. **URL:** *http://clifo.niwa.co.nz* Retrieved between Feb 2010 and Oct 2013.

Connell, J. H. & Snyder, R. L. (1989), 'Sprinkler spacing effects almond frost protection', *California Agriculture* **43**(1), 30 – 32.

Cremer, K. W. & Leuning, R. (1985), 'Effects of moisture on soil temperature during radiation frost', *Australian Forest Research* **15**, 33 – 42.

Darby, L. S., Allwine, K. J. & Banta, R. M. (2006), 'Nocturnal low-level jet in a mountain basin complex. Part 2: Transport and diffusion of tracer under stable conditions', *Journal of Applied Meteorology and Climatology* **45**(5), 740 – 753.

Darby, L. S., Allwine, K. J. & Banta, R. M. (2006), 'Nocturnal low-level jet in a mountain basin complex. Part 2: Transport and diffusion of tracer under stable conditions' Journal of Applied Meteorology and Climatology **45**(5), 740 – 753.

Davis, C. (2012), 'Frost damage to Austrian Vineyards' Drinks International, 23 May 2012. **URL:** *http://www.drinksint.com/news/fullstory.php/aid/2995*

Defant, F., (1951), 'Local winds', In: *Compendium of Meteorology*, T. M. Malone (Ed.), Boston, American Meteorological Society, pp 655 – 672.

Doesken, N. J., McKee, T. B. & Renquist, A. R. (1989), 'A climatological assessment of the utility of wind machines for freeze protection in mountain valleys', *Journal of Applied Meteorology* **28**(3), 194 – 205.

Doran, J. C. & Horst, T. W. (1990), 'The development and structure of nocturnal slope winds in a simple valley', *Boundary-layer Meteorology* **52**(1 – 2), 41 – 68.

Doran, J. C. (1991), 'The effects of ambient winds on valley drainage flows', *Boundary-Layer Meteorology* **55**(1-2), 177 - 19.

Economic impact of the New Zealand wine industry: An Nzier report to New Zealand wine growers, April 2009. **URL:** *http://www.nzwine.com/assets/sm/upload/v9/q6/e9/ls/NZIER_Rep_April_09.pdf*

Edwards, J. M. (2009), 'Radiative processes in the stable boundary layer: Part 2. The development of the nocturnal boundary layer', *Boundary-Layer Meteorology* **131**(2), 127 – 146.

Fernando, H. J. S. (2010), 'Fluid dynamics of urban atmospheres in complex terrain', *Annual Review of Fluid Mechanics* **42**, 365 – 389.

Funk, J. P. (1960), 'Measured radiative flux divergence near the ground at night', *Quarterly Journal of the Royal Meteorological Society* **86**, 382 – 389.

Ghielmi, L. & Eccel, M. (2006), 'Descriptive models and artificial neural networks for spring frost prediction in an agricultural mountain area', *Computers and Electronics in Agriculture* **54**(2), 101 – 114.

Graham, A. (2008), 'What exactly is a cool climate wine', Wine makers choice: Wine doctor blog, 12 September 2008.
URL: *http://winemakerschoicewinedoctor.blogspot.co.nz/2008/10/what-exactly-is-cool-climate-wine.html*

Grubišić, V., Doyle, J. D., Kuettner, J., Dirks, R., Cohn, S. A., Pan, L. L., Mobbs, S., Smith, R. B., Whiteman, C. D., Czyzyk, S., Vosper, S., Weissmann, M., Haimov, S., De Wekker, S. F. J. & Chow, F. K. (2008), 'The Terrain-induced Rotor Experiment. A field campaign overview including observational highlights', *Bulletin of the American Meteorological Society* **89**(10), 1513 – 1533.

Gudiksen, P. H. (1989), 'Categorisation of nocturnal drainage flows within the Brush Creek Valley and the variability of sigma theta in complex terrain', *Journal of Applied Meteorology* **28**(6), 489 – 495.

Gudiksen, P. H., Leone, JR., King, C. W., Ruffieux, D. & Neff, W. D. (1992), 'Measurements and modelling of the effects of ambient meteorology on nocturnal drainage flows', *Journal of Applied Meteorology* **31**(9), 1023 – 1032.

Gustavsson, T. (1995), 'A study of air and road-surface temperature variations during clear windy nights', *International Journal of Climatology* **15**(8), 919 – 932.

Gustavsson, T., Karlsson, M., Bogren, J. & Lindqvist, S. (1998), 'Development of temperature patterns during clear nights', Journal of Applied Meteorology **37**(6), 559 – 571.

Hafner, T. A. & Smith, R. B. (1985), 'Pressure drag on the European Alps in relation to synoptic events', *Journal of Atmospheric Science* **42**, 562 – 575.

Hanna, S. R. & Yang, R. (2001), 'Evaluations of mesoscale models' simulations of near-surface winds, temperature gradients, and mixing depths' *Journal of Applied Meteorology* **40**(6), 1095 – 1104.

Hauge, G. (2006), 'High resolution weather forecasting and predictability: Applications in complex terrain', PhD thesis, University of Bergen.

Hay, J. E. & Fitzharris, B. B. (1988), 'The synoptic climatology of ablation on a New Zealand glacier', *International Journal of Climatology* **8**(2), 201 – 215.

Hirdman, D. (2006), 'Sensitivity Analysis of the Mesoscale Air Pollution Model TAPM', MSc thesis, Department of Geography, University of Canterbury, Christchurch, New Zealand.

Hole, L.R. & Hauge, G. (2003), 'Simulation of a morning air temperature inversion break-up in complex terrain and the influence on sound propagation on a local scale', *Applied acoustics* **64**, 401 – 414.

Holland, T. & Smit, B. (2010), 'Climate change and the wine industry: Current research themes and new directions', *Journal of Wine Research* **21**(2), 125 – 136.

Hunt, E. D., Basara, J. B. & Morgan, C. R. (2007), 'Significant inversions and rapid in situ cooling at a well-sited Oklahoma mesonet station', *Journal of Applied Meteorology and Climatology* **46**(3), 353 – 367.

Hurley, P. (2008), 'TAPM V4. Part 1: Summary of some verification studies', *CSIRO Marine and Atmospheric Research Paper No. 26.*

Hurley, P. (2008), 'TAPM V4. Part 1: Technical Description', *CSIRO Marine and Atmospheric Research Paper No. 25.*

Integrated Data Viewer (IDV).
URL: http://www.unidata.ucar.edu/software/idv Last accessed 10 December 2013.

Ireland, W. (2005), *Frost and Crops. Frost Prediction and Plant Protection*, W. Ireland, Wellington.

Jackson, D. & Schuster, D. (1997), '*The production of grapes and wine in cool climates*', Lincoln University Press, New Zealand.

Jackson, D. I. & Cherry, N. J. (1988), 'Prediction of a districts grape ripening capacity, using a latitude temperature index', *American Journal of Enology and Viticulture* **1**, 19 – 28.

Jackson, D. I. & Lombard, P. B. (1993), 'Environmental and management practices affecting grape composition and wine quality – a review', *American Journal of Enology and Viticulture* **44**, 409 – 430.

Jiang, N. (2011), 'A new objective procedure for classifying New Zealand synoptic weather types during 1958 – 2008', *International Journal of Climatology* **31**(6), 863 – 879.

Jiang, N., Griffiths, G. & Dirks, K. N. (2011) 'Linking synoptic weather types to daily rainfall in Auckland', *Weather and Climate* **31**, 50 – 66.

Jiang, N., Griffiths, G. & Lorrey, A. (2013), 'Influence of large-scale climate modes on daily synoptic weather types over New Zealand', *International Journal of Climatology* **33**(2), 499 – 519.

Jiang, N., Hay, J. E. & Fisher, G. W. (2004) 'Classification of New Zealand synoptic weather types and relation to the Southern Oscillation Index', *Weather and Climate* **23**, 3 – 23.

Jin, J. & Wen, L. (2012), 'Evaluation of snowmelt simulation in the Weather Research and Forecasting model', *Journal of Geophysical Research* **117** (D10), 16pp.

Jones, G. V. & Davis, R. E. (2000), 'Using a synoptic climatological approach to understand climate – viticulture relationships', *International Journal of Climatology* **20**(8), 813 – 837.

Jones, G. V. & Hellman, E. (2003), '*Site assessment*', Oregon Viticulture Hellman, E. (ed.), 5thedition, Oregon State University Press, Corvallis, Oregon, pp. 44–50.

Jones, G. V., Duff, A. A., Hall, A. & Myers, J. W. (2010), 'Spatial analysis of climate winegrape growing regions in the Western United States', *American Journal of Enology and Viticulture* **61**(3), 313 – 326.

Jones, J. E., Wilson, S. J., Lee, G. & Smith, A. M. (2010), 'Effect of frost damage and pruning on current crop and return crop of Pinot Noir' , *New Zealand Journal of Crop and Horticulture Science* **38**(3), 209 – 216.

Kalma, J. D., Laughlin, G. P., Caprio, J. M. & Hamer, P. J. C. (1992), '*Advances in Bioclimatology – 2: The Bioclimatology of Frost. Its Occurrence, Impact and Protection'* Springer-Verlag, Berlin, Heidelberg.

Kaufmann, P. & Weber, R.O. (1996), 'Classification of mesoscale wind fields in the MISTRAL field experiment' *Journal of Applied Meteorology* **35**(11), 1963 – 1979.

Kenny, G. J. & Shao, J. (1992), 'An assessment of a latitude-temperature index for predicting climate suitability for grapes in Europe', *The Journal of Horticultural Science and Biotechnology* **67**(2), 239 – 246.

Kidson, J. D. (1994b), 'An automated procedure for the identification of synoptic types applied to the New Zealand region', *International Journal of Climatology* **14**(7), 711 – 721.

Kidson, J. W. & Watterson, I. G. (1995), 'A synoptic climatological evaluation of the changes in the CSIRO 9-level model with doubled CO_2 in the New Zealand region', *International Journal of Climatology* **15**(11), 1179 – 1194.

Kidson, J. W. (1994a), 'Relationship of New Zealand daily and monthly weather patterns to synoptic weather types', *International Journal of Climatology* **14**(7), 723 – 737.

Kidson, J. W. (1997), 'The utility of surface and upper air data in synoptic climatological specification of surface climatic variables', International Journal of Climatology **17**(4), 399 – 413.

Kidson, J. W. (2000), 'An analysis of New Zealand synoptic types and their use in defining weather regimes', *International Journal of Climatology* **20**(3), 299 – 316.

Kondo, H. (1995), 'The thermally induced local wind and surface inversion over the Kanto plain on calm winter nights', *Journal of Applied Meteorology and Climatology* **34**(7), 1439 – 1448.

Kondo, J., Kanechika, D. & Yasuda, N. (1978), 'Heat and momentum transfers under strong stability in the atmospheric surface layer', *Journal of Atmospheric Sciences* **35**(6), 1012 – 1021.

Kraus, H., Malcher, J. & Schaller, E (1985), 'A nocturnal low level jet during PUKK', *Boundary-Layer Meteorology* **31**(2), 187 – 195.

Lakes Environmental: Wind rose plots for meteorological data.
URL: http://www.weblakes.com/products/wrplot/index.html

Laughlin, G. P. & Kalma, J. D. (1987), 'Frost hazard assessment from local weather and terrain data', *Agricultural and Forest Meteorology* **40**(1), 1 – 16.

Laughlin, G. P. & Kalma, J. D. (1990), 'Frost risk mapping for landscape planning: A methodology', *Theoretical and Applied Climatology* **42**(1), 41 – 51.

Lehner, M. & Gohm, A. (2010), 'Idealised Simulations of Daytime Pollution Transport in a Steep Valley and its Sensitivity to Thermal Stratification and Surface Albedo' *Boundary-Layer Meteorology*, **134** (2), 327-351.

Leishman, N. J. (2005), 'Model sensitivity, performance, and evaluation techniques for the Air Pollution Model in south east Queensland', MSc thesis, School of Natural Resource Sciences, Queensland University of Technology.

Leone, J. M. Jr. & Lee, R. L. (1989), 'Numerical simulation of drainage flow in Brush Creek, Colorado', *Journal of Applied Meteorology* **28**(6), 530 – 542.

Mahrt, L. (1985), 'Vertical structure and turbulence in the very stable boundary layer', *Journal of the Atmospheric Sciences* **42**(22), 2333 – 2349.

Mahrt, L., Vickers, D., Nakamura, R., Soler, M. R., Sun, J., Burns, S. & Lenschow, D. H. (2001), 'Shallow drainage flows', *Boundary-Layer Meteorology* **101**(2), 243 – 260.

Manins, P. C. & Sawford, B. L. (1979a), 'Katabatic winds: A field case study', *Quarterly Journal of the Royal Meteorological Society* **105**(446), 1011 – 1025.

Manins, P. C. & Sawford, B. L. (1982), 'Mesoscale observations of upstream blocking', *Quarterly Journal of the Royal Meteorological Society* **108**(457), 427 – 434.

Mao, Q., Gautney, L. L., Cook, T. M., Jacobs, M. E., Smith, S. N. & Kelsoe, J. J. (2006), 'Numerical experiments on MM5-CMAQ sensitivityto various PBL schemes', *Atmospheric Environment* **40**(17), 3092 – 3110.

Marlborough District Council: Frost indicators and maps.
URL: http://www.marlborough.govt.nz/Environment/Climate/Reports-and-Special-Investigations/Frost-Indicators-and-Maps.aspx Accessed between March 2010 – March 2011.

Mattsson, J. O. & Nordbeck, S. (1981), 'Modelling cold air patterns', *Lund studies in Geography* **59**(A), 11pp.

McArtney, S., Chatterton, D. & Good, M. (2003), 'Dealing with frost: Describing vine response to frost damage and the impact of post-frost management on vine performance' Report to New Zealand Winegrowers, HortResearch Client Report 12037.

McDonald, C. (2012), 'Harsh frosts could cost 1000 tonnes of grapes, Otago Daily Times. URL: *http://www.odt.co.nz/regions/central-otago/233634/harsh-frosts-could-cost-1000-tonnes-grapes*

McGinley, J. A. & Goerss, J. S. (1986), 'Effects of terrain height and blocking initialisation on numerical simulation of alpine lee cyclogenesis', *Monthly Weather Review* **114**(8), 1578 – 1590.

McGowan, H. A. & Sturman, A. P. (1996), 'Interacting multi-scale wind systems within an alpine basin, Lake Tekapo, New Zealand', *Meteorology and Atmospheric Physics* **58**(1 – 4), 165 – 177.

McKee, T. B. & O'Neal, R. D. (1989), 'The role of valley geometry and energy budget in the formation of nocturnal valley winds', *Journal of Applied Meteorology* **28**(6), 445 – 456.

Nappo, C. J. & Snodgrass, H. F. (1981), 'Observations of night time winds using Pilot balloons in Anderson Creek Valley, Geysers, California', *Journal of Applied Meteorology* **20**(6), 721 – 727.

Neale, S. M. & Fitzharris, B. B. (1997), 'Energy balance and synoptic climatology of a melting snowpack in the Southern Alps, New Zealand', *International Journal of Climatology* **17**(14), 1595 – 1609.

Neininger, B. (1982), 'Mesoclimate measurements in the Upper Valais', *Annalen der Meteorologie* **19**, 105 – 107.

Ngan, F., Kim, H., Lee, P., Al-Wali, K. & Dornblaser, B. (2013), 'A study of nocturnal surface wind speed over-prediction by the WRF-ARW Model in Southeastern Texas', *Journal of Applied Meteorology and Climatology* **52**(12), 2638 – 2653.

Nolan, M. (2013), 'Analysis of local AWS and NCEP/NCAR reanalysis data at Lake El'gygytgyn, and its implications for maintaining multi-year lake-ice covers', *Climates of the Past* **9**, 1253 – 1269.

Noppel, H. & Fiedler, F. (2002), 'Mesoscale heat transport over complex terrain by slope winds – A conceptual model and numerical simulations', *Boundary-layer Meteorology* **104** (1), 73 – 97.

O'Steen, L. B. (2000), 'Numerical simulation of nocturnal drainage flows in idealized valley-tributary systems', *Journal of Applied Meteorology* **39**(11), 1845 – 1860.

Oke, T. R. (1987), *Boundary Layer Climates*, 2 edn, Routledge, London.

Oreskes, N., Shrader-Frechette, K. & Belitz, K. (1994), 'Verification, validation, and confirmation of numerical models in earth sciences', *Science* **263**(5147), 641 – 646.

Orgill, M. M., Kincheloe, J .D. & Sutherland, R. A. (1992), 'Mesoscale influences on nocturnal valley drainage winds in Western Colorado valleys', *Journal of Applied Meteorology* **31**(2), 121 – 141.

Pascoe, R. M. (1983), 'The climate and weather of Marlborough', New Zealand MetService Miscellaneous Publication **115**(12), 57pp.

Pinto, J. O., Parsons, D. B., Brown, S. Cohn., Chamberlain, N. & Morley, B. (2006), 'Coevolution of down-valley flow and the nocturnal boundary layer in complex terrain', *Journal of Applied Meteorology and Climatology* **45**(10), 1429 – 1449.

Polous, G. S. (1996), 'The interaction of katabatic winds and mountain waves', Ph.D. dissertation, Colorado State University, 297pp.

Polous, G. S., Bossert, J. E., McKee, T. B. & Pielke, R. A. (2000), 'The interaction of katabatic flow and mountain waves. Part 1: Observations and idealized simulations', *Journal of the Atmospheric sciences* **57**(12), 1919 – 1936.

Post, M. J. & Neff, W. D. (1986), 'Doppler lidar measurements of winds in a narrow mountain valley', *Bulletin of the American Meteorological Society* **67**(3), 274 – 281.

Poulos, G. & Zhong, S. (2008), 'An observational history of small-scale katabatic winds in mid-latitudes', *Geography Compass* **2**(1), 1 – 24.

Poulos, G. S., Blumen, W., Fritts, D. C., Lundquist, J. K., Sun, J., Burns, S. P., Nappo, C., Banta, R., Newsom, R., Cuxart, J., Terradellas, E., Balsley, B. & Jensen, M. (2002), 'CASES-99: A comprehensive investigation of the stable nocturnal boundary layer', *Bulletin of the American Meteorological Society* **83**(4), 555 – 581.

Powell, S. (2000), 'Nocturnal cold air drainage in complex terrain, Lake Tekapo, New Zealand', MSc thesis, Department of Geography, Victoria University.

Prabha, T. & Hoogenboom, G. (2008), 'Evaluation of the Weather Research and Forecasting model for two frost events', *Computers and Electronics in Agriculture* **64**(2), 234 – 247.

Prabhakaran, T., Hoogenboom, G. & Gopalakrishnan, S. G. (2007), 'Evaluation of WRF for frost warning and consequences of cold air pooling', *Eights WRF users' workshop, June 11 – 15, 2007*, National Centre for Atmospheric Research, Boulder, C.O.

Prtenjak, M. T. & Grisogono, B. (2002), 'Idealised numerical simulations of diurnal seabreeze characteristics over a steep change in roughness', *Meteorologische Zeitschrift* **11**(5), 345- 360.

Renwick, J. A. (2011), 'Kidson's synoptic weather types and surface climate variability over New Zealand', *Weather and Climate* **31**, 3 – 23.

Rotach, M. W. & Zardi, D. (2007), 'On the boundary-layer structure over highly complex terrain: Key findings from MAP', *Quarterly Journal of the Royal Meteorological Society* **133**(625), 937 – 948.

Sabatino, S., Buccolieri, R., Pulvirenti, B. & Britter, R. (2007), 'Simulations of pollutant dispersion within idealised urban-type geometries using CFD and integral models', *Atmospheric Environment* **41**(37), 8316 – 8329.

Salinger, K. J. & Mullen, A. B. (1999), 'New Zealand Climate: Temperature and precipitation variations and their links with atmospheric circulation 1930 – 1994', *International Journal of Climatology* **19**(10), 1049 – 1162.

Schmidli, J., Poulos, G. S., Daniels, M. H. & Chow, F. K. (2009), 'External influences on nocturnal thermally driven flows in a deep valley', *Journal of Applied Meteorology and Climatology* **48**(1), 3 – 23.

Schubert, S. & Henderson-Sellers, A. (1997), 'A statistical model to downscale local daily temperature extremes from synoptic-scale atmospheric circulation patterns in the Australian region', *Climate Dynamics* **13**(3), 223 – 234.

Scintec: Flat array SODAR SFAS with RASS interface.
URL:http://www.scintec.com/english/Web/Scintec/Details/A031002.aspx

Shapiro, A. & Fedorovich, E. (2007), 'Katabatic flow along a differently cooled sloping surface', *Journal of Fluid Mechanics* **571**, 149 – 175.

Skamarock, W. C. & Klemp, J. B. (2008), 'A time-split non-hydrostatic model for weather research and forecasting applications', *Journal of Computational Physics* **227**, 3465 – 3485.

Smith, R., Paegle, J., Clark, T., Cotton, W., Forbes, G., McGinley, J., Pan, H.-L. & Ralph, M. (1997), 'Local and remote effects of mountains on weather: Research needs and opportunities', *Bulletin of the American Meteorlogical Society* **78**(5), 877 – 892.

Smith, S. A., Brown, A. R., Vosper, S. B., Murkin, P. A. & Veal, A. T. (2010), 'Observations and simulations of cold air pooling in valleys', *Boundary-Layer Meteorology* **134**(1), 85 – 108.

Snyder, R. L. & Paulo de Melo-Abreu, J. (2005), 'Frost protection: Fundamentals, practice, and economics' *FAO Environment and Natural Resources Series* **10**, Rome.

Snyder, R. L., Paulo, de Melo-Abreu, J. & Matulich, S. (2005), '*Frost Protection: fundamentals, practice, and economics Vol 2*', Food and Agriculture Organisation of the United Nations, Rome.

Snyder, W. H., Thompson, R.S., Eskridge, R. E., Lawson, R. E., Castro, I. P., Lee, J. T., Hunt, J. C. R. & Ogawa, Y. (1985), 'The structure of a strongly stratified flow over hills: The dividing streamline concept', *Journal of Fluid Mechanics* **152**, 249 – 288.

Soler, M. R., Infante, C., Buenestado, P. & Mahrt, L. (2002), 'Observations of nocturnal drainage flow in a shallow gully', *Boundary-Layer Meteorology* **105**(2), 253 – 273.

Soltanzadeh, I., Azadi, M. & Vakili, G. A. (2011), 'Using Bayesian Model Averaging (BMA) to calibrate probabilistic surface temperature forecasts over Iran', *Annales Geophysicae* **29**, 1295 – 1303.

Sorbjan, Z. (1988), 'Structure of the stably-structured boundary layer during the SESAME-1979 experiment', *Boundary-layer Meteorology* **44**(3), 255 – 266.

Spring frost strikes in Reuilly, 17 April 2012.
URL: *http://jimsloire.blogspot.co.nz/2012/04/loire-frost-strikes-in-reuilly-html*

Stafne, E.T. (2007), 'Profile and challenges of the emerging Oklahoma grape industry',Oklahoma Cooperative Extension Service Pub. E-99.

Steeneveld, G. J., Mauritsen, T., de Bruijn, E. I. F., Vila-Guerau de Arellano, J., Svensson, G. & Holtsag, A. A. M. (2008), 'Evaluation of limited area models for the representation of the diurnal cycle and contrasting nights in CASES99', *Journal of Applied Meteorology and Climatology* **46**(3), 869 – 877.

Steeneveld, G. J., van de Wiel, B. J. H. & Holtslag, A. A. M. (2006), 'Modelling the evolution of the nocturnal boundary layer for three different nights in CASES-99', *Journal of Atmospheric Sciences* **63**(3), 920 – 935.

Steinacker, R. (1984), 'Area-height distribution of a valley and its relation to the valley wind', *Contributions to Atmospheric Physics* **57**, 64 – 71.

Steyn, D. G. & Galmarini, S. (2008), 'Evaluating the predictive and explanatory value of Atmospheric numerical models: Between relativism and objectivism', *The Open Atmospheric Science Journal* **2**, 38 – 45.

Stone, G. L. & Hoard, D. E. (1989), 'Low frequency velocity and temperature fluctuations in katabatic valley flows', *Journal of Applied Meteorology* **28**(6), 477 – 488.

Sturman, A. & Tapper, N. (1996), *The Weather and Climate of Australia and New Zealand*, 1 edn, Oxford University Press, Australia.

Sturman, A. P. & Quénol, H. (2013), 'Changes in atmospheric circulation and temperature trends in major vineyard regions of New Zealand', *International Journal of Climatology* **33**(12), 2609 – 2621.

Sturman, A. P. & Tyson, P. D. (1981), 'Sea breezes along the Canterbury coast in the vicinity of Christchurch, New Zealand', *Journal of Climatology* **1**(3), 203 – 219.

Sturman, A. P. (1987), 'Thermal influences on airflow in mountainous terrain', *Progress in Physical Geography* **11**(2), 183 – 206.

Sturman, A. P., Bradley, S., Drummond, P., Grant, K., Gudiksen, P., Kossman, M., McGowan, H. A., Oliphant, A., Owens, I. F., Powell, S., Sproken-Smith, R. & Zawar-Reza, P. (2003), 'The lake Tekapo experiment (LTEX): An investigation of atmospheric boundary layer processes in complex terrain', *Bulletin of the American Meteorological Society* **84**(3), 371 – 380.

Sturman, A. P., Fitzsimons, S. J. & Holland, L. M. (1985), 'Local winds in the Southern Alps, New Zealand', *Journal of Climatology* **5**(2), 145 – 160.

Sturman, A. P., Trewinnard, A. C. & Gorman, P. A. (1984), 'A study of atmospheric circulation over the South Island of New Zealand (1961 – 1980)', *Weather and Climate* **4**, 53 – 62.

Thatcher, M. & Hurley, P. (2010), 'A customisable downscaling approach for local-scale meteorlogical and air pollution forecasting: Performance evaluation for a year of urban meteorological forecasts', *Environmental Modelling and Software* **25**, 82 – 92.

Thompson, B. W. (1986), 'Small-scale katabatics and cold hollows', *Weather* **41**(5), 146 – 153.

Trought, M. C. T., Howell, G. S. & Cherry, N. (1999), 'Practical considerations for reducing frost damage in vineyards', Report to the New Zealand Wine Growers: 1999.

Van de Weil, B. J. H., Moene, A.F., Steeneveld, G.J., Baas, P., Bosveld, F.C. & Holtslag, A. A. M. (2010), 'A conceptual view on inertial oscillations and nocturnal low-level jets', *Journal of the Atmospheric Sciences* **67,** 2679 – 2689.

Verdes, P. F., Granitto, P. M. & Navone, H. D. (2000), 'Frost prediction with machine learning techniques', Proceedings of the 5th Argentine congress on computer science, pp 1423 – 1433.

Waldhuter, L. (2013), 'Barossa grape growers devastated by frost' ABC rural, 18 September 2013.
URL: *http://www.abc.net.au/news/2013-10-18/barossa-frost-damage/5031590*

Wang, H., Skamarock, W. C. & Feingold, G. (2009), 'Evaluation of scalar advection schemes in the Advanced Research WRF model using large eddy simulations of aerosol-cloud interactions', *Monthly Weather Review* **137**(8), 2547 – 2558.

Weigel, A. P., Chow, F. K., Rotach, M. W. (2007), 'On the nature of turbulent kinetic energy in a steep narrow alpine valley', *Boundary-layer Meteorology* **123**(1), 177 – 199.

Whiteman, C. D. & Doran, J. C. (1993), 'The relationship between overlying synoptic-scale flows and winds within a valley', *Journal of Applied Meteorology* **32**(11), 1669 – 1682.

Whiteman, C. D. & Zhong, S. (2008), 'Downslope flows on a low-angle slope and their interactions with valley inversions. Part 1: Observations', *Journal of Applied Meteorology and Climatology* **47**(7), 2023 – 2038.

Whiteman, C. D. (1982), 'Breakup of temperature inversions in deep mountain valleys: Part 1. Observations', *Journal of Applied Meteorology* **21**(3), 270 – 289.

Whiteman, C. D. (1990), 'Observations of thermally developed wind systems in mountainous terrain', Chapter 2 in Atmospheric Processes over Complex Terrain, *Meteorological Monographs* **23**(45), 5 – 42, American Meteorological Society, Boston, Massachusetts.

Whiteman, C. D., Bian, X. & Zhong, S. (1997), 'Low-level jet climatology from enhanced rawinsonde observations at a site in the Southern Great Plains', *Journal of Applied Meteorology* **36**(10), 1363 – 1376.

WRF model physics options and references.
URL: *http://www.mmm.ucar.edu/wrf/users/wrfv3.5/phys_references.html* Last accessed on 28 Feb 2014.

Yamada, T. & Bunker, S. (1989), 'A numerical model study of nocturnal drainage flows with strong wind and temperature gradients', *Journal of Applied Meteorology and Climatology* **28**(7), 545 – 554.

Yarnal, B., Comrie, A. C., Frakes, B. & Brown, D. P. (2001), 'Developments and prospects in synoptic climatology', *International Journal of Climatology* **21**(15), 1923 – 1950.

Zardi, D. & Whiteman, C. D. (2012), '*Diurnal Mountain Wind Systems: Chapter 2 in Mountain Weather Research and Forecasting*' (Chow, F. K., DeWekker, S. F. J. & Snyder, B. (Eds.)). Springer, Berlin.

Zhang, D. –L. & Zheng, W. (2004), 'Diurnal cycles of surface winds and temperatures as simulated by five boundary-layer parameterisations', *Journal of Applied Meteorology* **43**(2), 157 – 169.

Zhang, Y., Sartelet, K., Wo, S. –Y. & Seigneur, C. (2013), 'Application of WRF/Chem-MADRID and WRF/Polyphemus in Europe – Part 1: Model description, evaluation of

meteorologicalpredictions, and aerosol–meteorology interactions', *Atmospheric Chemistry and Physics* **13**(14), 6807 – 6843.

Appendix

The following six SODAR plots provide additional examples of meteorological features revealed by each of the three case studies in Chapter 7. In SODAR plots 1 and 2, strong ridge top winds penetrate partially into the Awatere Valley. The synoptic winds are strong enough to prevent the formation of thermally-induced down-valley drainage, yet remain decoupled from the valley surface. Under predominantly clear skies, the very light near-surface winds allow the formation of radiation frost. SODAR plot 3 illustrates a similar example in the Wairau Valley at Rapaura, when strong west-south-westerly winds descend to within 30 – 40 m of the valley floor.

SODAR plots 4 and 5 provide two further examples of low-level jet formation at Rapaura in the Wairau Valley under clear, stable boundary layer conditions. In SODAR plot 4 the LLJ commences very close to the surface (30 m), but rapidly increases in speed and height. It extends to 400 m AGL 4 hours after initiation, with a distinct wind speed maximum detectable between 90 – 170 m above the ground. Data is only available till 7 am on SODAR plot 5, however, the later development (2am) of a LLJ is clearly discernable following the easing and eventual decoupling of easterly (up-valley) synoptic winds. In this case the LLJ continued until late morning (11am).

SODAR plot 6 illustrates a further example of LLJ development in the Awatere Valley. In this case the wind speed maximum is diffuse between 120 to over 380 m AGL. It also occurs later in the morning and continues for some time after sunrise.

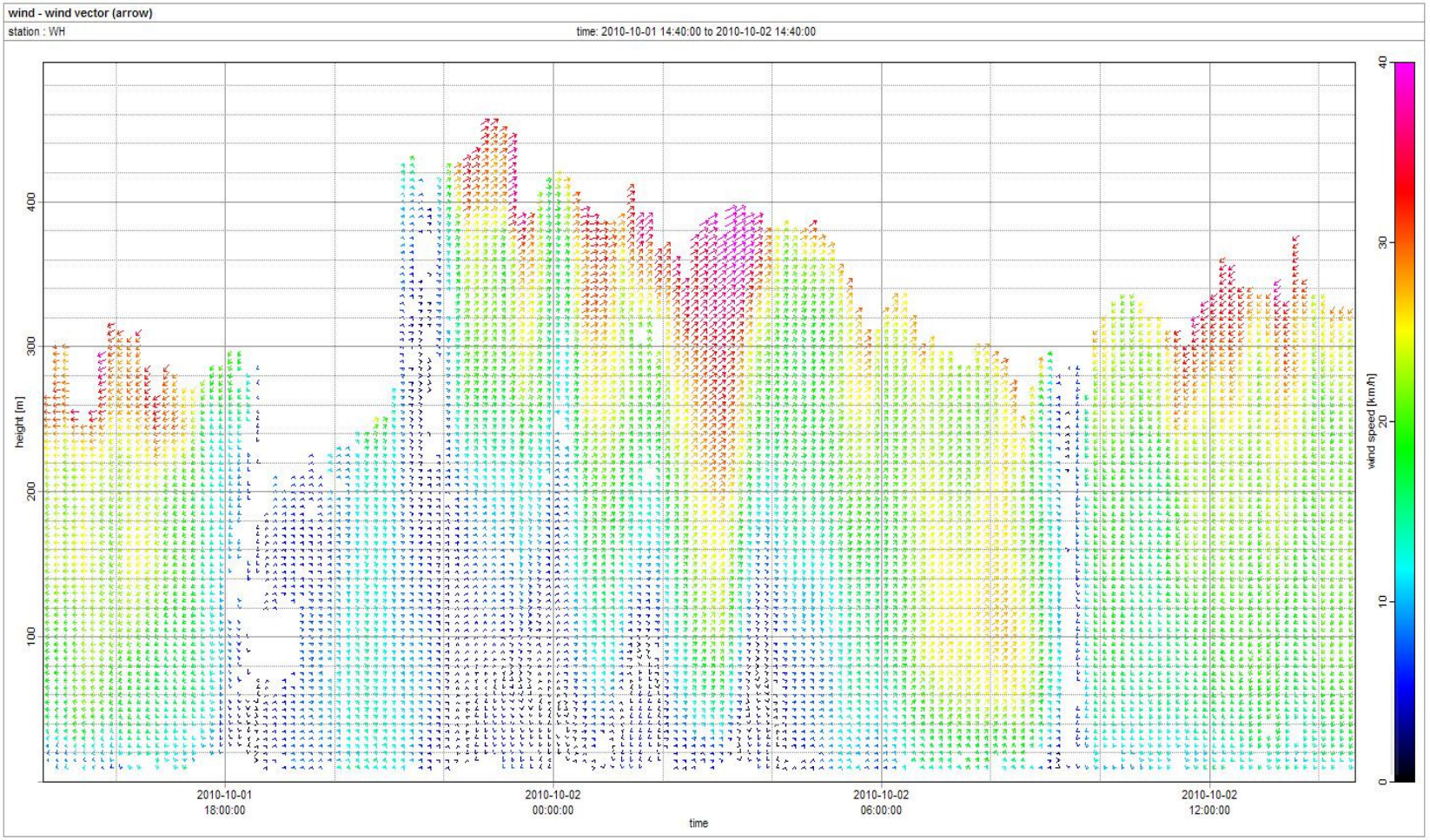

SODAR plot 1, October 1 – 2 2010, Awatere Valley. Strong westerly winds on surrounding ridge tops overnight prevent the formation of thermally induced drainage flows. Winds remain decoupled from the Awatere Valley AWS and result in localized frost.

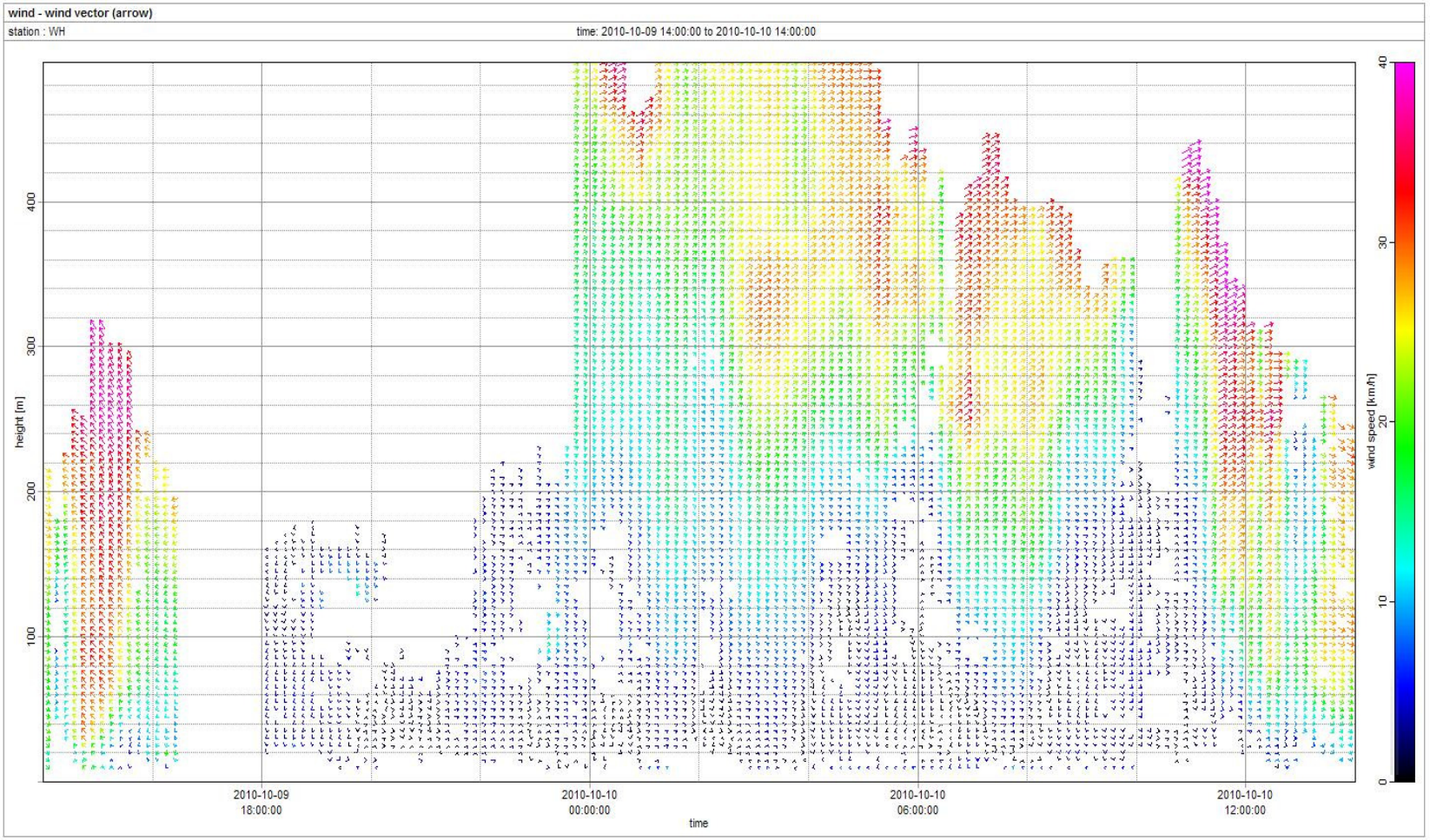

SODAR plot 2, October 9 – 10 2010, Awatere Valley. Further example of strong west – south-west winds upon surrounding ridge tops. The synoptic winds penetrate to within 80 m of the valley floor at times, but are not sufficient to ventilate at the Awatere AWS. The very light near-surface winds result in near-frost conditions.

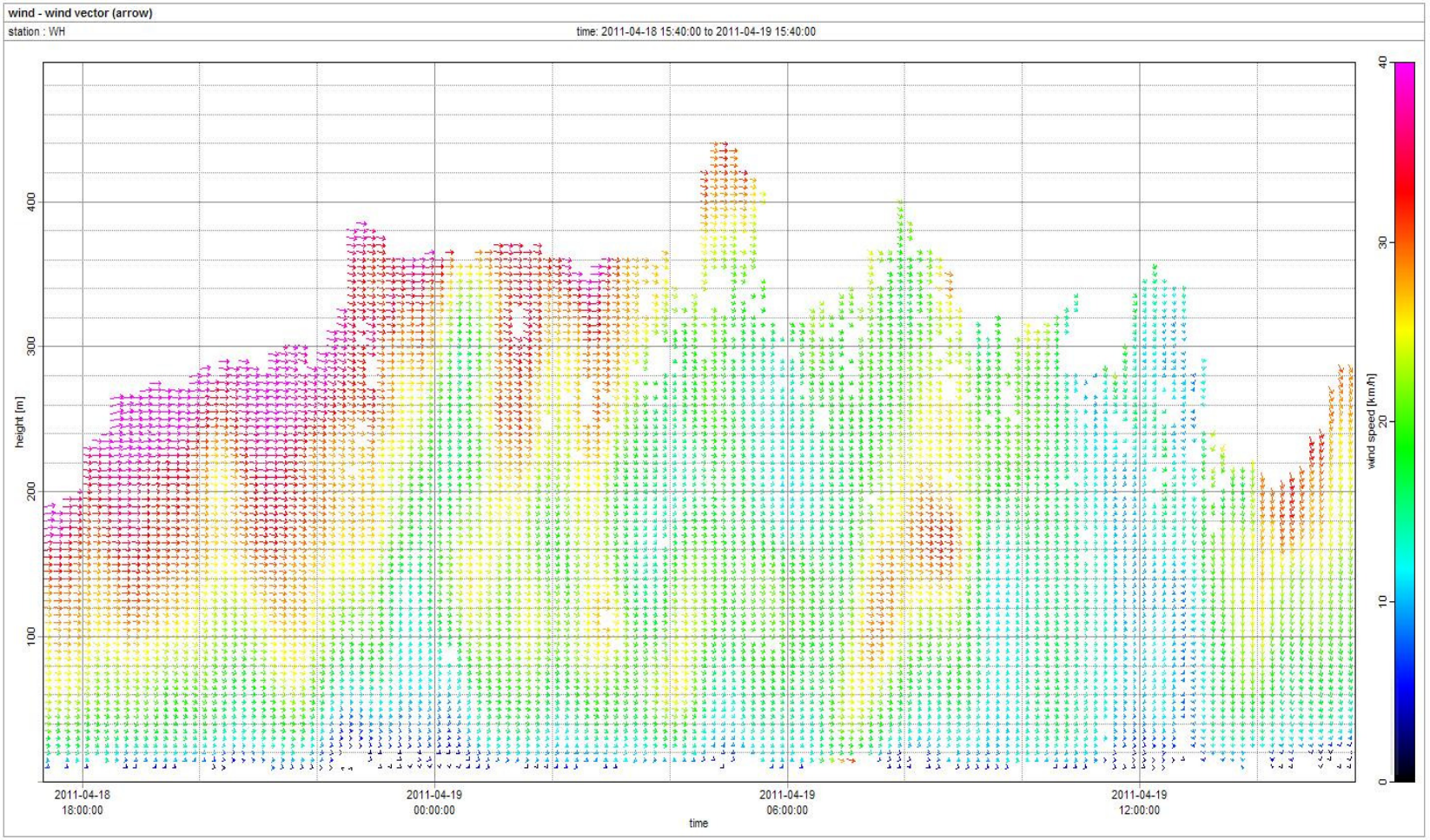

SODAR plot 3, 18 – 19 April, Rapaura, Wairau Valley. Strong westerly winds are recorded to within 40 – 60 m above the valley floor, but terrain induced shelter provides a shallow layer of very light winds near the surface. The very light near-surface winds augment localised frost conditions for a time.

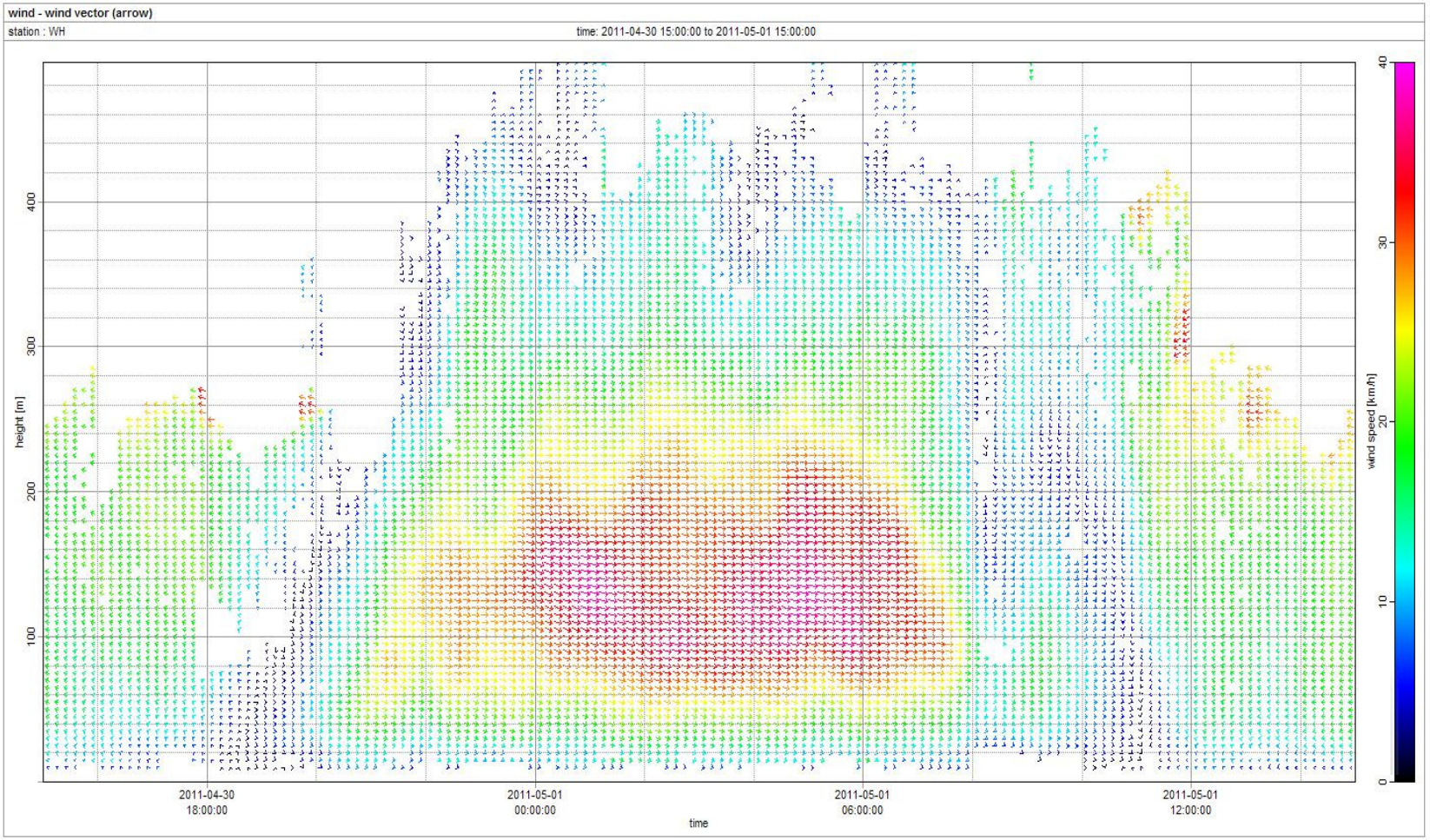

SODAR plot 4, 30 April – 1 May 2011, Rapaura, Wairau Valley. The formation of a low-level jet is present from 8 pm. Wind speed maximums occur between 60 – 200 m AGL.

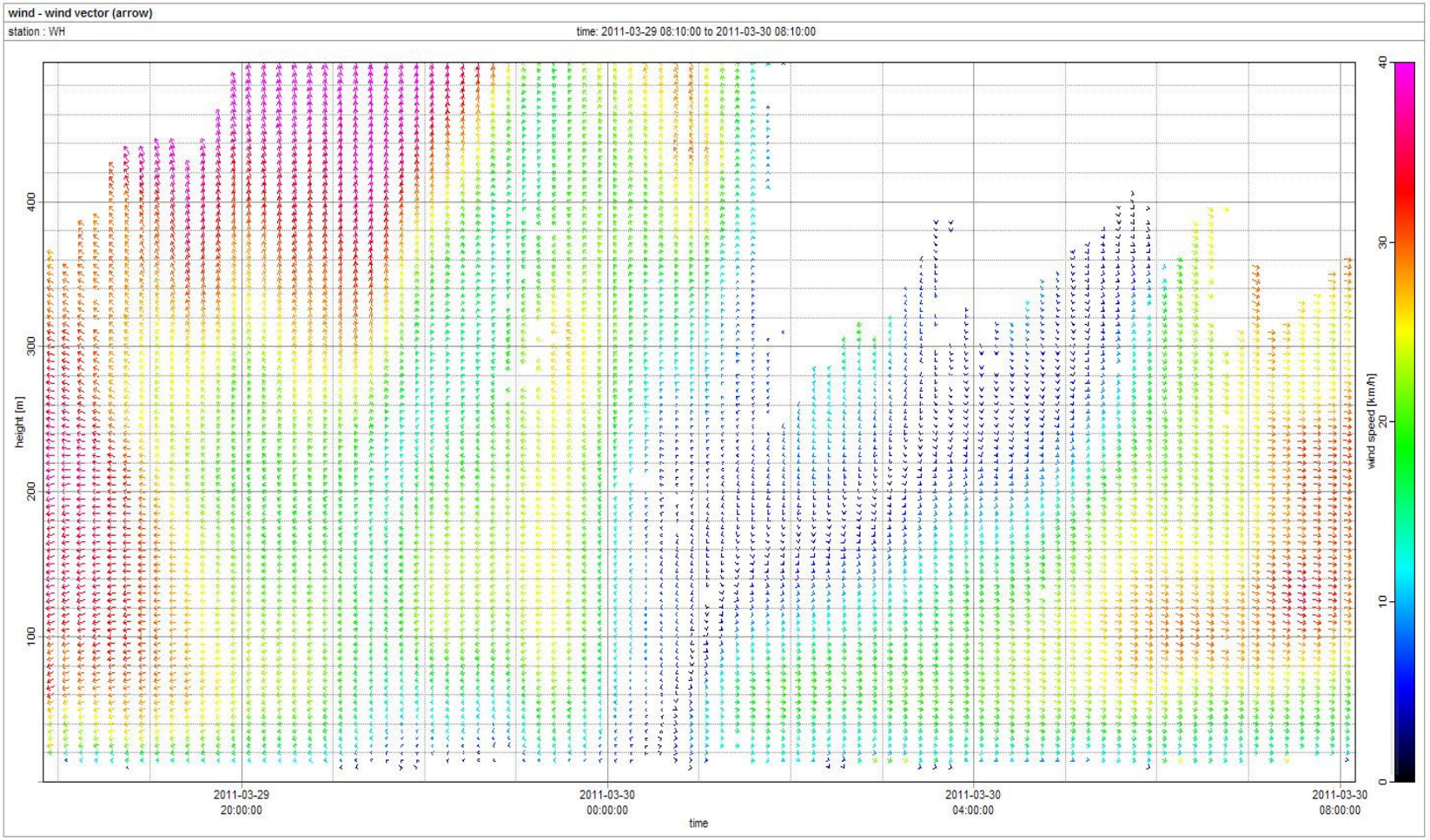

SODAR plot 5, 29 – 30 March 2011, Rapaura, Wairau Valley. The late development of a low-level jet from 1 am, as south-south-easterly synoptic winds ease above the region. Data is only available till 8am 30 March, however, the low-level jet remains well developed.

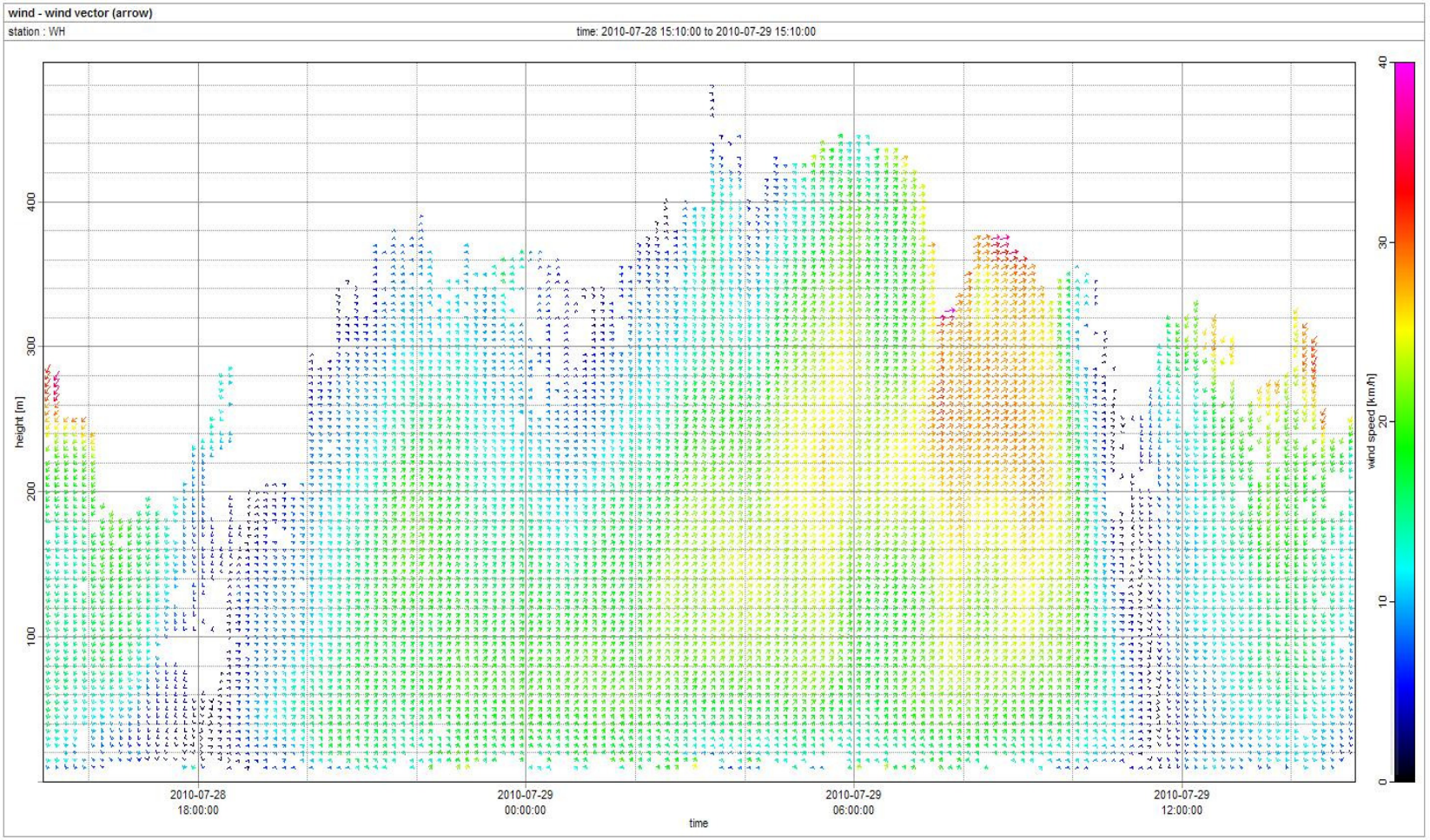

SODAR plot 6, 28 – 29 July 2010, Awatere Valley. Development of thermally-induced drainage winds, with low-level jet features. The LLJ continues within the valley until 11 am the following morning. Despite light ridge top winds, strong near-surface winds at the Awatere AWS prevent the formation of frost.